Doctoral Thesis

Ultimate Behavior and Safety of Tower Cranes Installed in High-rise Buildings under Construction at the Time of an Earthquake

by

Yoshitaka Ushio

September 2019

Graduate School of Simulation Studies
University of Hyogo

Summary of this thesis

It is important to determine and apply the measures to prevent fatal tower crane accidents at construction sites during earthquakes because these accidents negatively and seriously impact construction projects, may result in losses of life and tremendous repair costs, and distort the construction schedule. In many cases, construction contractors follow the less stringent structural design criteria applying only to cranes because tower cranes are facilities and structures that are needed only for a short term (e.g., less than two years) and construction costs and time effectiveness are often emphasized over safety measures. .

Chapter 1 presents the background and objectives of this thesis. The background briefly explains the seismic design criteria for tower cranes in Japan and details a serious tower crane accident caused by an earthquake. It occurred in 2002 during the construction of the Taipei 101 Building (101 stories); the accident was experienced by the author as the project director. In this tower crane accident, two cranes located at a height of more than 200 m from the ground fell down due to the site joint failure of tower crane mast, leading to the death of five people, injuring approximate 20 people, and seriously damaging the building itself and neighborhood.

The objectives of this thesis are highlighted as follows:

(1) To confirm the resonance effects of a tower crane seismic responses with the building, where the tower crane is installed, at construction sites of high-rise building, and propose countermeasures to prevent those effects and to minimize tower crane failures,

(2) To propose a new design method for end-plate-type tensile bolted joints that are commonly applied to the site joints of tower crane masts owing to their site workability. The method uses the calculation results obtained using a supercomputer by an application of static elastoplastic finite element analysis (LS-DYNA R 9.2.0 _ Rev. 119543, which was developed by Livermore Software Technology Company(LSTC)), to a tower-crane-mast structural models with extremely finely shaped solid elements, and

(3) To develop a modeling method for tower crane mast structures by creating a hybrid element model comprising solid, shell, and beam elements for seismic response non-linear FEM analysis (LS-DYNA) to enable structural engineers to grasp the precise dynamic ultimate behavior of mast site joints during earthquakes, and to promote better structural design.

Chapter 2 describes the earthquake responses of tower cranes at construction sites using simulation methods and discusses the amplification of the tower crane response due to resonance effects between the building and the tower crane during an earthquake. The analysis was performed using the "Dynamic PRO" computer software on a 14-story building designed according to the latest seismic design criteria. The lumped-mass models for six construction stages were prepared for seismic analysis using linear and non-linear structural models of the building. El Centro NS (v_{max} = 50 cm/s and v_{max}=32.25 cm/s) seismic loads were applied with a 3% damping ratio of the building and the tower crane structures. The seismic load (v_{max} = 50 cm/s) was large enough that some of the designed buildings' structural members should have experienced plastic deformation, and the seismic load (v_{max}=32.25 cm/s) was the level that the designed buildings' structural members were all within elastic range.

The results showed seriousness of the resonance effects caused by their close natural frequencies. Based on the corresponding results, the countermeasures such as changing the stiffness of the building frame and tower crane mast to prevent such resonance effects are proposed and discussed.

Chapter 3 proposes a new design method for end-plate-type tensile bolted joints that are commonly applied to the site joints of tower crane masts. End-plate-type tensile bolted joints possess good workability for the joining of vertical members, such as posts of a tower crane mast, during assembly and disassembly, and moreover, it is structurally capable of transmitting large loads efficiently. However, the problem is that the design of the joints is difficult and complicated because of the joint condition that the outer surface of the mast needs to be flat to enable climbing of the tower crane. Therefore, depending on the shapes of the post members of the mast, special joints such as large-diameter bolted (greater than 30 mm) and eccentric-bolted tension joints are applied to the site joints.

This new design method uses the calculation results obtained using a supercomputer through static elastoplastic finite element analysis (LS-DYNA) applied to structural models with extremely fine cubic-shaped solid elements with side lengths of 2.5 mm. To prove the effectiveness of this method, the conventional design method was also described. Using the design method proposed in this chapter, it is possible to realize not only more precise and reliable joint designs but also the design of various complicated joints in consideration of the construction conditions such as the pre-tension axial force on the bolts.

Chapter 4 proposes the modeling of a tower crane mast structure for seismic response non-linear FEM analysis. Consequently, the author created a new hybrid element model (HEM) composed of beam, shell, and solid elements that not only expressed the detailed ultimate behavior of the site joints of a tower crane mast, such as the stresses on individual solid elements of end plates and bolts, axial tension force of each bolt, and gap between the two end plates, etc. during an earthquake but also suppressed any increase in the total calculation time and revealed its behavior using LS-DYNA and a supercomputer. El Centro NS (v_{max} = 100 cm/s) was applied as a seismic load with 3% of the damping ratio of the structural model. The case study on the seismic responses of the joint models with diferent initial pretention forces of bolts was also done using this simulation analysis. This result suggested for end-plate-type tensile bolted joints that initial pretention axial force of bolts should be critical factor for designing of safer joints.

The simulations using the proposed structural model make it possible to provide effective and useful information for designing safe joints to prevent brittle disruptions of tower cranes during earthquakes while taking into consideration site workability (control of the bolt pre-tension axial force, etc.) and economy.

Finally, this thesis recommends a computer-simulation method, which can generally be less expensive and can take more parameters into account in the study than experiments with specimens that are common in studies on the mechanical behavior of joints in steel structures. Therefore, when an analytical model that allows more reproducibility and less computation time as this thesis proposed is devised, the computer simulation tool become very useful and effective for precise and reliable design of steel structure joints.

Table of Contents

Chapter 1

Introduction

1.1 Background

For about 30 years the author had been working for Nippon Steel Corporation and been engaged in the overseas steel construction projects, construction of high-rise buildings such as the Hong Kong Bank of China Building (70th Floors), the Taipei 101 Building (101st Floors), etc. and long span buildings such as the Hong Kong Airport Terminal Building (Getines and Ushio (2000), etc. Each steel construction project was very difficult in terms of both schedule and technical aspects and he also experienced a serious accident due to a natural disaster.

Particularly, during construction of the Taipei 101 Building, which was the tallest building in the world when it was built, there was so fatal catastrophic disaster that two tower cranes were collapsed and fell down to the ground from about 230 m above the ground level by the earthquake on March 31, 2002 (Loh *et al.* 2003 and Ushio *et al.* 2017). This disaster caused great damages such as 5 human deaths, approx. 20 injuries and serious damage of the building under construction, etc.

After the accident, the investigation of the causes including the earthquake response analysis, was carried out by the Taipei structural Engineers Association and concluded " The strength of the mast of the tower crane falling down was satisfied with the seismic design criteria in both Taiwan and Japan, but the seismic loading on the tower crane was significantly amplified, 6 times compared with the case of the tower crane being installed on the ground, due to the resonance effect between the tower crane and the building where the tower crane was installed and consequently the seismic load exceeded the design load to be applied", and in addition "The structure system of the mast was so brittle that the bolt joints were destructed before the jointed members yielded."

In the case of the Hyogo-ken Nanbu Earthquake in Japan, collapse and fall accidents of tower cranes have been reported (Takanashi 2005), but there was no human damage as the earthquake broke out very early morning. The detail is explained in Appendix.

Among the themes related to earthquake countermeasures at construction sites, those for tower cranes are especially important. An accident involving the collapse of a crane during the construction of a high-rise building has serious consequences, such as human death and injury, enormous repair costs, and significant delays in construction.

In many cases, however, because a tower crane is a temporary facility and structure due to its short-term use (e.g., less than 2 years), the cost and time effectiveness are often emphasized over safety measures and construction contractors sometimes follow only the structural design criteria for the crane but do not take further consideration and countermeasures to prevent serious accidents during powerful earthquake similar to those for permanent buildings.

As for the seismic design load in the structural design criteria for cranes in Japan, two types of crane standards exist for protection against earthquake; one is the Construction Code of cranes and the other is the Japan Crane Association standard. The Construction Code has legal force and specifies that all the cranes must be designed with a uniform value of lateral seismic factor of 0.2 in accordance with the JIS B 8821 (2013) and JIS 8831 (2004) standard. In case the combined design force includes short-term loads such as seismic or wind loads, the allowable stress of the structural members and the connections is 1.3 times (seismic) or 1.15 times (wind) greater than the allowable stress under long-term loading of the structure. It is considered that the application of these design criteria, in terms of being economical and safe, is reasonable, and a common and

standard practice prevalent in Japan, which is a country subject to frequent and intensive earthquakes.

The Japan Crane Association standard (JCA1101) specifies the seismic modification coefficient calculated by considering the structures where the crane is fixed in 2008 (Kobayashi 2017). Furthermore, these criteria were revised in 2018 in consideration of ISO standard (ISO 1131 (2016)). The Seismic design criteria recommended by the Japan Crane Association have been improving.

The earthquake countermeasures are different depending on the locations where the tower crane is fixed. Especially the tower crane used in the construction sites located in the densely populated area of the city are more dangerous. However, since the tower crane is reused many times and used in different places (geographical locations, structures with tower cranes on, etc.), it could not be assumed as a temporary structure. In addition, a tower crane operator manipulates different types of tower cranes for a long period of time, in consideration of their safety at the time of earthquake, the design criteria for short-term use basis should not be applied.

Furthermore, when a tower crane is installed in a high-rise building, the tower crane rises according to the construction progress, and the structural characteristics (natural period) of the building with the tower crane installed changes according to the construction progress. Then, at the stage where the natural period of the building approaches the one of the tower cranes, an unexpected earthquake load is applied to the tower crane due to the resonance effects which was the cause of the disaster of the Taipei 101 Building (Takanashi 2007 and Ushio *et al.* 2017). The probability of an earthquake occurring at this stage is considerably low. However, considering the seriousness of the accident, it is necessary to take measures against earthquake resistance as the case of emergency. In consideration of the above, the seismic design standard of the tower crane need not only to be further revised but also to establish the design tools for tower crane seismic design.

Another point to be discussed is the design criteria for the connections of the crane mast, between mast units, and the mast to the crane machine deck. Since the structural frame of the tower crane is a temporary structure, these frames should be reused several times. Therefore, the site connections of the mast units, which consist of the lattice frame with four H-shaped columns, horizontal members and bracings in case of the crane used for Taipei 101 Building construction, should be designed such that the site-assembling and disassembling of these mast units can be easily carried by considering the schedule and costs. Therefore, it seems to be the one of the reasons why the standards do not require the bolt connections to be stronger than the connected structural members (AIJ Recommendation), which means that the failure of the mast should not be at the bolt connections but at members such as the H-shaped columns. However, considering that the bolt connection failure as shown in Fig.1-1 is one of typical failure patterns of the climbing-type tower cranes like the cases of the Taipei 101 building and the buildings in the Hyogo-ken Nanbu Earthquake in 1995, this criteria on the mast unit connections similar to permanent building structures is recommended to be mandatorily applied to the crane design, and also strong joints with easier assembling and disassembling should be designed.

Actually, in the case of Taipei 101 Building, for restart of the construction, the study of the site connections was done but it was found that the connections to satisfy both this recommended requirement and construction workability could not be realized. Consequently, it was concluded that these connections were designed as the connections

with welds and bolts, as shown in Fig.1-2, to make the mast scrapped after the dismantle because the engineers had not enough time and knowledge to design the suitable connections in order to manufacture the new cranes for the scheduled restart of the construction. If the project team had used suitable and applicable design method of those connections, they would not have wasted the money for site work by making scrapping.

Therefore, in order to solve the abovementioned site-joint problems, the accurate design of the site-joins of the temporary structures such as tower crane masts is required and it will be realized by grasping the detailed information of the behaviors of the joints under earthquakes by reproducing such dynamic behaviors precisely and realistically using computer simulations.

Fig. 1-1 Destruction of a tower crane mast of the Taipei 101 Building

(a) Bolted web and welded flange

(b) Cover plates welded for compensation of bolt hole section area loss

Fig. 1-2 Site joints of mast of the new tower cranes installed after the accident in the Taipei 101 Building

1.2 The purposes of this research and outline of the contents

According the experiences the author had, the resonance effects to a tower crane with the building where the tower crane is fixed, and site joints of a tower crane mast are key issues to prevent the fatal disaster of tower cranes at earthquake. Therefore, the purposes of this research are as follows:

(1) To confirm the resonance effects of a tower crane seismic responses with the building, where the tower crane is installed, at construction sites of the high-rise building, and propose countermeasures to prevent those effects and to minimize tower crane failures,
(2) To propose a new design method for end-plate type tensile bolted joints that are commonly applied to the site joints of tower crane masts owing to their site workability. The method uses the calculation results obtained using a supercomputer by an application of static elastoplastic finite element analysis (LS-DYNA R 9.2.0 _ Rev.119543, which was developed by Livermore Software Technology Company(LSTC)), to a tower-crane-mast structural models with extremely finely shaped solid elements, and
(3) To develop a modeling method for tower crane mast structures by creating a hybrid element model comprising solid, shell and beam elements for seismic response non-linear FEM analysis (LS-DYNA) to enable structural engineers to grasp the precise dynamic ultimate behavior of mast site joints during earthquakes, and to promote better structural design.

Chapter 2 describes the earthquake responses of tower cranes at construction sites using simulation methods and discusses the amplification of the tower crane response due to resonance effects between the building and the tower crane during an earthquake. The analysis was performed on a 14-story building designed according to the latest seismic design criteria. The lumped-mass models for six construction stages were prepared for seismic analysis using linear and non-linear structural models of the building. El Centro NS (v_{max} = 50 cm/s and v_{max}=32.25 cm/s) seismic load was applied with a 3% damping ratio of the building and the tower crane structures. The seismic load (v_{max} = 50 cm/s) was large enough that some of the designed buildings' structural members should have experienced plastic deformation, and the seismic load (v_{max}=32.25 cm/s) was the level that the designed buildings' structural members were all within elastic range. The results showed seriousness of the resonance effects caused by their close natural frequencies.

This analysis was conducted using the "Dynamic PRO" computer software. Based on the corresponding results, the countermeasures such as changing the stiffness of the building frame and tower crane mast to prevent such resonance effects are discussed and proposed.

One of the causes of brittle tower crane collapses was the destruction of the site joints of the tower crane masts. Chapter 3 proposes a new design method for end-plate type tensile bolted joints that are commonly applied to the site joints of tower crane masts. A high-tensile-strength tensile bolted joint possesses good workability for the joining of vertical members, such as the posts of a tower crane mast, at the time of assembly and disassemble, and moreover, it is structurally capable of transmitting large loads efficiently. However, the problem is that the design of the joints is difficult and complicated because the outer surface of the mast needs to be flat to enable climbing of the tower crane. Therefore, depending on the shapes of the post members of the mast, special joints such as large-diameter bolted (greater than 30 mm) and eccentric-bolted tension joints are applied to the site joints.

This new design method uses the calculation results obtained using a supercomputer through static elastoplastic finite element analysis (LS-DYNA) applied to structural models with extremely fine cubic-shaped solid elements with side lengths of 2.5 mm. To

prove the effectiveness of this method, the conventional design method (JSS IV 05-2004) was also described. Using the design method proposed in this chapter, it is possible to realize not only more precise and reliable joint designs but also the design of various complicated joints in consideration of the construction conditions such as the pre-tension axial force on the bolts. Furthermore, this method is applicable not only to tower crane masts but also to bolted tension joints in all structures.

Chapter 4 proposes the modeling of a tower crane mast structure for seismic response non-linear FEM analysis. Consequently, the author created a new hybrid element model (HEM) composed of beam, shell, and solid elements that not only expressed the detailed ultimate behavior of the site joints of a tower crane mast, such as the stresses on individual solid elements of end plates and bolts, axial tension force of each bolt, and gap between the two end plates, etc. during an earthquake but also suppressed any increase in the total calculation time and revealed its behavior using LS-DYNA and a supercomputer. In addition, the case study on the seismic responses of the joint models with diferent initial pretention forces of bolts was done using this simulation analysis. This result suggested for end-plate-type tensile bolted joints that initial pretention axial force of bolts should be critical factor for designing of safer joint and recommended that the pretention force, 75% of bolt yield strength, specified in AIJ Recommendation (2012), shuld be reduced to the proper value in consideration of loading condition of the joint using of the suitable analysis like the method proposed. El Centro NS (v_{max} = 100 cm/s) was applied as a seismic load with 3% of the damping ratio of the structural model.

It is also possible to replace the detailed joint model of HEM with an alternative detailed joint model that could be used for any types of tower-crane mast joint. The simulations using the proposed structural model make it possible to provide effective and useful information for designing safe joints to prevent brittle disruptions of tower cranes during earthquakes while taking into consideration site workability (control of the bolt pre-tension axial force, etc.) and economy.

Finally, this thesis recommends a computer-simulation method, which can generally be less expensive and can take more parameters into account in the study than experiments with specimens that are common in studies on the mechanical behavior of joints in steel structures. Therefore, when an analytical model that allows more reproducibility and less computation time as this thesis proposed is devised, the computer simulation tool become very useful and effective for precise and reliable design of steel structure joints.

Chapter 2.

Resonance effects on tower cranes in a normal office building designed according to the Japanese Building Code

The contents of this chapter are according to the following references:

Ushio, Y., Okano, M. and Nagano, Y. (2017), "The earthquake response of climbing-type tower cranes installed in high-rise buildings in consideration of various situation under construction", *Proceedings of 16th World conference on Earthquake Engineering, Santiago, Chile*. No.3403

Ushio, Y., Okano, M., Shirai, M. and Nagano, Y. (2018), "The Seismic Response Analysis of Steel structure Building in Consideration of Construction Progress No.1 to No.3", Summary research reports presented at the annual conference in Hiroshima, organized by the Architectural Institute of Japan (AIJ) Aug. 2017, Structure Field Ⅱ、P57-62

2.1 Introduction

A self-climbing tower crane is raised along with the high-rise building for which it is being used, according to construction progress. At same time, if the natural frequency of the building under construction reaches that of the tower crane, the resonance caused by their close natural frequencies leads to an amplification effect.

At the Taipei 101 Building, seismographs at each of three ground-surface locations near the construction site measured the maximum acceleration as 193, 100, and 57 Gal; it was assumed that the earthquake was of medium intensity, with an acceleration of about 100 Gal. This is supported by the fact that very few other buildings in Taipei City collapsed during that earthquake (Loh *et al.* 2003). According to an investigation into the causes of the accident (Investigation Reports 2002), including an analysis of the tower crane carried out by the Taipei Structural Engineers Association after the accident, it was concluded that "*The strengths of the masts of the fallen tower cranes satisfied the seismic design standards of Taiwan and Japan, but the collapse of the crane was due to the destruction of the masts, caused by the amplification effect of the building in which they were installed and the amplified load considerably exceeded the design load.*" The difference between the natural periods of a building and tower crane greatly affects the crane's response to an earthquake because its height increases during construction. Because the resonance is amplified with the building vibrations, the earthquake load applied to a tower crane mast and temporary support structure may be several times larger as it was when the crane is installed on the ground (Takanashi 2007 and Ai *et al.* 2013).

In this chapter, the tower crane's responses to the earthquake, considering the construction progress, were studied using simulation methods. The tower crane's response to amplification caused by resonance between the building and crane during a powerful earthquake was confirmed (Ushio *et al*. 2017 a, b). Based on these results, we investigated countermeasures to prevent such resonance by changing the stiffness of the building frame and tower crane mast (Ushio *et al*. 2017a).

2.2 Modeling of the building and tower crane for the analysis

In the seismic design of buildings by the calculation of critical load capacity, which was introduced as one of the performance-type design methods, together with the latest revision of the Japanese Building Code (1998), the following items should be checked:

1. The building should not exceed the damage limit for an earthquake encountered at least once during its service life (a medium earthquake occurring about once in several decades).
2. The building should not exceed the safety limit for an extremely rare earthquake ground motion (a large earthquake occurring once every several hundred years).

The effects on a tower crane caused by resonance between a building and the crane have been studied for a typical office building with 14 stories (total floor area: 10,258 m^2, height: 63.3 m), designed according to the above-mentioned revised Japanese Building Structural Design Code, which has been published in the book titled "Examples of

Structural Design/Structural Member Sections" (2007). The structural frame is shown in Fig. 2-2, and the tower crane's location (KCP-H1020) is shown in Fig. 2-1.

The tower crane shown in Fig. 2-1 was used in the simulation. Its specifications are shown in Table 2-1.

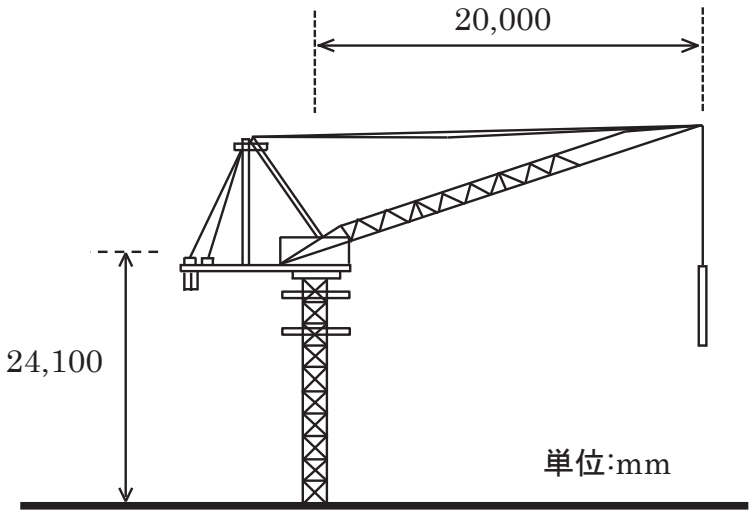

Fig. 2-1 Schematic of the tower crane (KCP.H-1020 type)

Table 2-1 Tower crane specifications

Height (H_T) [m]	Weight (M_T) [kN]	Initial Stiffness (k_T) [kN/cm]	Yield Point (Qi) (kN)
24.1	120	12.12	146

To construct this building, the frame was divided into five tiers (penthouse excluded), and the self-climbing tower crane was fixed on the top floor of each tier. It was also assumed that all the construction work of the structural frame, such as welding, bolt fastening, and floor concreting, was completed for the floor to which the tower crane would climb. A seismic response analysis was carried out at each construction stage, as shown in Fig. 2-3. In this analysis, a two-dimensional frame system with only one direction of seismic load, X1 to X6, was applied.

The lumped mass models of the six construction stages for the seismic analysis are shown in Fig. 2-4 (a); their structural characteristics are linear and nonlinear. The hysteresis restoring force characteristics of the nonlinear model is shown in Fig. 2-4 (b), and the relevant values are listed in Table 2-2. The damping ratio is proportional to the stiffness of the frame, which was determined as 0.03.

El Centro NS (v_{max} =50 cm/s) was applied as the seismic load. This seismic load was so large that some of the building's structural members should have experienced plastic deformation, because this building was designed in accordance with the latest Japanese structural design code. This analysis was carried out using the "Dynamic PRO" computer software developed by Union System Inc.

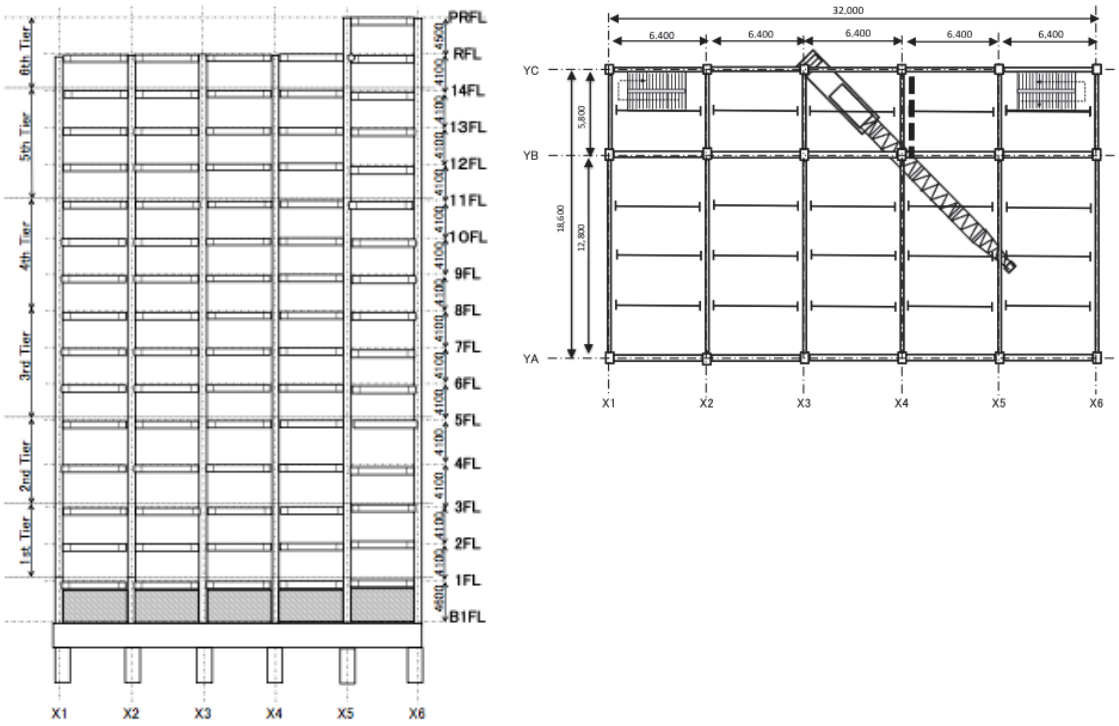

Fig. 2-2 Elevation and floor plan of the S Office and location of the tower crane

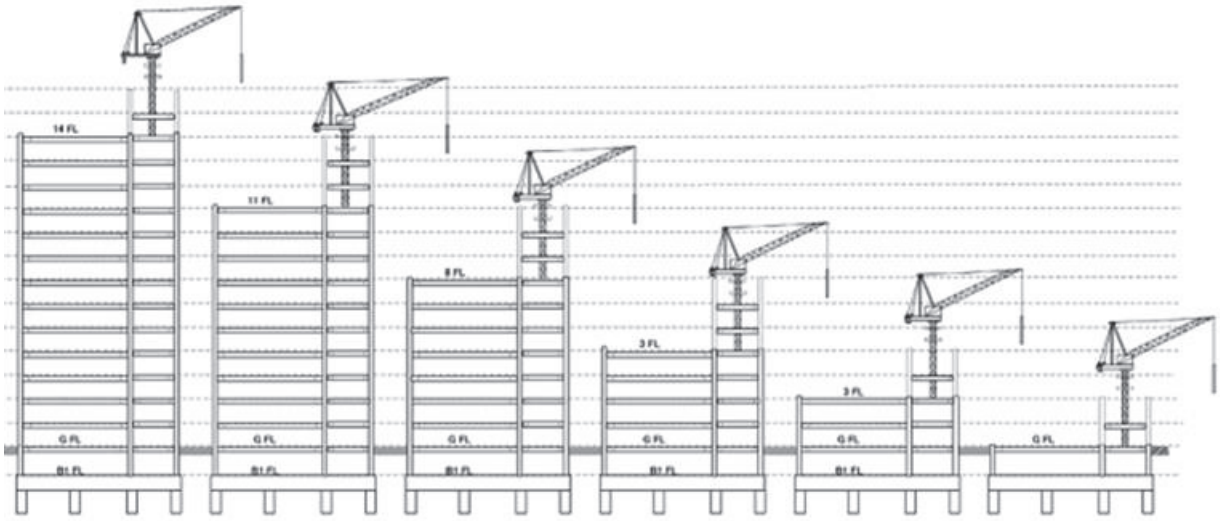

Stage 6 TC on 14th Floor | Stage 5 TC on 11th Floor | Stage 4 TC on 8th Floor | Stage 3 TC on 5th Floor | Stage 2 TC on 3rd Floor | Stage 1 TC on 1st Floor

Fig. 2-3 Tower crane locations for the six stages

.

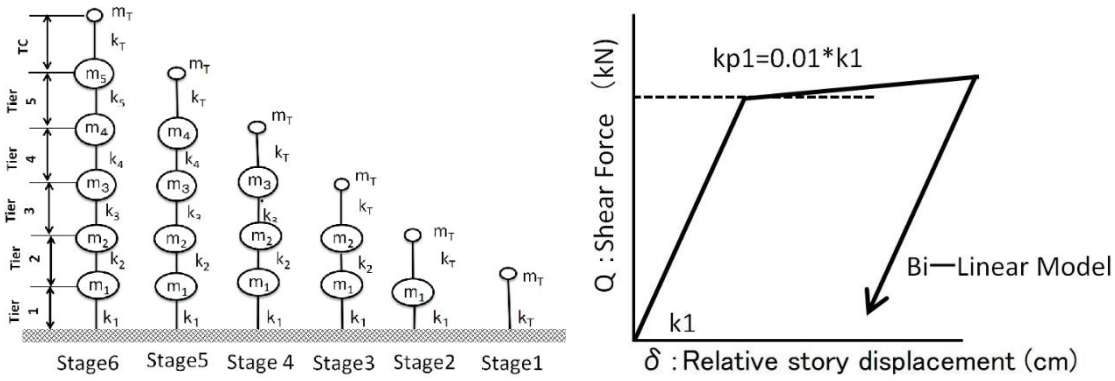

(a) Lumped mass model (b) Hysteresis restoring force characteristics

Fig. 2-4 Lumped mass model of each stage of tower crane locations

Table 2-2 Values of the lumped mass model of the building structural system

Tier No.	Height of each Tier (cm)	Weight of Lumped Mass (kN)	Stiffness in Elastic Range (kN/cm)	Max. Elastic Capacity (kN)	Hysteresis Restoring Force Characteristics
TC	2,410	120	12.1	146	Bilinear
5	1,232	16,017	1,435	8,841	Bilinear
4	1,230	16,240	1,781	10,955	Bilinear
3	1,230	16,415	2,026	12,462	Bilinear
2	820	11,030	3,315	13,592	Bilinear
1	880	11,122	4,302	18,930	Bilinear

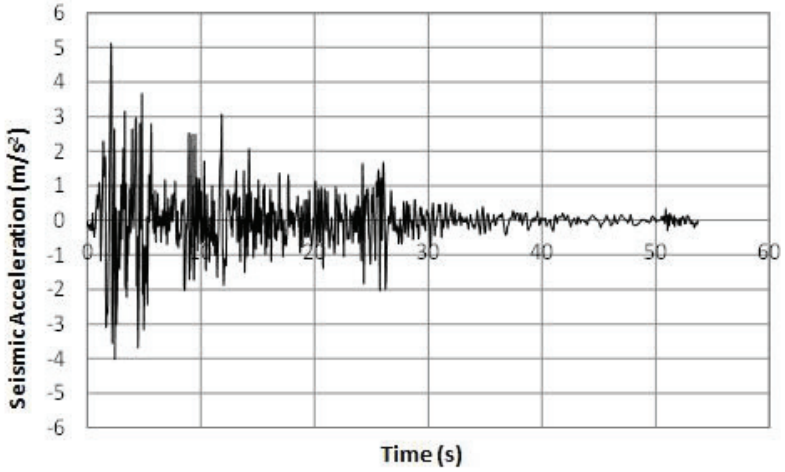

Fig. 2-5 Acceleration wave of El Centro NS level 2: normalized as v_{max} = 50 cm/s.

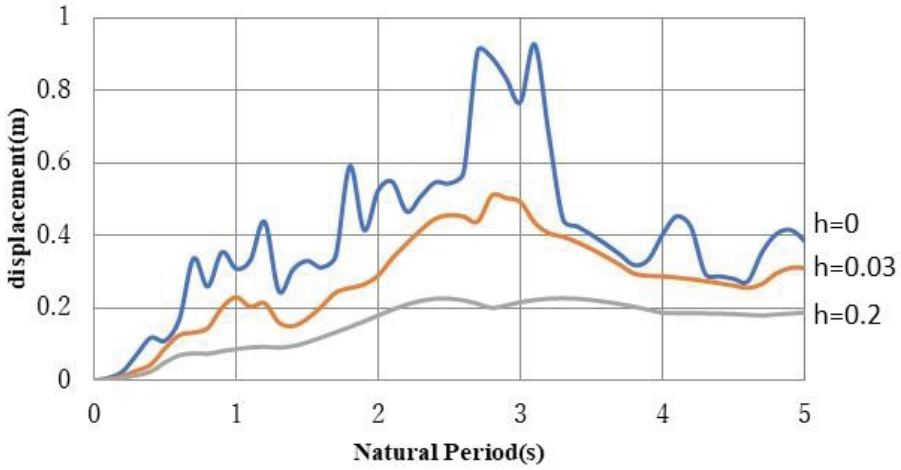

Fig. 2-6 Response spectrum of El Centro NS (1940).

2.3 Comparison of the analysis results between the cases of elastic and elastoplastic building models, and resonance of the building and earthquake

We investigated the effect of plasticizing the building under construction, in which the tower crane was installed, on the crane's response to an earthquake. If the plasticizing's influence was significant, we could implement an earthquake resistance countermeasure by giving its function to the tower crane's temporary supports. Accordingly, Figures 2-7 (a) and (b) show the drifts of each building tier and the tower crane at construction Stages 2 to 6. Also, Table 2-3 shows the results of the maximal drift of each tier at Stage 4, obtained through seismic response analysis of the building linear and non-linear models (although the crane is non-linear in both models). Figures 2-8 (a) and (b) show the response history loop of the drift and shear force of each tier and tower crane mast at Stage 4 in the linear and non-linear models.

From these figures, the maximal drift exceeded 1/100 in the first tier at Stage 3 and in the second tier at Stage 4, regardless of the use of a tower crane in the buildings during construction. There is a point during building construction when the building's response to the earthquake is higher than it is after completion. This behavior of a building under construction is thought to be caused by resonance between the building and the earthquake ground motion. This resonance exists because the first peak of the displacement response spectrum, caused by the earthquake ground motion, occurs at around 1 second in case of El Centro NS (1940) (as shown in Fig. 2-6) and because its natural period is close to that of the building under construction at Stages 3 and 4.

For the tower crane, Fig. 2-9 shows that the responses of the tower crane top are amplified because of the resonance effects between the building and crane, and between the building and the earthquake ground motion, for the linear and non-linear structural systems. The amplification is about double in the nonlinear model and 2.5 times in the linear model compared to that at Stage 1, in which the tower crane is fixed to the ground. A comparison of the seismic response analysis results between the linear and non-linear models shows that building plasticization reduces the tower crane's response to the

earthquake. The result confirms that the earthquake energy absorption by the tower crane's temporary support system is effective for reducing the earthquake response.

The largest drift of the tower crane is at Stage 4 in the elastic model and at Stage 3 in the elastoplastic model. As mentioned previously, these amplified responses are influenced mainly by the resonance between the building and ground motion in the elastic model and between the building and tower crane in the elastoplastic model.

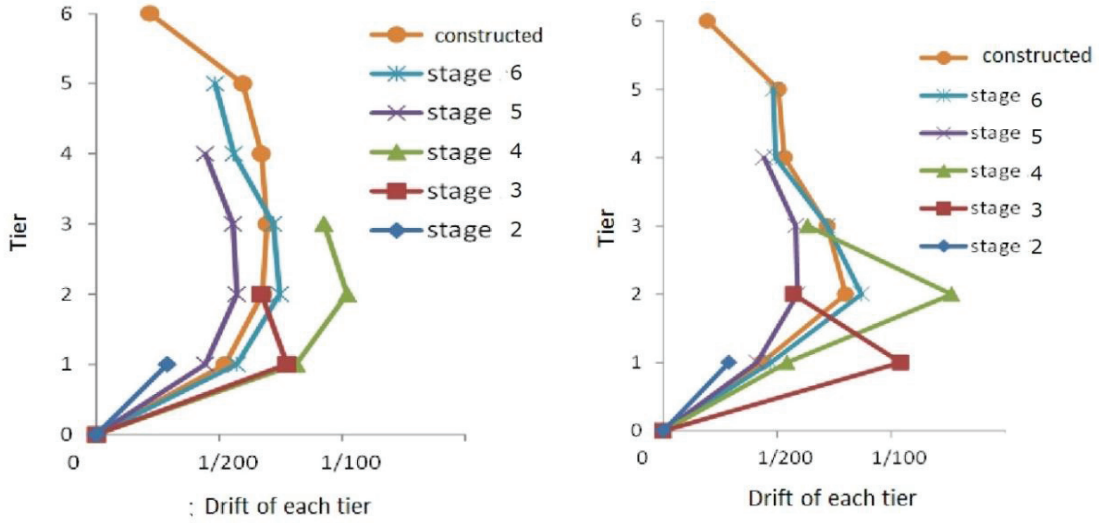

(a) Linear model (b) Nonlinear model

Fig. 2-7 Drift of each tier in the linear and nonlinear models.

Table 2-3 Maximum drift angle of each tier at Stage 4 in the elastic and inelastic models

Tier	Maximum Drift Angle (radian)	
	Elastic Building Model	Inelastic Building Model
Tower Crane	1/65	1/97
3	1/108	1/158
2	1/98	1/79
1	1/123	1/184

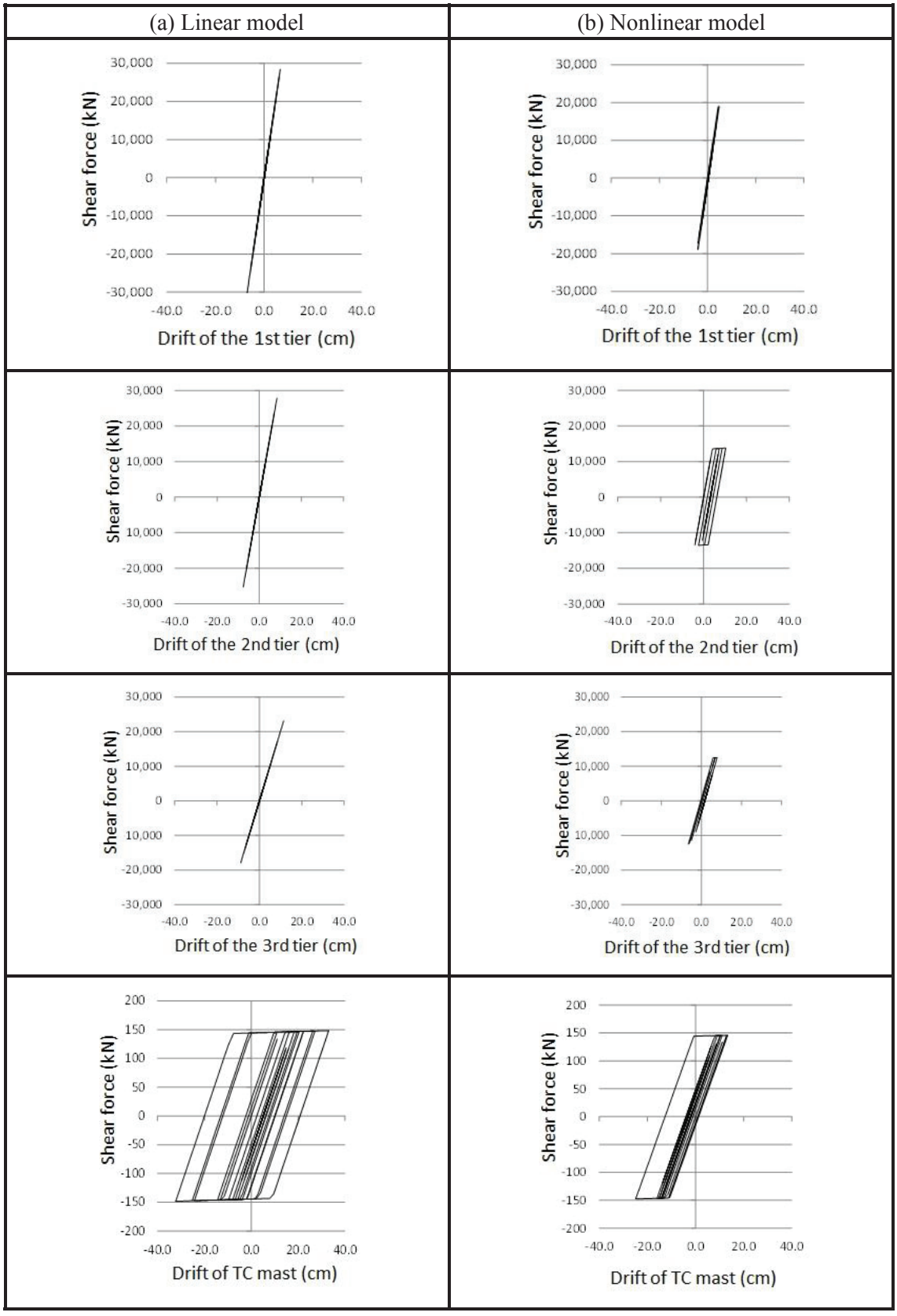

Fig. 2-8 Hysteresis loops of drift (cm) and shear force (kN) at Stage 4

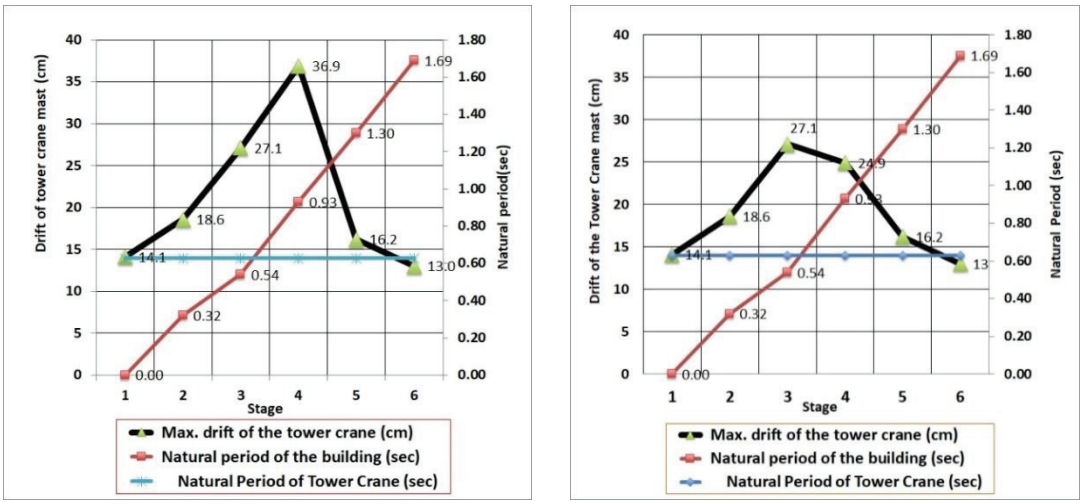

(a) Linear model (b) Nonlinear model

Fig. 2-9 Natural period of the building and response of the tower crane at each stage.

2.4 Resonance between the building and tower crane

An earthquake response analysis of the crane was performed at Stage 3, in which the natural periods of the building under construction and tower crane were closest (building: 0.54 s, crane: 0.63 s) and where the response of the crane was large, using an earthquake ground wave whose intensity was reduced to a level (v_{max} = 32.25 cm/s) from the intensity of El Centro NS, level 2 (v_{max} = 50 cm/s) so that the seismic response of the building fell within the elastic range. In addition, in Stage 4, where the difference between the natural periods was slightly larger than in Stage 3, the same analysis was performed using the same ground motion level input (v_{max} = 32.25 cm/s).

Under the two earthquake intensity levels (v_{max} = 32.25 and 50 cm/s) at Stages 3 and 4, Figures 2-10 and 2-11 (respectively) show the time response history of the seismic responses (drift) of the tower crane top. Figures 2-12 and 2-13 show the hysteresis curves of the drift and shear force of the tower crane, and Figures 2-14 (a) and (b) show the maximal drift of each building tier and the crane at Stages 3 and 4.

Figures 2-10 and 2-12 show almost no difference between the seismic responses of the tower crane under two earthquake intensity levels (v_{max} = 32.25 and 50 cm/s) at Stage 3, in which the natural periods of the building and crane are close. On the other hand, Figures 2-11 and 2-13 show some difference between the responses under the two earthquake intensity levels at Stage 4 (the natural period of the building under construction is 0.93 s, slightly different from that of the tower crane, which is 0.63 s). The tower crane's response under the more intense earthquake is obviously larger. In addition, from Figures 2-10 to 2-14, the tower crane's response at Stage 3 is much larger than that at Stage 4. Even if the earthquake intensity level is smaller, and the response of the building is larger, the response of the tower crane is larger at Stage 3 than at Stage 4.

As discussed in Section 2.3, it is again confirmed that the response at Stage 4 is affected by the resonance of the earthquake ground motion and building and the response at Stage 3 is affected by the resonance of the building and tower crane.

From these figures, in the case of an earthquake with an intensity level exceeding the building's safety limit, i.e., an extremely rare earthquake ground motion (such an earthquake has occurred once every several hundred years), the earthquake energy is absorbed by the plasticized building, and the energy transferred to the tower crane is reduced. On the other hand, for an earthquake ground motion level which causes the building to respond within the elastic range, the earthquake energy is transmitted to the tower crane through the building, with small damping, and that produces a large response caused by the resonance effects. In other words, the resonance between the building and crane can lead to serious damage to the crane, even in relatively small earthquakes. Therefore, countermeasures to suppress the resonance are necessary in addition to the seismic design of the building itself.

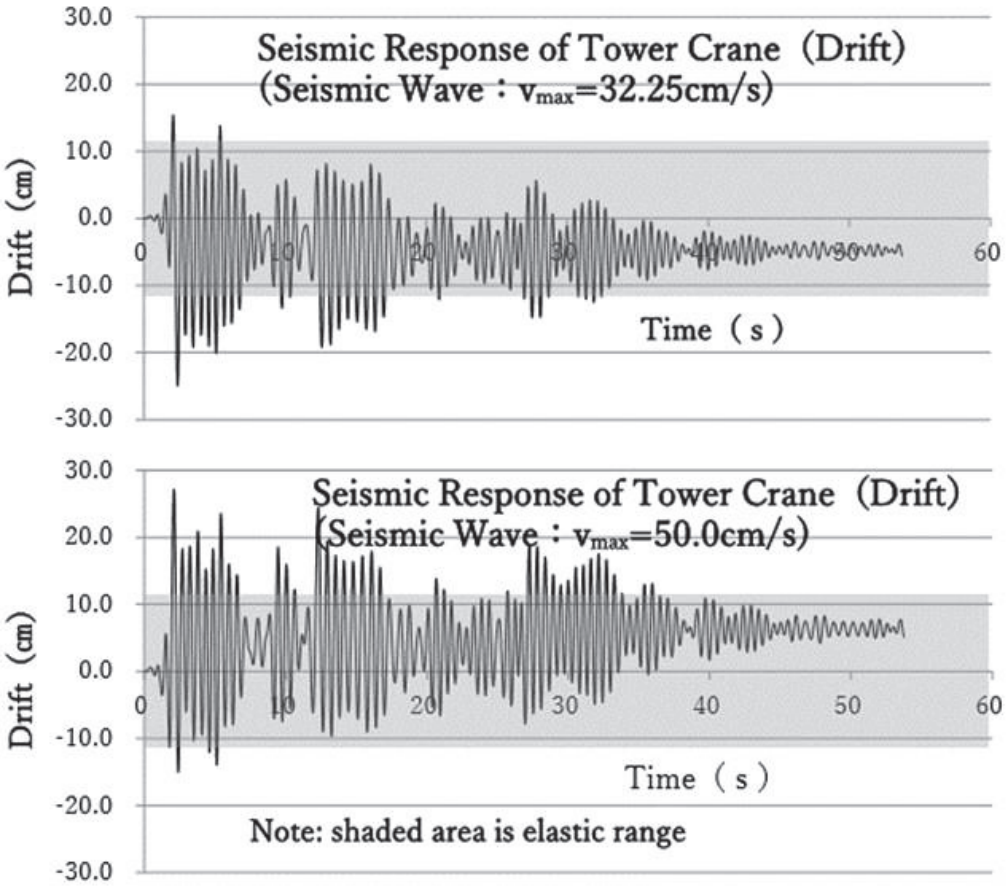

Fig. 2-10 Seismic response (drift) of the tower crane at Stage 3
(seismic wave: v_{max} = 32.25 and 50 cm/s)

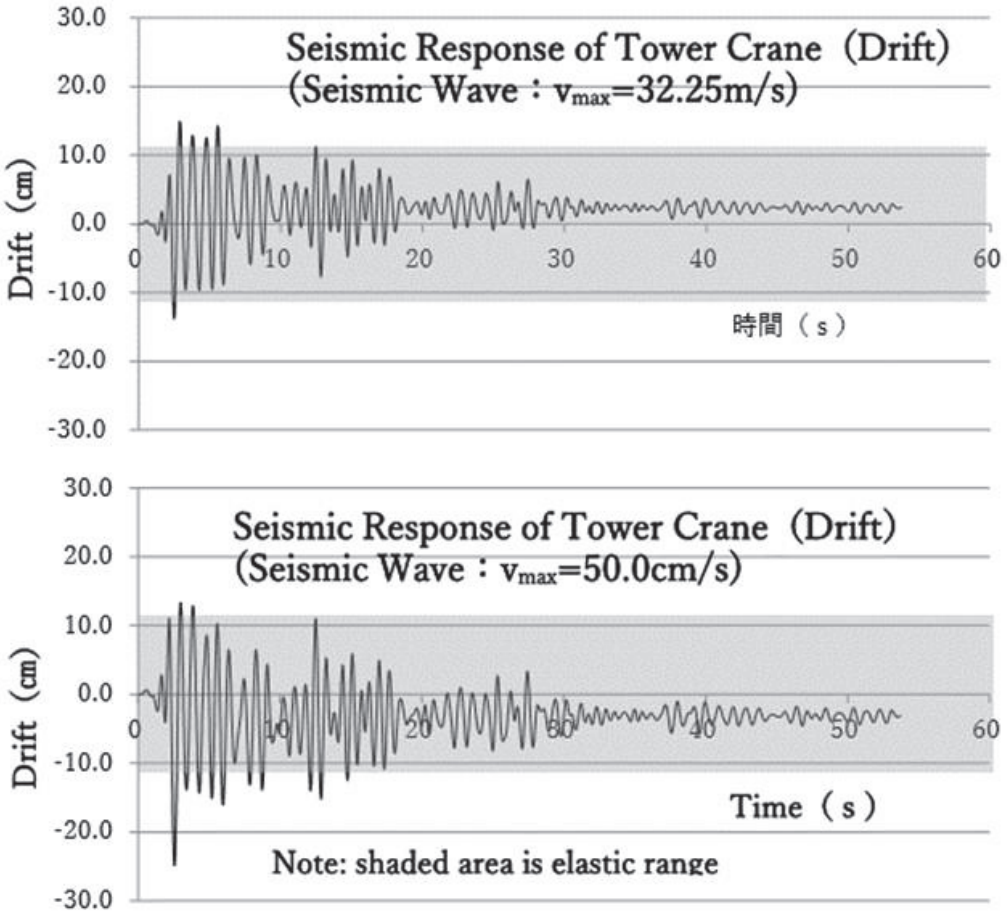

Fig. 2-11 Seismic response (drift) of tower crane at Stage 4
(seismic wave: v_{max} = 32.25 and 50 cm/s)

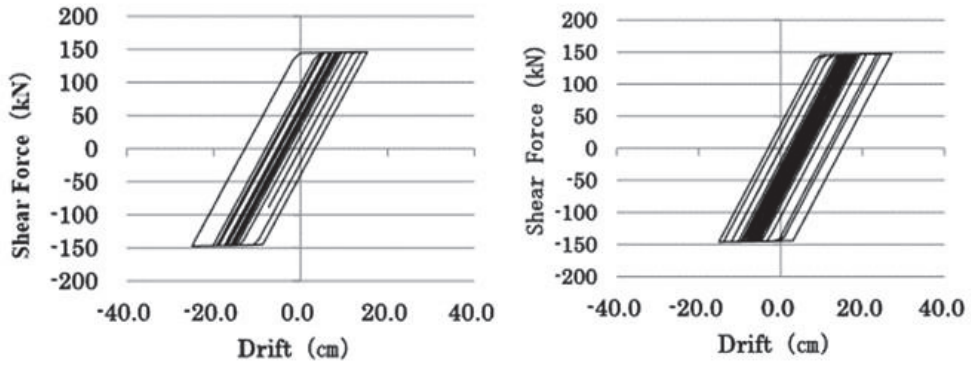

(a) Earthquake wave (v = 32.25 cm/s) (b) Earthquake wave (v = 50 cm/s)

Fig. 2-12 Hysteresis curves of drift and shear force of the tower crane under two earthquake intensity levels at Stage 3.

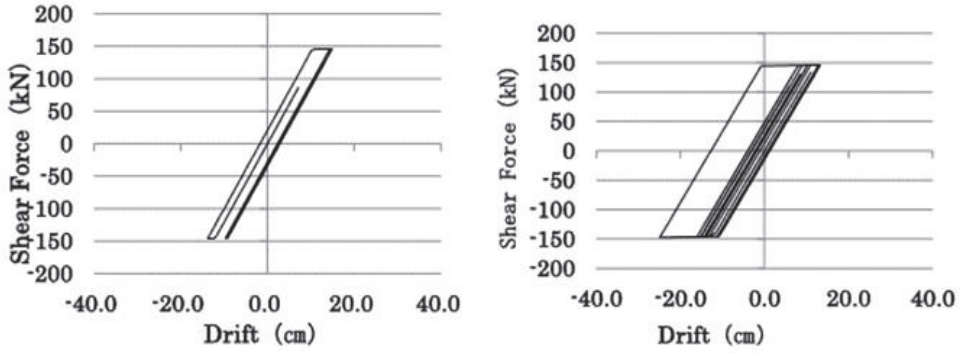

(a) Earthquake wave (v_{max} = 32.25 cm/s) (b) Earthquake wave (v_{max} = 50 cm/s)

Fig. 2-13 Hysteresis curves of drift and shear force of the tower crane under two earthquake intensity levels at Stage 4.

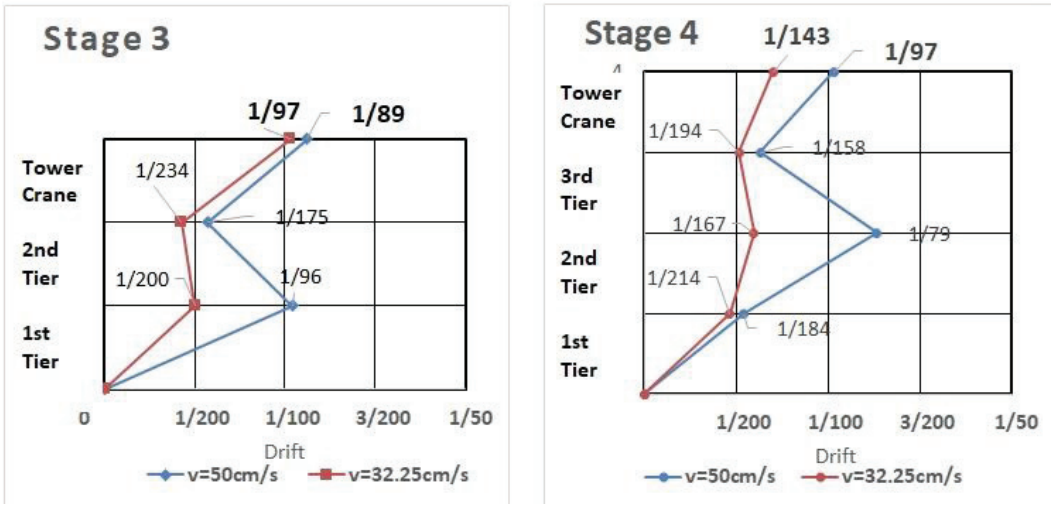

Fig. 2-14 Maximal drift of each tier of the building and the tower crane.

2.5 Countermeasures for the prevention of resonance effects

For countermeasures to prevent this resonance effect, the following two measures are studied:

(1) Changing the building structure's stiffness to adjust the building's natural period

(2) Changing the tower crane mast stiffness to adjust the crane's natural period

(1) Case study considering an increase or decrease in the building frame stiffness

As a countermeasure to the tower crane response amplification, the natural period of the building structure, to which the crane is fixed, is changed. This is done by increasing or decreasing the building frame stiffness by installing temporary bracings (H300 x 300 x 8 x 8) and applying pin joints for the girder-to-column connections. The four cases shown in Table 2-4 are considered for analysis.

Table 2-4 Modification of the structural frame during construction (Stage 3)

	Framing Floor Plan	Elevation of the Building Frame
Case 1	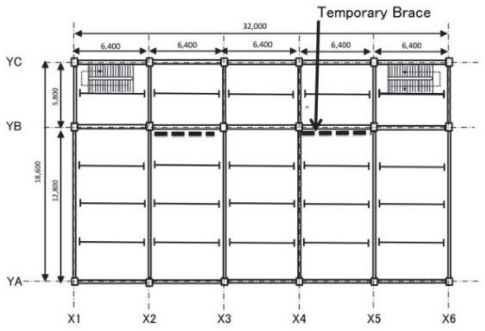	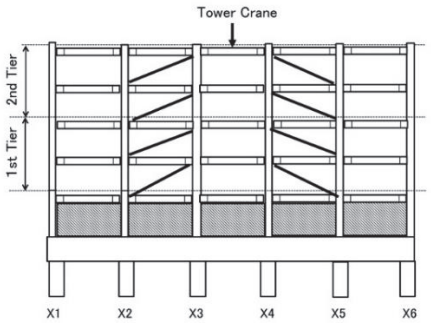
Case 2	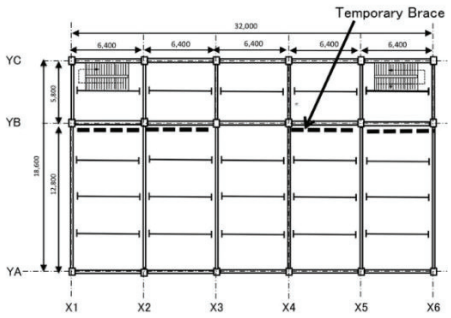	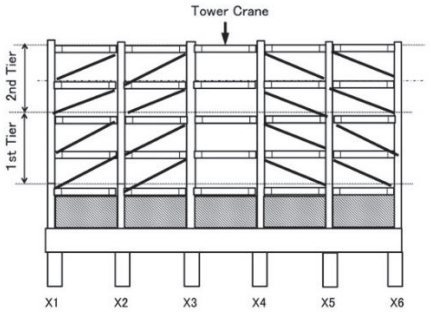
Case 3	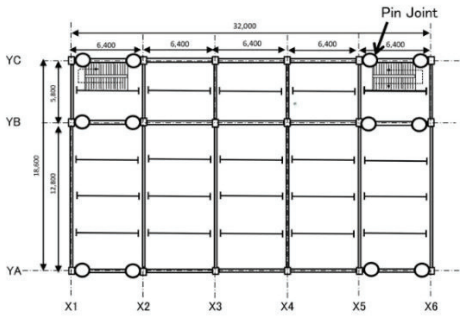	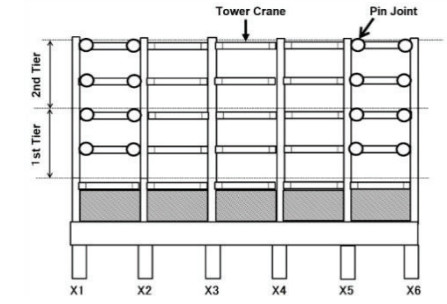
Case 4	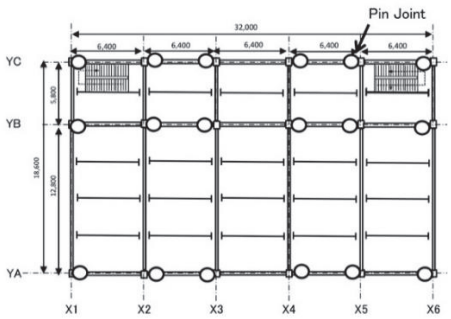	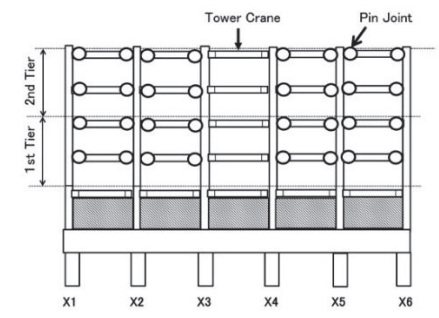

The seismic analysis results are shown in Table 2-5 and Fig. 2-15. From these results, the change in building frame stiffness, because of the temporary installation of bracings and pin joints, is effective for reducing the tower crane's seismic response amplification. However, it is also considered to be a problem since these measures may affect the construction cost and schedule. In addition, in the case of pin joints, the possibility of building failure should be carefully studied.

Table 2-5 Natural period of the building for each stage and maximal deflection of the tower crane top

	Natural period of the building in each case	Max. drift of the tower crane top (cm)	%
Original	0.54	27.1	100
Case 1	0.45	20.9	77
Case 2	0.39	18.2	67
Case 3	0.70	23.1	85
Case 4	1.04	10.8	40

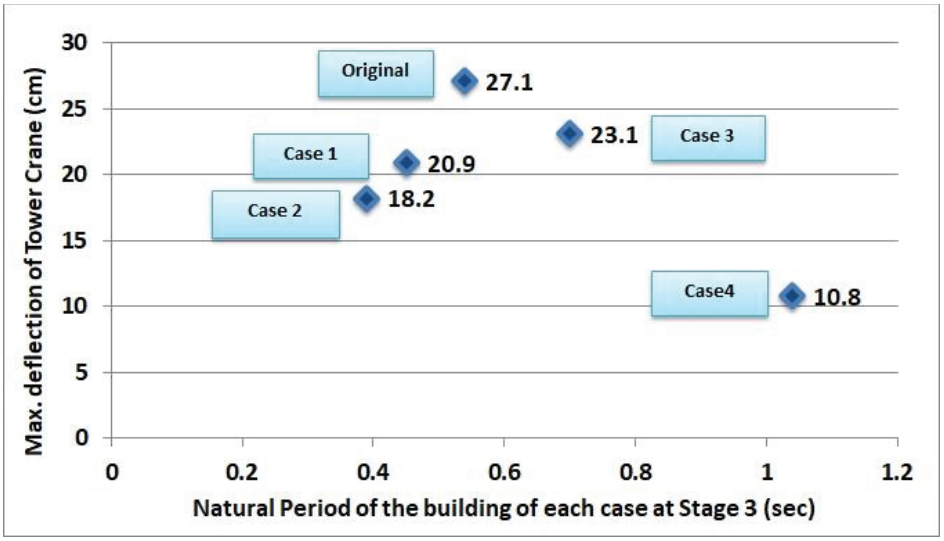

Fig. 2-15 Natural period of the building in each case and maximal drift of the tower crane top

.

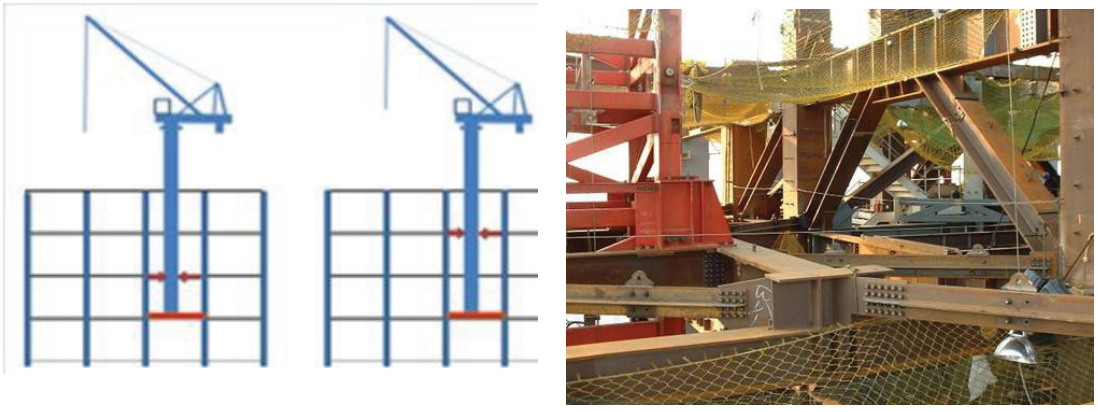

(a) Length adjustment of the extended mast (b)Temporary supporting frame for the tower crane

Fig. 2-16 Tower crane temporary support structure

(2) Stiffness of the tower crane mast and the temporary supporting frame structural system

When a climbing crane's fixing system consists of a pin joint on the base and a roller joint on the mast, as shown in Fig. 2-16, the tower crane's mast length can be adjusted by changing the level of the roller joint between the mast and building by installing additional horizontal temporary supporting frames. If the extended mast length is shortened, the natural period of the tower crane is reduced, which decreases the resonance effect between the crane and building.

In addition, designing a temporary supporting frame by considering the frame stiffness and plastic deformation, e.g., by introducing damping devices, will help reduce the magnitude of the tower crane's response to the earthquake.

2.6 Conclusion

This chapter used simulation methods to describe the tower crane's response to an earthquake considering the construction progress. It also discussed the response amplification caused by resonance between the building and crane and between the building and earthquake ground motion during an earthquake. The analysis was done on a 14-story building designed according to the latest seismic design criteria. Lumped mass models of the six construction stages were prepared for seismic analysis; the building structural models were linear and nonlinear. El Centro NS (v_{max} = 50 cm/s and v_{max}=32.25 cm/s) seismic load was applied with a 3% damping ratio of the building and the tower crane structures. The seismic load (v_{max} = 50 cm/s) was large enough that some of the designed buildings' structural members should have experienced plastic deformation, and the seismic load (v_{max}=32.25 cm/s) was the level that the designed buildings' structural members were all within elastic range. The results showed seriousness of the resonance effects caused by their close natural frequencies.

Based on these results, focusing on resonance between the building and tower crane, countermeasures, such as changing the building frame and tower crane mast stiffness, were discussed and proposed to prevent such resonance effects for the safe planning of construction work in seismic-zone countries.

Chapter 3

A new design method for site-joints of the tower crane mast by non-linear FEM analysis

The contents of this chapter are based on the following reference:

Ushio, Y., Saruwatari, T. and Nagano, Y. (2019b)," A new design method for site-joints of the tower crane mast by non-linear FEM analysis" (2019), Advances in Computational Design, An International Journal, (Accepted for next publication)

Ushio, Y., Saruwatari, T., Nagano, Y. (2018), "Non-linear analysis on the end plate connections of tower crane mast structure", Research reports presented at the 2018 annual conference organized by the Kinki branch of the Architectural Institute of Japan, Structure field, 249-252

3.1 Introduction

Among the themes related to earthquake countermeasures at construction sites, those for tower cranes are particularly important. An accident involving the collapse of a crane during the construction of a high-rise building has serious consequences, such as human injury or death, enormous repair costs, and significant delays in construction. However, given that a tower crane is a temporary structure, the cost and time effectiveness are often emphasized over safety.

The mast structure is critical for the earthquake resistance of tower cranes. In particular, the site joints of the mast are very critical structural system. There was a typical example of an earthquake-related tower crane accident during the construction of a high-rise building, Taipei 101 Building in Taiwan, where the author was in charge of construction work at the site as the project director. In this accident, the end-plate-type tensile bolted joints of the tower crane mast collapsed. In order to prevent such an accident, attention should be paid to the structural design of tower crane mast joints. Therefore, this chapter focuses on the design of site bolt joints of tower crane masts and proposes a new simulation-based design method. Specifically, a design method/procedure with static elastoplastic FEM analysis using a supercomputer is proposed. This method is based on the current allowable stress design criteria for end-plate-type tensile bolted joints joining a tower crane mast blocks on site.

Although many papers on FEM elastoplastic analysis of end-plate type tensile bolted joints have been published in the past, their contents are to prove the validity of the proposed design formula or to study the mechanical behavior and performance of the joints, etc. On the other hand, this paper proposes a design method/procedure for site joints of tower crane masts (end-plate type tensile bolted joints) that directly use the results obtained by using a supercomputer and LS-DYNA, which is the software for FEM elastoplastic analysis. In this analysis, in order to maximize the reproducibility, based on the performance of the computer, a model comprising minimal hexahedrons elements of 2.5 mm on each side was adopted to obtain more accurate design.

The mast of a climbing-type tower crane is close to 50 m long, but it is transported in lengths of several meters owing to transport restrictions and then assembled at the site. The mast is later disassembled for reuse after the construction is completed. Therefore, such cranes are assembled with bolt or pin joints. Considering the cost of materials, fabrication, and site work, an end-plate-type tensile bolted joint is generally used for the site joints. An end-plate type tensile bolted joint has good workability at the time of assembly and disassembly for the jointing of vertical members, such as the posts of a crane mast, thus making it structurally capable of transmitting a large load efficiently. This results in a reduction in the number of bolts required and the number of holes to be drilled at the factory, as well as enabling bolt tightening work at the time of construction; these factors make the construction process economical. Furthermore, it is an advantage that the rigidity of the joint portion is also high owing to the contact force caused by the high pre-tensioned axial force introduced into the high-strength bolt.

However, the problem is that the design conditions of the joints are more severe because the outer surface of the mast needs to be flat for climbing the tower crane. Depending on the shapes of the post members of the mast, large-diameter bolted joints (greater than 30 mm), eccentric-bolted tension joints, etc., are applied for site joints (Fig. 3-1). In the case of the abovementioned Taiwan high-rises, large-diameter (45 mm diameter) high-strength bolts were used for the joints. For the post members of tower cranes in Japan, rectangular shape steel tubes are normally used for large cranes, and angle-shaped steel are used for small cranes; thus, many eccentric bolt tensile joints, such

as (b) and (c), are observed (Ushio *et al*. 2019c). The use of H-shaped steel posts (a) was adopted for the tower crane that collapsed in the Taiwan high-rise during the earthquake.

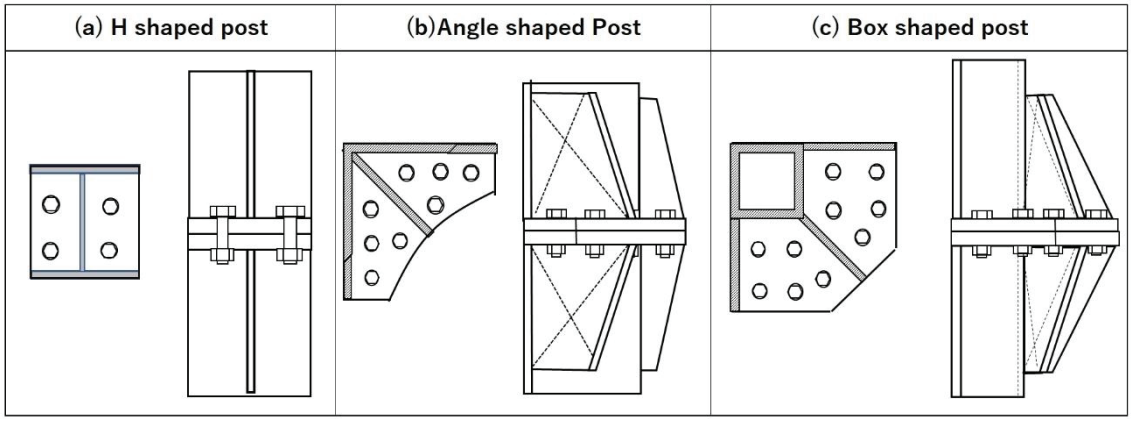

Fig. 3-1 Typical site joints of a tower crane mast

Given the easy disassembly and reuse of bolts, the pre-tension axial force on the bolts of tower crane mast joints is smaller than that on the high-strength bolts used for buildings, as specified by the AIJ recommendation (2012). Therefore, the pre-tension axial force on the bolts should also be taken into consideration in the design.

3.2 Outline of the joint design

3.2.1 Two design methods for end-plate-type tensile bolted joints

Figure 3-2 shows the design flow diagram for the end-plate-type tensile bolted joint. The blue frame and red frame represent the conventional method and the design procedure proposed in this paper respectively.

High-strength tensile bolted joints have been studied by many researchers on a design method for the T-joint (split tee types and end-plate-types) described in JSS IV 05-2004. There are still many studies on this subject such as by Yang *et al.* (2013) and by Wang *et al.* (2015). Given the complicated mechanical properties of this joint type owing to the effect of the prying action force caused by the rigidity of the end plate, arrangement of the bolts and pre-tensioned axial forces on the bolts, there are some problems with the design method. To understand these mechanical properties and devise a design formula, a method of confirmation by experiments was used. However, the use of this approach to create an accurate design formula for all types of joints would be costly and time consuming. Therefore, the details of joints are often simplified such that the design formula can be universally applied to the design of a joint. Herein, this method is referred to as the "conventional design method."

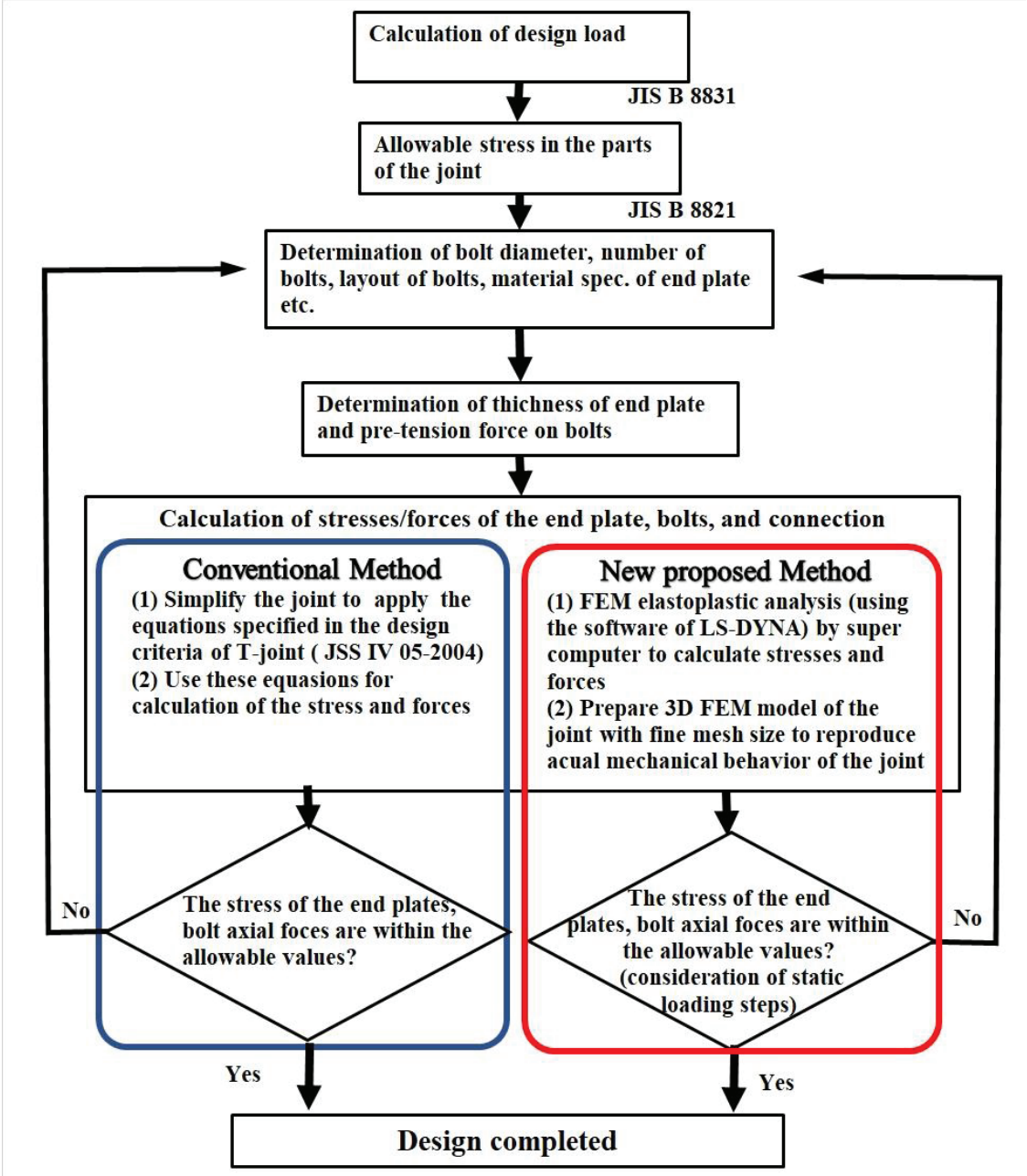

Fig. 3-2 Joint design flow and areas covered in the new design method

In contrast, with advances in analysis software and improvements in the calculation speed of supercomputers, structures can be accurately and easily reproduced along with their dynamic behavior via computer simulations. This approach would allow the accurate creation of a design for all types of joints. Furthermore, if it is applied to the site joints of a tower crane mast, it will provide us with a structural system and design method that is safe, cost efficient and workable. This forms the basis of the proposed new design method.

Table 3-1 lists the advantages and disadvantages of the abovementioned design methods.

The author uses the mast joint of a tower crane of which details and capacity are similar to those of the tower crane that collapsed in the earthquake during the construction of the Taipei 101 Building.

Table 3-1 Advantages and disadvantages of the two design methods

Item	Conventional	Proposed
(1) Applicable to all types of joints (see Figs. 1–3)		✓
(2) Accurate calculation of stresses and forces on joint parts		✓
(3) Accurate calculation of the effects of the prying action to the stresses and forces on the joint parts		✓
(4) Accurate calculation of the effects of the pre-tension force of the bolts to the stresses and forces on the joint parts		✓
(5) Calculation time and cost	✓	

3.2.2 Design load calculation

The Japanese seismic design standards for tower cranes are specified in JIS B 8821 (2013) and JIS B 8831 (2004).

Regarding earthquake loads, the standard specifies that "to apply a horizontal load that is 20 percent of its own weight, regardless of whether it is the traveling type or fixed type, but not to consider the seismic horizontal load of the weight suspended by rope, but in case that dynamic analysis of the structure against an earthquake is done, this condition need not be applied." In this standard, the seismic load is taken into consideration in load combination C (hoisting load + self-weight load + seismic load + heat load) out of load combinations A, B, and C. Considering that load combination C is the most critical for the structural design of this type of tower crane, the stresses and forces on the structural members calculated under that combination are compared with the allowable stresses.

For the calculation of the design load acting on the site joint portion of the tower crane mast, a 3D truss of the mast structure is analyzed by the application of the load of condition C, including the seismic load specified in JIS B 8831 (2004). By assuming the load combination of a tower crane of 500 tm (25 t × 20 m) capacity (similar to the one that collapsed during the earthquake in Taiwan), the forces applied to the mast members are calculated, and the maximum tensile force on the post member is found to be 2148 kN. Meanwhile, the tensile force acting on one bolt is 537 kN. Furthermore, the sizes of the mast frame members are designed based on member stresses calculated under the condition of this designed load. The calculation of the design load in load combination C is shown in Fig. 3-3.

For the design load on the joint, only a tensile load of 537kN per mast post was considered, because the shear load is small and can be resisted by the friction between the end plates.

JIS B 8831 (2004) specifies that the value of the seismic load shall be the load equivalent to 20% of the vertical static load on the crane. A tower crane is defined as being a temporary structure (short installation duration); therefore, construction costs and work efficiency constitute a greater concern. In the standard defining the earthquake resistance of a tower crane, the applied safety factor is lower than that for permanent buildings. However, considering the seriousness of the damage that could be caused by an earthquake disaster involving a tower crane, Takanashi (2007) indicated that the design

acceleration specified by the seismic design standard for cranes is insufficient for those cases in which a crane connected to a building is influenced by the seismic response of that building as well as the ground characteristics (seismic wave characteristics). In response, JCAS 1101 (2008), a seismic design guideline for cranes, was issued, and a new design seismic load and design method for overcoming these problems were proposed. Recently, the new standard ISO11031 (2016) standard on seismic design of cranes was approved by the related member countries in 2016, and the seismic design guideline in Japan such as JCAS 1101 (2008) was updated in April 2018 to reflect this ISO11031 (2016) as described by Kobayashi (2017).

However, as for earthquake-resistant design loads, the value calculated based on JIS B 8831 (2004) was adopted in this chapter because this study focuses on the design method.

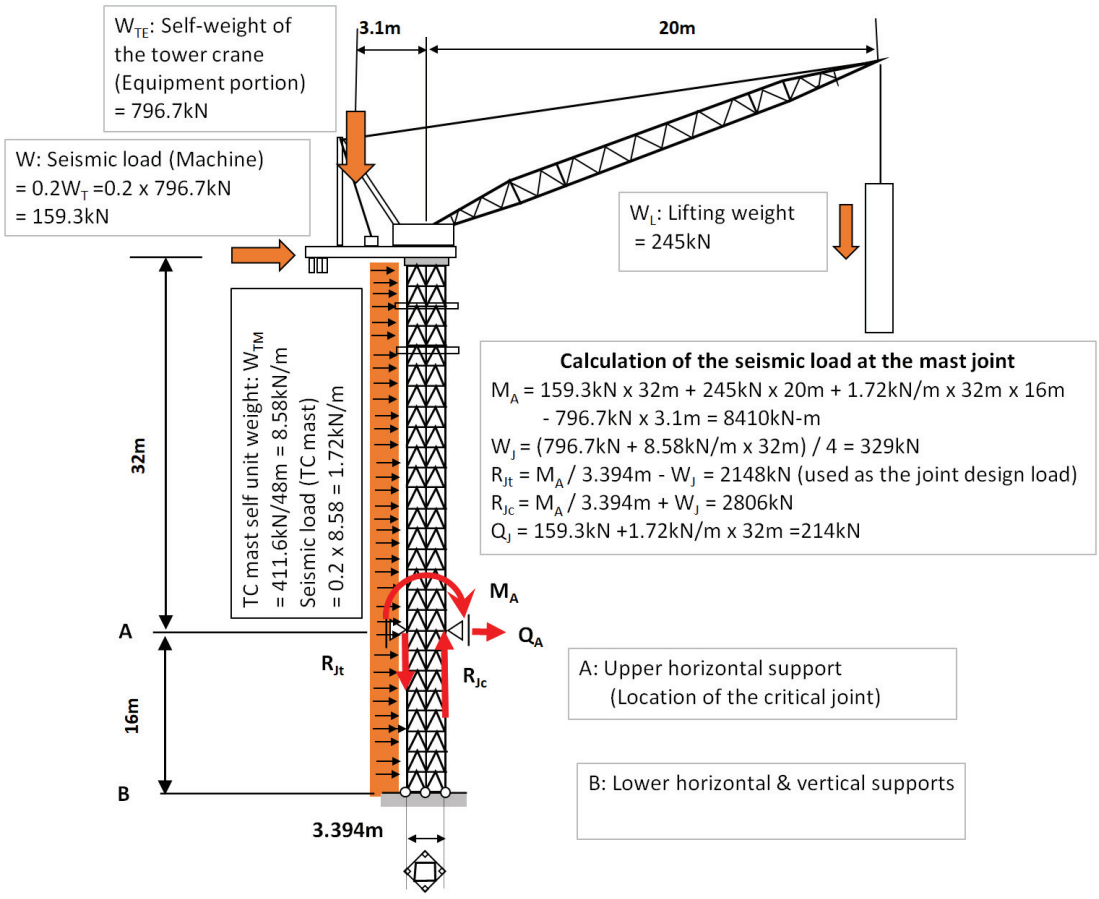

Fig. 3-3 Loading condition with seismic loading for the design of the crane structure

3.2.3 Allowable stresses in joint parts for tower crane mast design

The allowable stresses for the structural design of tower cranes are given by the safety factor method and specified in JIS B 8821 (2013): "The basic allowable stress σ_a shall be the smaller value of either the yield point (or 0.2% strain yield strength) or tensile strength

of the material divided by the strength factor given in Table 3- 2 for each load combination given in JIS B8831 (2004).”

Table 3-2 Strength factors

Load Combination	Strength Factor	
	For Yield Point	For Tensile Strength
Load combination A	1.5	1.8
Load combination B	Value for load combination A divided by 1.15	Value for load combination A divided by 1.15
Load combination C	Value for load combination A divided by 1.3	Value for load combination A divided by 1.3

- The yield point of the end plate σ_y = 340 N/mm^2 and the tensile strength σ_u = 500 N/mm^2
- The yield point of bolts σ_{By} = 900 N/mm^2 and tensile strength σ_{Bu} = 1000 N/mm^2

Therefore, the allowable stress σ_{Ba} in the bolt and the allowable stress σ_a in the end plate are determined as follows based on the JIS standard:

$$\sigma_a = \sigma_y/(1.5/1.3) = 340/1.154 = 295 \text{ N/mm}^2 \quad (1)$$

$$\sigma_{Ba} = \sigma_{Bu}/(1.8/1.3) = 1000/1.385 = 722.0 \text{ N/mm}^2 < \sigma_{By}/(1.5/1.3) = 779.9 \text{ N/mm}^2 \quad (2)$$

According to JIS B 1082 (2009), the effective cross-sectional area of the bolt is A_{se} = 1306 mm2 in the case of M45 bolts. Therefore, the allowable axial force on M45 bolts is 943 kN.

3.2.4 Determination of diameter, strength, and number of bolts in the Joint

The diameter, strength, and number of bolts are first determined temporarily so that the total tolerable bolt tensile strength of the joint is greater than the allowable tensile strength of the post member of the tower crane mast. In this case, four M45 hexagon bolts of strength class 10.9 are taken. Depending on the analysis results, this content may be changed if necessary.

The allowable tensile strength of four bolts = 4 × 1000 (Nmm^2) / 1.385 × 1306 mm^2/1,000 = 3772 kN

The allowable tensile strength of an H-shaped steel post = 340 (N/mm^2) / 1.154 × 11800 mm^2 = 3477 kN

3.3 Conventional method for the end-plate-type tensile bolted joint design

3.3.1 Application of design criteria JSS IV 05-2004

Regarding the design criteria for high-strength tensile bolted joints, given that there is no provision concerning the design method in the abovementioned JIS B8821 (2013), the design criteria for T-joints specified in JSS IV 05-2004 are determined suitable for the design of this type of joints.

To use these criteria, as shown in Fig. 3-4, this tower crane mast joint is simplified as one in which the web portion of the H-shaped steel post is ignored, and all tensile forces act only on the flanges. Consequently, the design criteria for a T-joint may be applied to the bolted tension joint of a tower crane mast post that is made of H-shaped steel. In consideration of the prying action of the joint, the bolt tensile force and end plate bending stress can be calculated.

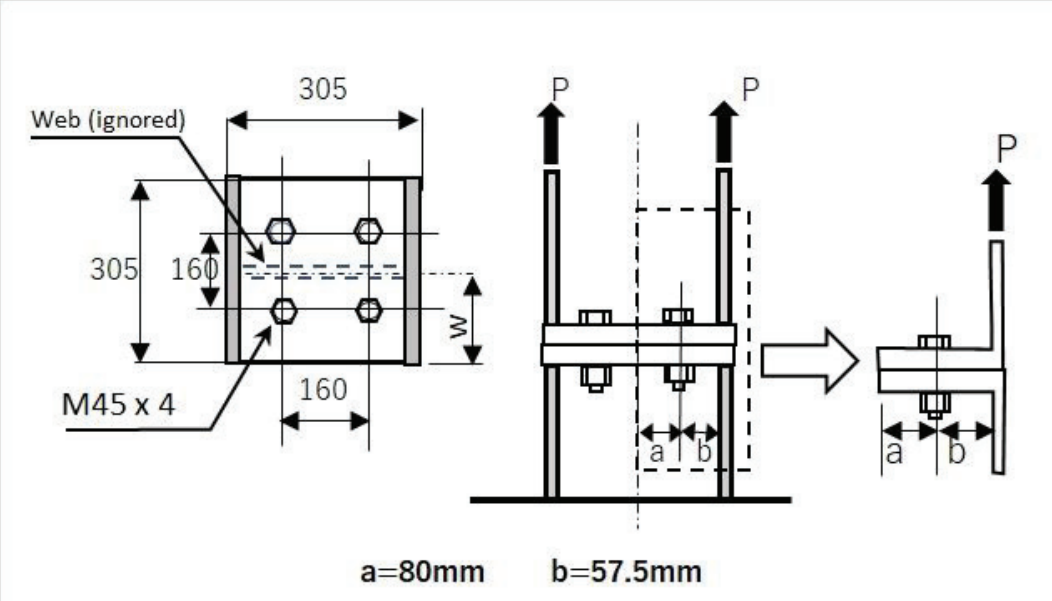

Fig. 3-4 Modeling of the joint for design

3.3.2 Design of T-joints according to the design criteria in JSS IV 05-2004

3.3.2.1 Basic concept of the design criteria in JSS IV 05-2004

According to these criteria, the design and checking of a T-joint should be performed in consideration of the fact that the joint behavior depends on its flange thickness. When a tensile force acts on a T-joint, the joint behaves differently depending on the size of the T-flange thickness, and the limit states reaching the allowable stress level are generally classified into three types (Fig. 3-5). Thereafter, the design and checking should be performed for each state.

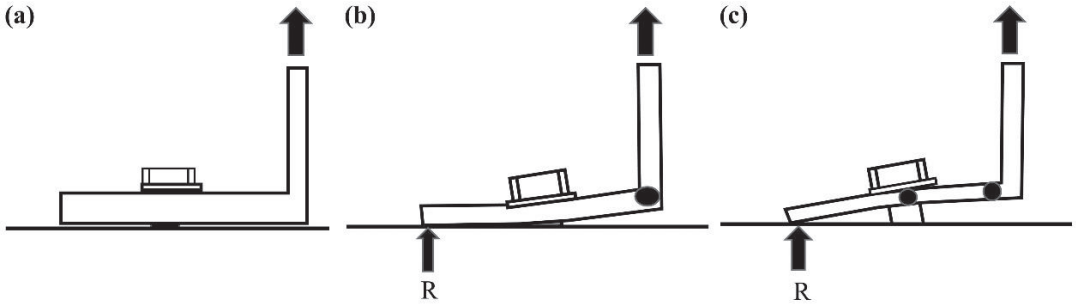

Fig. 3-5 Behavior of a T-joint depending on flange thickness (JSS IV 05-2004)

(a) The case in which a T-flange is thick, and the bolt stress reaches its allowable stress before the T-flange
(b) The case in which the T-flange thickness is between (a) and (c) and both the bolt stress and T-flange stress reach an allowable level
(c) The case in which the T-flange is thin and reaches its allowable stress before the bolt

3.3.2.2 Checking the Axial Force on the Bolts (the parameters are listed in the Appendix)

(1) When the work force P is a tensile force, the axial force B per bolt is obtained using Eq. (3) or (4):

$$B = B_0 (1 + p), \quad where \quad P < B_0 \tag{3}$$
$$B = P (1 + p), \quad where \quad P \geqq B_0 \tag{4}$$

(2) The axial force per bolt that becomes the maximum will satisfy Eq. (5):

$$\frac{B}{A_{se}} \leq \sigma_{Ba}. \tag{5}$$

In these equations, p is the prying action force coefficient, which can be obtained from the following equations:

(1) $P \geq B_0$,

$$p = \{0.7845 - 0.1278(w/120)\} - [\{-0.1991 + 0.3644(w/120)\} + \{0.0130 - 0.0076(w/120)\}t](P/B_0), \tag{6}$$

(2) $P < B_0$,

$$p = [\{1.6949 - 4.4147(w/120) + 3.1598(w/120)^2\}(t/d)^3 + \{-8.2310 + 21.1358(w/120) - 15.2549(w/120)^2\}(t/d)^2 + \{13.0538 - 33.4313(w/120) + 24.3475(w/120)^2\}(t/d) + \{-5.8936 + 16.4708(w/120) - 12.1872(w/120)^2\}](P/B_0)^3 + [\{-1.3371 + 2.5566(w/120) - 1.8194(w/120)^2\}(t/d)^3 + \{6.8885 - 12.3107(w/120) + 8.8723(w/120)^2\}(t/d)^2 + \{-12.5142 + 20.9008(w/120) - 15.1267(w/120)^2\}(t/d) + \{6.5631 - 9.2754(w/120) + 6.9223(w/120)^2\}](P/B_0)^2 + [\{0.1994 - 0.4645(w/120) +$$

$0.3351(w/120)^2\}(t/d)^3 + \{-1.0977 + 2.3260(w/120) - 1.6283(w/120)^2\}(t/d)^2 + \{1.7329 - 3.2528(w/120) + 2.3300(w/120)^2\}(t/d) + \{-0.9846 + 1.6253(w/120) - 1.1807(w/120)^2\}](P/B_0)$. (7)

The prying action force is $p = 0$ when the coefficient obtained by Eqs. (6) and (7) is negative. However, $p = 0.3333$ when the coefficient exceeds 0.3333.

3.3.2.3 T-flange stress inspection

(1) The bending stress check of the T-flange shall be performed at the center position of the bolt and the joint position with the T-web.
(2) For the calculation of the T-flange bending moment, the bolt axial force acts as a concentration force on the bolt center, whereas the prying action force can be calculated as the concentration force acting on the flange edge.
(3) The bending stress of the T-flange should satisfy Eqs. (8) and (9):

$$\sigma_{bf}=\frac{M_b}{W_b} \leq \sigma_a \quad , \tag{8}$$

$$\sigma_{wf}=\frac{M_w}{W_w} \leq \sigma_a, \tag{9}$$

a) where the working force P is greater than or equal to the pre-tension axial force on the bolt B_0:

$$\sigma_{wf} = \frac{M_w}{W_w} = \frac{6(ap-b)P}{wt^2}, \tag{10}$$

$$\sigma_{bf} = \frac{M_b}{W_b} = \frac{6apP}{w_n t^2}, \tag{11}$$

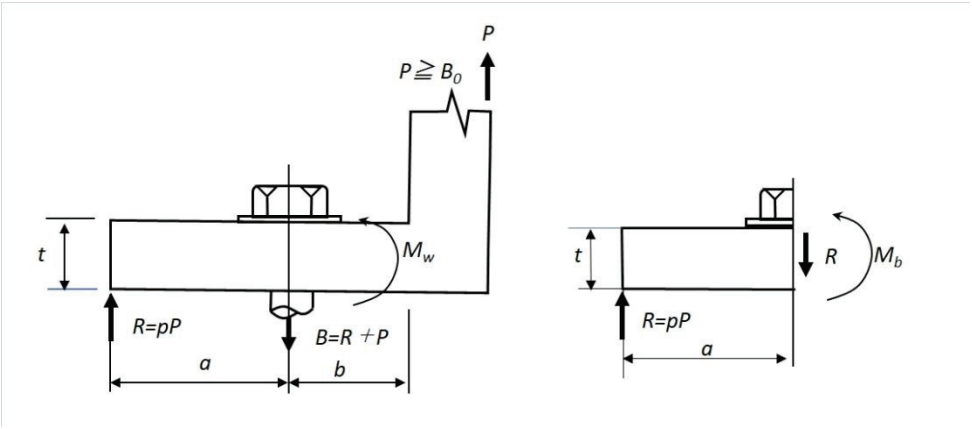

(a) Calculation of M_w (b) Calculation of M_b

Fig. 3-6 P is greater than or equal to the pre-tension axial force on the bolt B_0

b) where the working force P is less than the pre-tension axial force on the bolt B_0:

$$\sigma_{wf} = \frac{M_w}{W_w} = \frac{6\left(ap\frac{B_0}{P} - b\right)P}{wt^2}, \tag{12}$$

$$\sigma_{bf} = \frac{M_b}{W_b} = \frac{6a\{(p+0.25)\frac{B_0}{P} - 0.25\}P}{w_n t^2}. \tag{13}$$

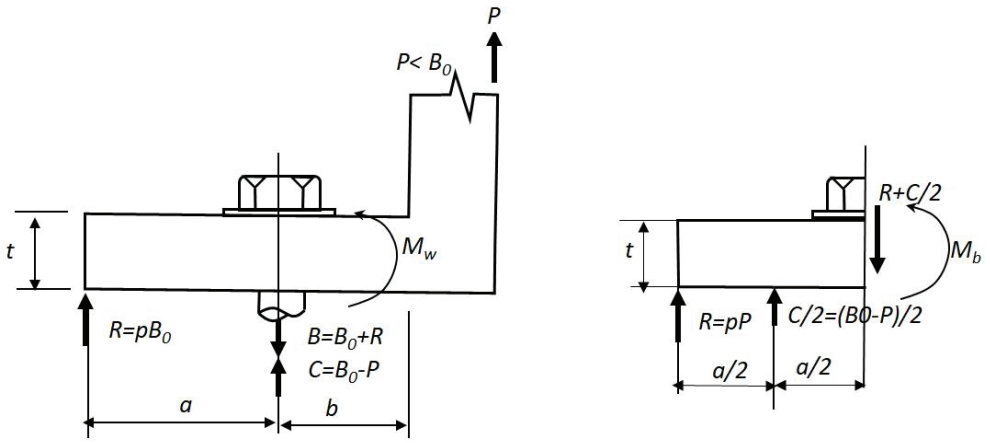

(a) Calculation of M_w (b) Calculation of M_b

Fig. 3-7 P is less than the pre-tension axial force on the bolt B_0

3.3.3 Design results for the joint

The yield strength of the end plate steel is 340 N/mm^2. By using JSS IV 05-2004, the tensile stress of the bolt against the design load and the bending stress of the end plate were calculated and compared with the allowable stresses and forces. Fig. 3-8 shows the results, which are the calculated key values for the 14 cases: the two cases of pre-tension axial force (B_0) (75% and 50% of the bolt yield axial force (B_y)) and the seven cases of end plate thickness (t), i.e., 30, 40, 50, 55, 60, 65 and 70mm, for each of the pre-tension axial forces on the bolts. The axial forces on the bolts were calculated from this prying action force coefficient (p), which was calculated from the criteria in JSS IV 05-2004.

According to the results, the thickness of the end plate should be 64 mm and more when the pre-tension axial force on the bolts is 75% of their axial yield strength and 52 mm and more when it is 50% (Fig. 3-8). The end plate is the first part to reach the allowable stress (in the corner near the flange of the post), and it can be seen that there is an enough margin for the bolt strength. This means that a bolt reaches the allowable tensile stress, σ_{Ba}, in case the end-plate thickness is 47 mm when the pre-tension axial force on the bolts is 75% of their axial yield strength, and that all bolts are within the allowable tensile stress regardless of thickness of the end plates when it is 50%. Furthermore, as the pre-tension axial force of the bolt decreases, the bolt axial force (B) corresponding to the same design load decreases.

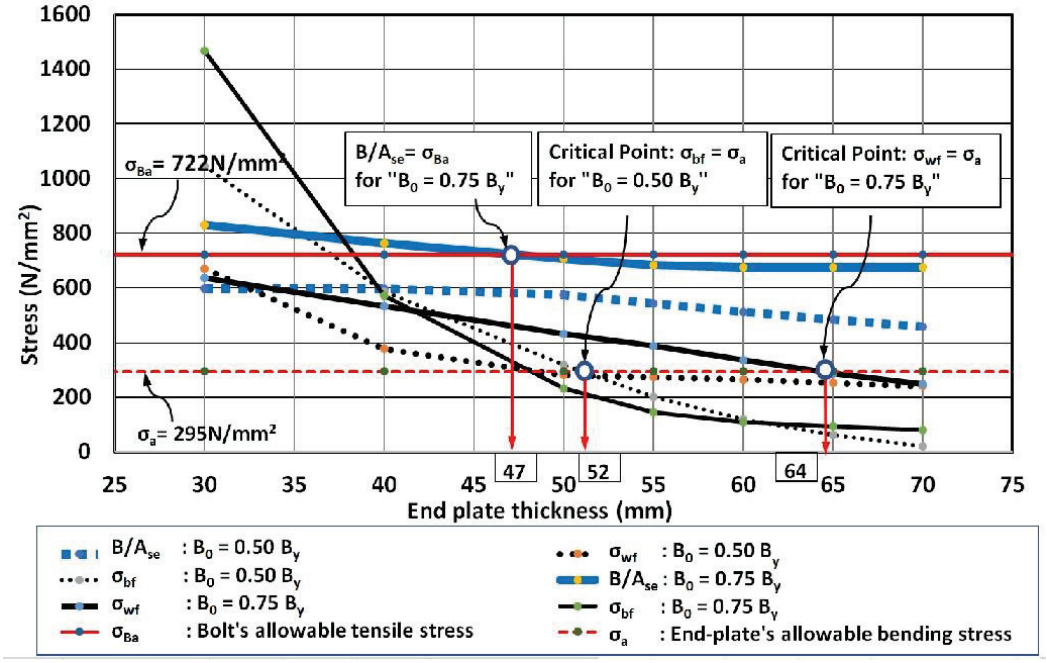

Fig. 3-8 Verification of bolt tensile stresses and end-plate bending stresses

3.4 A new design method using the elastoplastic finite element method (LS-DYNA)

3.4.1 Numerical analysis of the tensile bolted joint using LS-DYNA

Numerical calculation by the finite element method was performed to analyze the behavior of the tower crane mast joint in detail. To perform the massive parallel calculations, we used the supercomputer system of University of Hyogo.

3.4.1.1 Numerical calculation method

For the calculation, we used LS-DYNA R 9.2.0 _ Rev. 119543, which was developed by Livermore Software Technology Company (LSTC). This software employs an explicit scheme, and it can calculate large-scale problems at high speed. It is suitable for analyzing nonlinear problems, including those involving large deformations, and it is possible to stably calculate buckling and fracture phenomena. Therefore, the collapse of a structure and the ultimate proof stress can be accurately evaluated. Furthermore, given that the software can accurately analyze the contact state between parts by using its own contact algorithm, it can accurately model and evaluate the assembled structure by bolt joining. Therefore, this software should be suitable for the numerical analysis in this research. The recent good application examples of this software refer to Mizushima et al. (2018) for full-scale steel structures .

3.4.1.2 Modeling of the end-plate–type tensile bolt joint

(1) Model overview

The in-situ joint of the tower crane mast was modeled by cutting at locations 450 mm above and below the joining face. All members were modeled as solid elements for which a 2.5 mm mesh size was decided on the basis of one side, and the minimum plate thickness of 10 mm was divided into three or more parts. For the shape of the joint, H-shaped steel posts (H - 305 × 305 × 10 × 15), large-diameter M 45 hexagon bolts, and end plates with thicknesses of 30, 50, and 70 mm were prepared. The number of elements in the models was from 930,000 to 1,400,000, and the number of nodes was from 1 to 1.5 million. Figure 3-9 schematizes the model. Figure 3-10 shows an image of the mesh size.

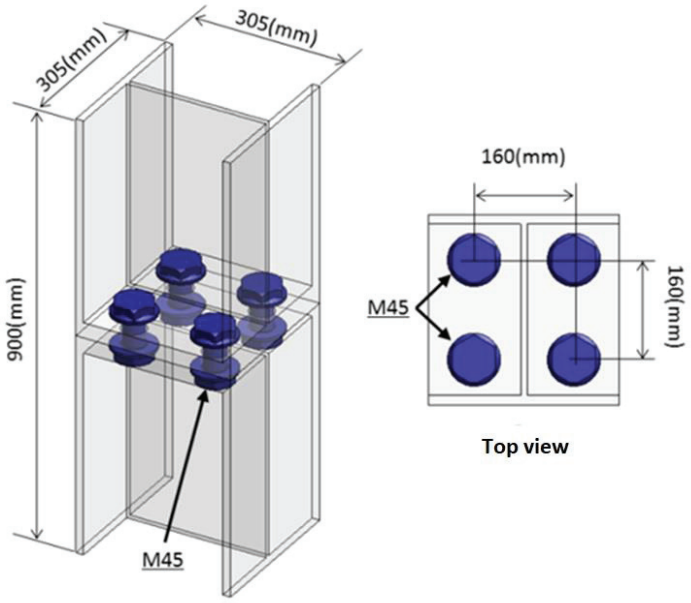

Fig. 3-9 Outline of the model

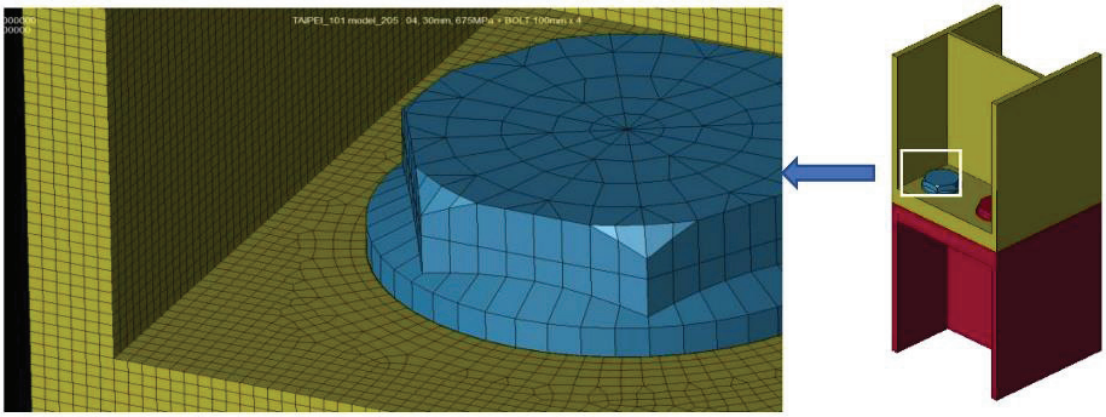

Fig. 3-10 Mesh size for modeling

(2) Material model

An elastoplastic material model (* MAT_PLASTIC_KINEMATIC) (LS-DYNA KUM

I, II) that is included in the software and considers kinematic hardening was used for the modeling of material properties. In this model, both kinematic (β = 0) and isotropic hardening (β = 1) can be obtained by setting the hardening parameter β (0 < β < 1). In this analysis, kinematic hardening (β = 0) was used (Fig. 3-11). In order to reproduce the actual behavior with high accuracy, the stress-strain characteristics of the material should be obtained by material testing of actual members. However, since this paper focuses on design procedures using simulation, appropriate assumptions were used.

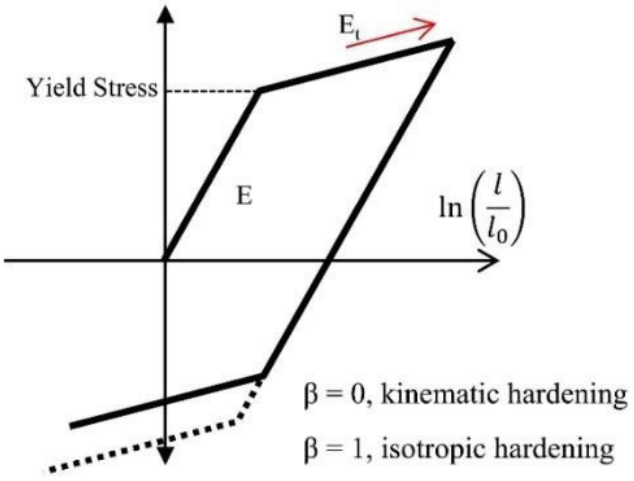

Fig. 3-11 Hardening of the elastoplastic material

It is also possible to consider the fracture behavior after yielding, which is used for modeling general metal materials, composite materials, plastics, and similar materials. Although it is also possible to consider the influence of the strain rate, no shock load was applied in this analysis; thus, it was excluded. Furthermore, the breakage of elements was not considered. Table 3-3 lists the properties of the materials used.

Table 3-3 Material properties

	Young's Modulus (E) (MPa)	Hardening (E_t) (MPa)	Density (ton/mm^3)	Poisson's Ratio	Yield Strength (MPa)
H-shape & plate	206,000	0.01E	7.89E−09	0.3	340
Bolt	210,000	0.01E	7.89E−09	0.3	900

(3) Contact condition

The bolted joint connecting members were modeled in as real a situation as possible by defining the contact conditions on the surface between the end plates welded to the upper and lower posts and between the washer and end plate. The contact conditions are controlled by the "constrained method" using the contact determination function (* CONTACT_AUTOMATIC_ SURFACE_TO_SURFACE) (LS-DYNA KUM I, II) included in the software. The friction coefficient for these contact surfaces was assumed as 0.1.

(4) Loading conditions

By completely fixing the lower end of the mast site joint, force is applied with a displacement of +5 mm at the upper end, in the tensile direction. To suppress the impact load during the time between the start and end of loading in each loading step, the slopes of the load curve at the start and end are made gentle. Figure 3-12 shows the loading condition, and Figure 3-13 shows the loading displacement curve for suppressing the impact load.

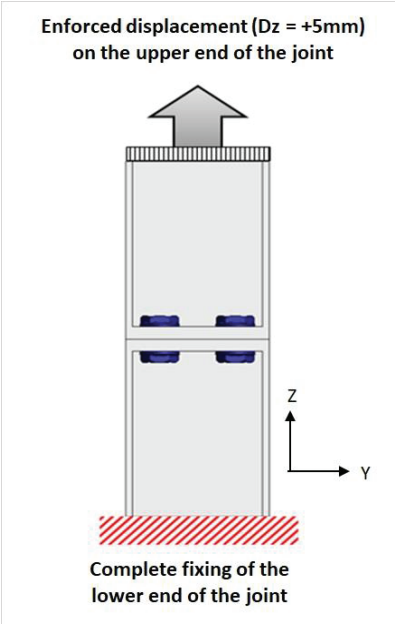

Fig. 3-12 Loading condition

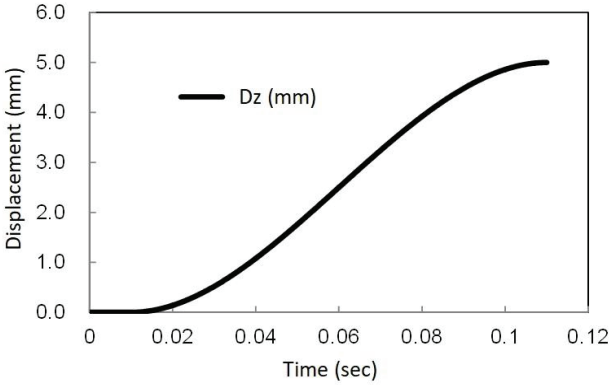

Fig. 3-13 Displacement curve to suppress the impact load

3.4.1.3 Joint types for analysis

The mast site joints of a tower crane that is generally used for steel high-rise buildings were chosen as the models for analysis. We chose to analyze the same type of tower crane that suffered from collapse during the previously mentioned earthquake. The key members of the joints are composed of H305 × 305 × 10 × 15 (σ_y = 340 N/mm^2) as the post member and M45 (Class 10.9) bolts. Furthermore, the seven analysis model cases shown in Table 3-4 were chosen using the following three items as parameters and were analyzed by LS-DYNA for each case. The allowable tension strength of each joint was then calculated according to the crane structural standard (JIS B 8821 (2013)). When selecting the joint types for analysis, the eccentric end-plate–type tensile bolted joint with six bolts, which is difficult to design with high precision using the conventional design method described in Section 4, was also added to the analysis target:

(1) Thicknesses of end plates (30, 50, and 70 mm)

(2) Number of bolts (two type of joints shown in Fig. 3-14)

(3) Pre-tension axial force on bolts (rates of bolt yield strength: 50% and 75%)

Table 3-4 Seven cases for analysis models

	1	2	3	4	5	6	7
Name	H4-3075	H4-3050	H4-5075	H4-5050	H4-7075	H4-7050	H6-5075
Thickness	30 mm	30 mm	50 mm	50 mm	70 mm	70 mm	50 mm
No. of bolts	4	4	4	4	4	4	6
Pre-tension	75%	50%	75%	50%	75%	50%	75%

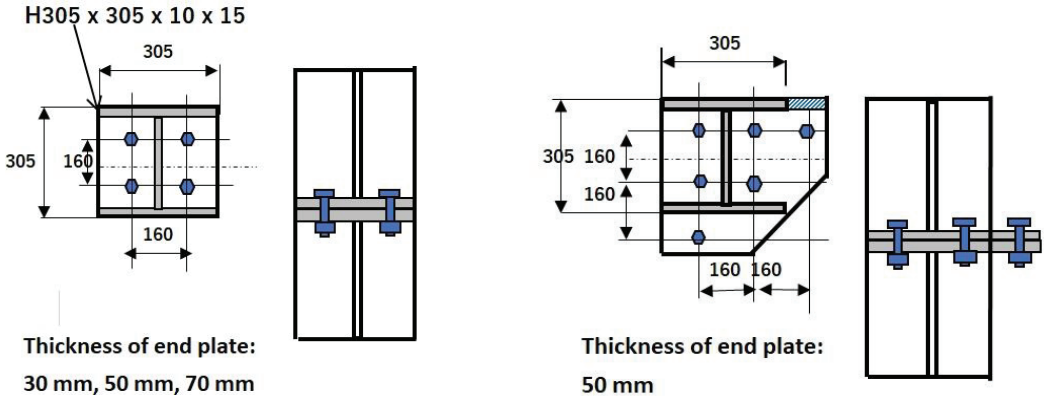

(a) Four-bolts joint
(same as the joint in the Taiwan case)

(b) Six-bolts joint
(add two bolts)

Fig. 3-14 Joint detail of the models for analysis

For example, in the case of H4-3075, the analyzed models are named as follows: sectional shape of the post (H-shaped steel), 4; number of bolts, 30; thickness of the end plate (30 mm), 75; pre-tension force on bolts (% to bolt yield strength: 75%)
Figure 3-14 shows the arrangements of bolts and stiffeners in four- and six-bolt joints.

3.4.2 Analysis results used for the joint design

As specified in JSS IV 05-2004, the bolt axial force considering the prying action force and bending stress in the end plate are verified for joint design to ensure that they are within the allowable values (JIS B 8821 (2013)).
From the analysis result data obtained by LS-DYNA, three types of numerical data listed below are extracted for each loading step. The parts of the joint are meshed as finely as possible to solid elements, and a more realistic situation is reproduced. Therefore, it should be assumed that the following numerical data can be calculated with high accuracy:

(1) Axial tensile forces on the bolts (section force)

(2) Tensile forces on the joint (tensile force acting on post)

(3) Von Mises stresses in the end plate solid elements.

Items 1 and 2 above were calculated using the functions incorporated in LS - DYNA,

but it was difficult to calculate item 3. For this item, in the case wherein the maximal value among the von Mises stresses of all solid end plate elements is compared with the allowable bending stresses of the end plates in this joint design, such an allowable stress design method is impractical because some elements may have high stress owing to stress concentrations. After examining the distribution of von Mises stresses in the end plates, it was concluded that the solid element groups with high von Mises stress values should be determined (Fig.3-16). It was also concluded that the average values of the stresses in the solid elements of each group should be calculated, and the highest of the average values should be taken as the design stress of the end plate. The elements at the corners of the H-shaped steel post and the edge of the plate, which are subject to concentrated stress, were excluded.

In this determination, the von Mises stresses in the elements at the surface of the end plate during loading steps 20, 23, 26, and 29 were observed using contour diagrams. This was performed to visualize the size of the stresses considering that the stress in a surface element of the end plate is dominated by bending in the out-of-plane direction. Figure 3-15 shows the contour diagram for analyzed model H4-5075 as an example.

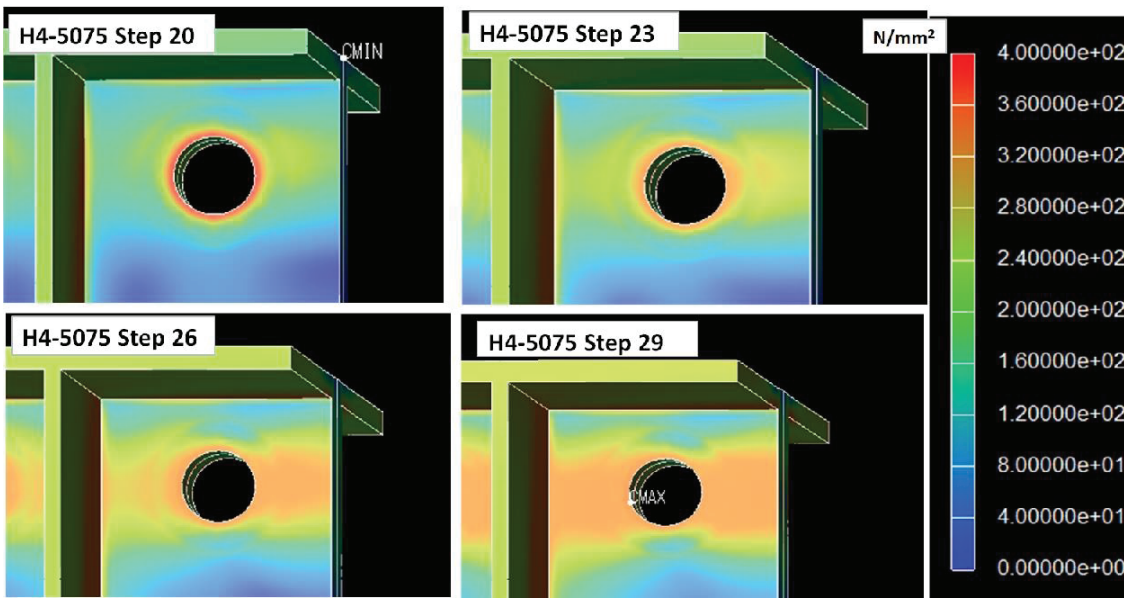

Fig. 3-15 Contour diagram of the von Mises stress in the end plates of analyzed model H4-5075

Figure 3-17 shows the transition of the von Mises stress in each element for the loading steps for the two end plate element groups marked in Fig. 3-16. Furthermore, by using the above method, the stress transition values for the end plate design of the seven analyzed models are shown in Figure 3-18. This design stress varies considerably depending on the thickness of the end plate, and there is little influence caused by the increase in the bolt pre-tension axial force and by the number of bolts.

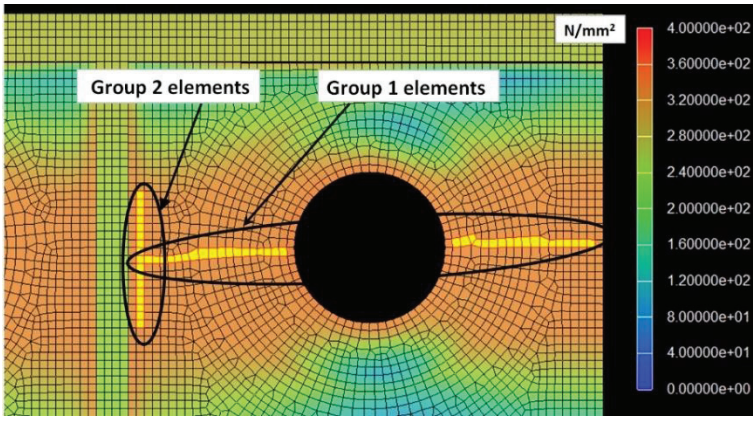

Fig. 3-16 Solid element groups with high von Mises stresses in the end plate

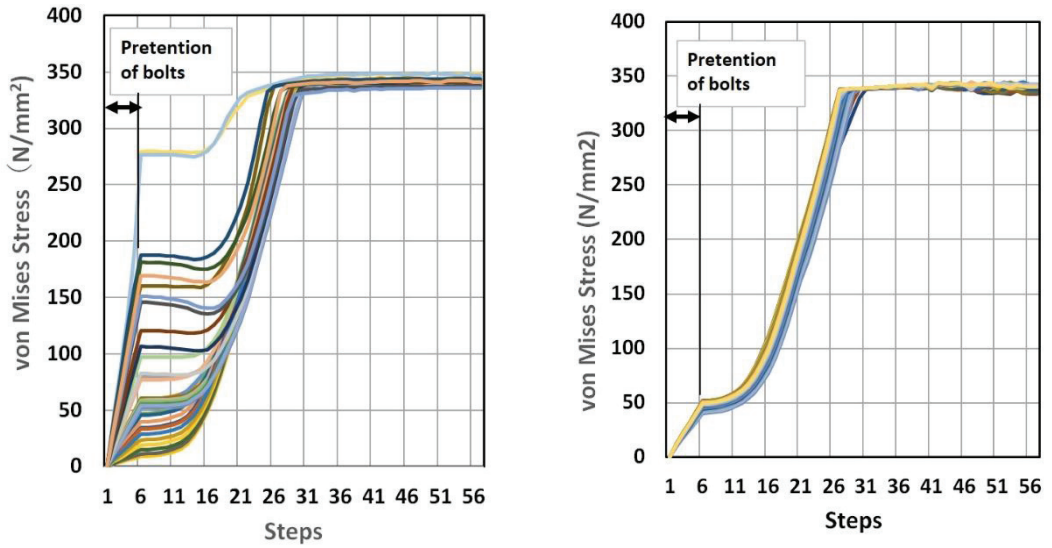

(a) von Mises Stress of Group 1 elements (b) von Mises Stress of Group 2 elements

Fig. 3-17 Von Mises stresses of groups 1 and 2 elements at each loading step

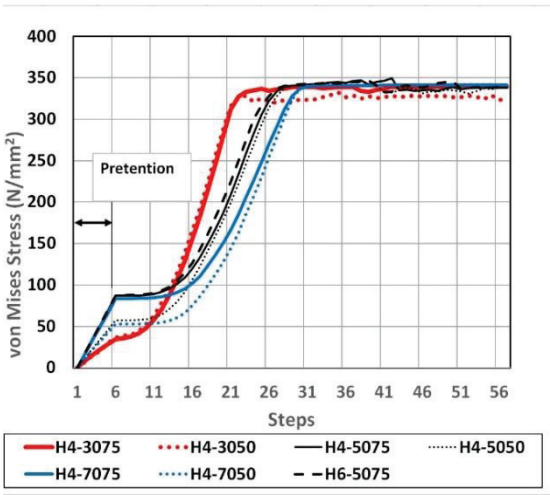

Fig. 3-18 Bending stresses of the end plates of the seven analyzed models to be used for design

3.4.3 New design pattern to obtain the allowable tensile strength of the joints

For the joints listed in Table 3-4, Figs. 3-19 to 3-22 illustrate how to obtain the design tensile strength of the end-plate–type tensile bolted joint using the analysis results calculated by LS-DYNA, according to JIS B 8821(2013).

The design procedure is specifically explained in Fig. 3-19(a). This figure shows the three transition curves of the following stresses and forces (described in Section 3.4.2) for each loading step obtained from the LS-DYNA analysis:

(1) Axial tensile forces on the bolts (section force)

(2) Tensile forces on the joint (tensile force acting on post)

(3) Von Mises stresses in the end plate solid elements

The left vertical axis of the graph represents the von Mises stress (N/mm^2), whereas the right vertical axis represents the tensile force (kN) corresponding to the values of the bolt axial forces and the tensile load on the joint for one bolt. Furthermore, the allowable bending stress (σ_a) of the end plate and the allowable tensile strength (B_a) of the bolt specified in JIS B 8821 (2013) are indicated by thin horizontal dotted and solid lines respectively. The loading steps at which the axial force of the bolt and the design von Mises stress of the end plate reach their allowance values (stipulated in JIS B 8821 (2013)) are obtained from the graphs. The steps are indicated by the point of intersection between the solid line of B_a and the transition curve of the bolt axial force (a black bold solid line), and the point of intersection between the dotted line of σ_a and the transition curve of the design von Mises stress of the end plate (a black bold dotted line).

The tensile load (a red bold solid line) at the loading step at which one of the two points first reaches the allowable values is used as the allowable tensile strength of the tensile bolted joint. Given that the graph shows the loading force for one bolt, the allowable tensile strength of the joint is calculated by multiplying the number of bolts by the value obtained from the graph. Figure 3-19(b) shows the design results when the pre-tension bolt axial force is 50 percent of the bolt yield strength.

By using this design method and the analysis results calculated by LS-DYNA, it is possible to design end-plate–type tensile bolted joints even if they have complicated shapes. Moreover, the joint design can consider the bolt pre-tension axial force.

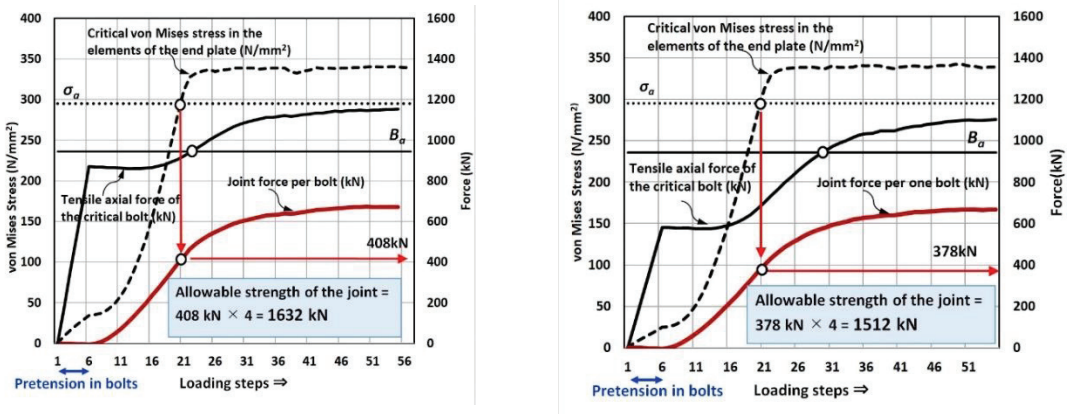

(a) H4-3075 (b) H4-3050

Fig. 3-19 Calculation of the allowable strength of joint models H4-3075 and H4-3050

For the remaining five models shown in Table 3-4, the design results obtained by this method are shown in Figs. 3-20 to 3-22. For the easy comparison of the graphs for the cases of joints with four bolts, two cases with different bolt pre-tension axial forces are shown side by side for each plate thickness.

Table 3-5 summarizes the design results, such as the allowable tensile strengths of the joint models in Table 3-4:

Using the abovementioned method with LS-DYNA, even for eccentric-tensile bolted joints in which the post members are angle shaped or rectangular tube steel, engineers can design the joints to a more accurate level according to JIS B 8821 (2013).

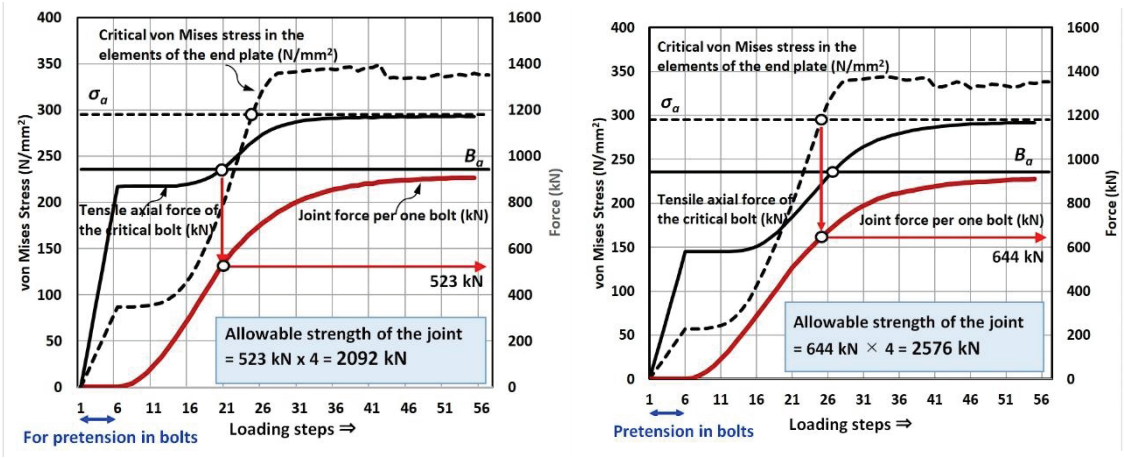

(a) H4-5075 (b) H4-5050

Fig. 3-20 Calculation of the allowable strength of joint models H4-5075 and H4-5050

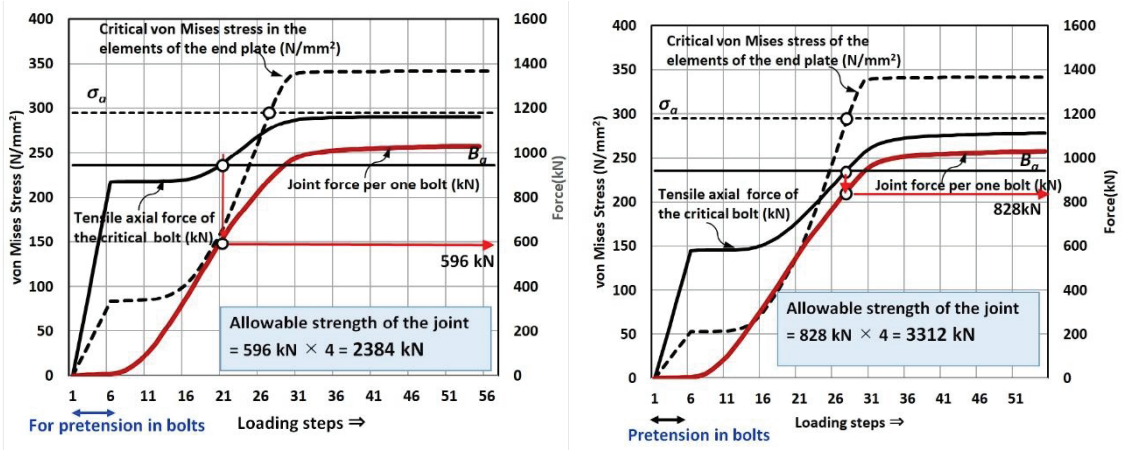

(a) H4-7075 (b) H4-7050

Fig. 3-21 Calculation of the allowable strength of joint models H4-7075 and H4-7050

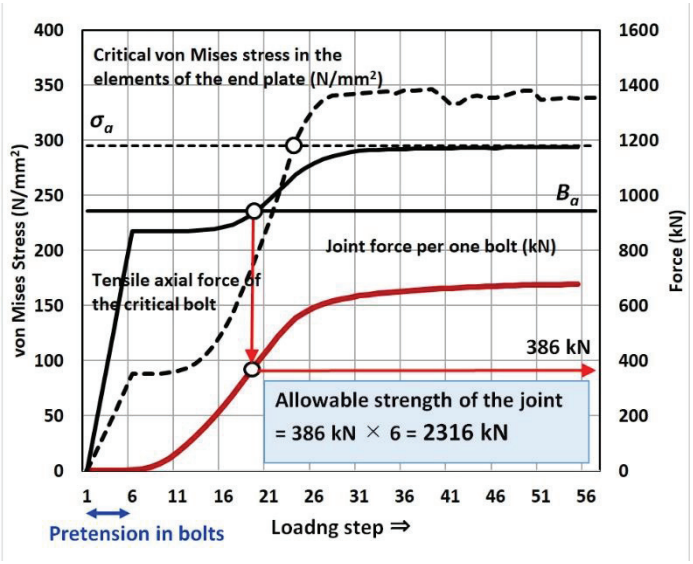

Fig. 3-22 Calculation of the allowable strength of joint model H6-5075

Table 3-5 Allowable strengths of the joint models

	Joint type	Number of bolts	EPL Thickness (mm)	Pre-tension of each bolt*1	Allowable tensile strength of the joint (kN)	Failure pattern (first part to reach its allowable stress)
H4-3075	1	4	30	75%	1632	End plate
H4-3050	1	4	30	50%	1512	End plate
H4-5075	1	4	50	75%	2092	Bolts
H4-5050	1	4	50	50%	2576	End plate
H4-7075	1	4	70	75%	2384	Bolts
H4-7050	1	4	70	50%	3312	Bolts
H6-5075	2	6	50	75%	2316	Bolts

*1: Rates to yield strength of the bolt (1170kN = 0.9kN/mm^2 x 1301mm^2)

3.5 Advantages of the new design method versus the conventional method

Based on the design results shown in Fig. 3-8 and Figs. 3-19 to 3-22, the advantages of the new design method using LS-DYNA compared with the conventional design method based on JSS IV 05-2004 are described below:

(1) Accuracy of the calculation of end plate thickness

Table 3-6 shows the thickness of the end plate calculated by both design methods. Although there is no significant difference between the obtained thicknesses of the end plates, the design result obtained using LS - DYNA is somewhat more economical (smaller plate thickness) and reliable because engineers can accurately grasp the stress situation of each part of the joint.

Table 3-6 Comparison of the design method results

Design Method	Bolt's pre-tension	No. of bolts*1	Thickness of the end plate (mm)	First part to reach Allowable Stress
Conventional method (JSS IV 05-2004)	B_0=0.75B_y	4	64	End plate
	B_0=0.50B_y	4	52	End plate
Proposed method (Elastoplastic FEM (LS-DYNA))	B_0=0.75B_y	4	55*2	Bolt
	B_0=0.50B_y	4	45	End plate (close to the bolt)

* 1 Adopted bolt: size M 45, material JIS B 1051, strength classification 10.9
* 2 Calculated by the proportional distribution from the results of the analyzed models with an end plate thickness of 70 mm (H4-7075 and H4-7050)

(2) Accurate understanding of the fracture pattern of joints

In the conventional design method based on JSS IV 05-2004, Figure 3-8 shows that for H4-5075 and H4-5050 with different pre-tension axial forces on the bolts, the end plate first reached the allowable stress, and the bolt still had a room to reach the allowable stress. On the contrary, with the new design method using LS-DYNA, as shown in Fig. 3-20 (a), the bolt first reached the allowable stress in the H4-5075 model. The reason for the difference in the fracture pattern seems to be the difference of accuracy of the results calculated by two methods. For example, the prying action force on the bolts calculated according to the JSS IV-2004 criteria is underestimated when the end plate is thicker as explained in Fig. 3-23 which shows the bolt tension force against end plate thicknesses calculated by the conventional and the proposed methods under the design load of 537kN per bolt for comparison. For end-plate-type tensile bolted joints, it is normally required for the structural design to avoid the brittle fracture that occurs in bolts. Therefore, using the new design method, engineers can accurately grasp the fracture pattern of the joint, find measures to prevent brittle fracture, and produce flexible designs.

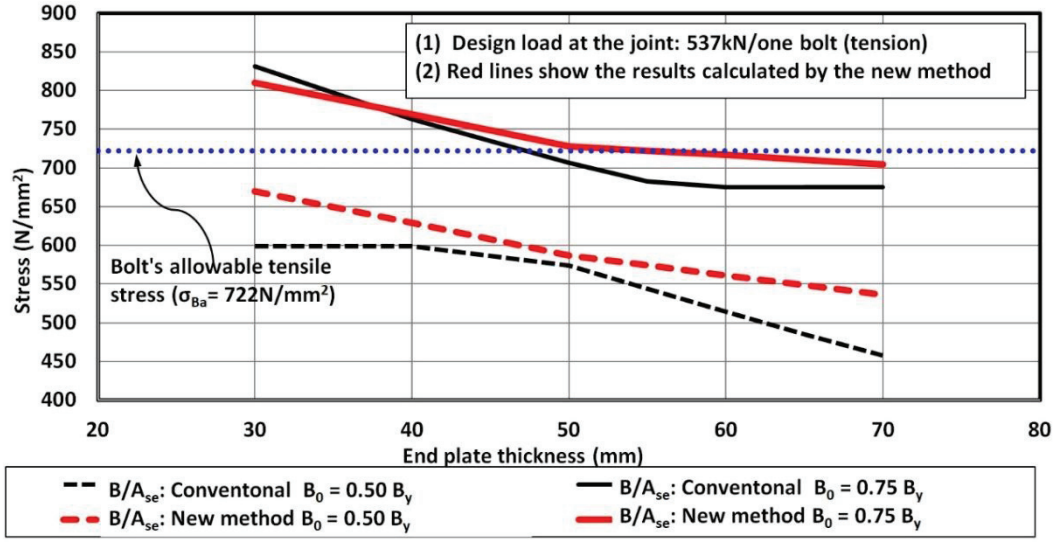

Fig. 3-23 Tension forces of bolts calculated using the conventional and new proposed methods

(3) Design considering construction conditions

The conventional design method calculates the tensile stress in the bolt and the bending stress in the end plate based on the design load and compares these stresses with the allowable values. By contrast, the new design method calculates the various stresses

and forces at the loading steps from the introduction of the pre-tension axial force on the bolt to the loading on the joint. Therefore, according to the new method, it is possible to design joints in consideration of construction conditions such as the magnitude and variation of the pre-tension axial forces to be applied to the bolts at the time of construction as well as the fabrication and construction accuracy of the joints, etc. Figures 3-20 and 3-21 show that when the thickness of the end plate is thicker (50 and 70 mm), the allowable tensile strength of the joint increases by 23% at 50 mm of the thickness of the end plate and by 39% at 70 mm by lowering the pre-tension axial force on the bolt from 75% to 50% of the bolt yield strength.

(4) Application to complicated joints

Regarding the joints (Figures. 3-1(b) and (c)) for which the modeling to T-joints is difficult, the conventional design method cannot be accurately applied for the design. Even if it is applied, the designed joints will be uneconomical joints with a high safety factor. Therefore, a highly accurate design can be created using the new method. Figure 3-22 shows the design results of the joint (H6-5075) reinforced by two additional bolts; this joint is difficult to model as a T-joint. The results obtained using the new method show that any eccentricity causes each bolt in the joint to have a biased tension force such that the allowable joint force must be determined based on the bolt with the largest tension load. As such, the joint is not efficient. This problem could be solved by changing the critical bolts to the ones having larger diameter. This proposed design method can thus overcome the problems associated with such joint design.

3.6 Conclusion

A new design method that uses the static elastoplastic finite element method (LS-DYNA) has been described for an end-plate-type tensile bolted joint, which is generally applied at the site bolt joints of a tower crane mast. For the on-site joints of the tower crane mast that are assembled on site, the design must satisfy all the relevant requirements, including ease of assembly/dismantling work in the field, safe collapse pattern (avoid breakage from bolts, etc.) and strength. To this end, a minimal element FEM analysis model must be analyzed using a supercomputer and the highly reproducible analysis results must be directly used in the design. By applying this method to, for example, a complex eccentric-tension bolt joint, the engineers can realize a detailed design in consideration of many parameters such as the enlargement of diameter of the bolts in response to a larger load in the joint, proper pre-tension of bolts, optimization of the bolt layout. Such designed joints, however, require the application of sufficient quality control during construction as usual.

The design method proposed in this paper makes it possible to design the joint that achieves both workability and strength. In addition, we are confident that this new design method will help improve the earthquake resistance of tower cranes. Furthermore, this method is applicable not only to tower crane masts but also to bolted tension joints in all structures.

3.7 Parameters

P : Tensile force acting on one bolt under design load (kN)
B_0 : Pre-tension axial force of a bolt (kN)
w : Width of a T-flange per one bolt (mm) (Fig. 3-2)
w_n : Net width of a T-flange per one bolt (mm)
t : Thickness of an end plate (mm)
B : Axial force of a bolt (N)
B_y : Yield strength of a bolt (kN)
d : Nominal diameter of a bolt (mm)
A_{se} : Effective cross-sectional area of the threaded portion of a bolt (mm^2)
p : Prying action force coefficient
σ_{Bu} : Ultimate tensile strength of bolts (N/mm^2)
σ_{Ba} : Allowable tensile stress of bolts (N/mm^2)
$\sigma_{B\,y}$: Yield strength of bolts (N/mm^2)
σ_{bf} : Bending stress of a T-flange at a bolt location (N/mm^2)
σ_{wf} : Bending stress of a T-flange at a T-web location (N/mm^2)
σ_{vm} : von Mises stress of end plate (N/mm^2)
σ_a : Allowable bending stress of a T-flange steel material (N/mm^2)
M_b : Bending moment of a T-flange at a bolt location (N · mm)
M_w : Bending moment of a T-flange at a T-web location (N · mm)
W_b : Section modulus of a T-flange at a bolt location
W_w : Section modulus of a T-flange at a T-web location

Chapter 4

Elastoplastic FEM analysis of earthquake response for the field-bolt joints of a tower crane mast

The contents of this chapter are based on the following reference:

Ushio, Y., Saruwatari, T. and Nagano, Y.（2019a）“ Elastplastic FEM analysis of earthquake responsee for the field-bolt joints of a tower crane mast” (January 2019), *Advances in Compuational. Design, International journal,* **4** (1), 53-72

4.1. Introduction

Safety measures for tower cranes are extremely important among the seismic countermeasures at high-rise building construction sites. In particular, the collapse of a tower crane from a high position is a very serious catastrophe (Zrnic *et al.* 2011). A typical example of such an accident due to an earthquake is the case of the Taipei 101 Building, which occurred on March 31, 2002. In that accident, two tower cranes collapsed because of failure of the site joints of the tower crane mast during an earthquake. The amplification effect of the resonance of the tower crane and building and the resulting unexpected load on the joints is regarded as the cause of the collapse.

In the steel structure of a permanent building, the joints of members such as columns, beams, and bracings should be designed with a strength that is greater than that of the jointed members (AIJ Recommendation, 2012). However, for temporary structures that are premised on being dismantled, such as a tower-crane mast, the efficiency of site work is taken into consideration, and the joining portion has details that are easy to install and dismantle. However, there are cases in which such joints are not as strong as the joined members.

In chapter 3, an end plate–type bolt tensile joint (also applied to the crane of Taipei 101), which is commonly used for tower-crane masts on sites due to their excellent workability, a static nonlinear FEM analysis was carried out. Subsequently, a new tower-crane joint-design method using those analysis results was proposed (Ushio *et al.* 2019b). In order to reproduce the actual static behavior of the joint parts for this method, taking into consideration supercomputer calculation times, this analysis model was created by subdividing joint parts such as end plates, bolts, and posts into solid elements, with an average size of 2.5 mm per side.

In the case of a huge earthquake such as the Nankai Earthquake, which is expected to occur in the future, and as descrived in chapter 2, the amplification of seismic loads due to resonance with the building in which a tower crane is installed, it is expected that tower-crane masts may be destroyed by the resulting unexpected load. In that case, it is also expected that the breaking of bolts at the site joints of a tower crane mast will cause a serious disaster, like the one that occurred at the Taipei 101 Building.

Therefore, it is necessary to prevent the collapse of tower cranes by designing and taking measures on the construction site for the joints, through intensive study on the detailed ultimate mechanical behavior of tower-crane mast joints during an unexpected earthquake. As for an analysis to obtain the detailed mechanical behavior, it is conceivable to model all of the structural members of a tower-crane mast with solid elements and perform a finite element method (FEM) elastoplastic earthquake-response analysis. However, in the case of seismic-response analysis, the calculation of a large number of steps is required, and considering current computer technology, such an analysis is not realistic in terms of calculation time.

The purpose of this chapter was to create a new hybrid element model (HEM) that not only expressed the detailed behavior of the site joints of a tower-crane mast during a large earthquake but also suppressed any increase in the total model-analysis calculation time and revealed that behavior through computer simulation. The hybrid-element model was composed of three element types: beam elements, shell elements, and solid elements. In the proposal, we compare the analysis results between the HEM and beam element model

(BEM), which is composed only of the beam elements, and confirms the effectiveness of the proposed model.

4.2 Simulation model

4.2.1 Numerical calculation method

For the calculation, we used LS-DYNA R 9.2.0_Rev. 119543, which was developed by the Livermore Software Technology Corporation (LSTC). This software employs an explicit scheme, and it can calculate large-scale problems at high speed. It is suitable for analyzing nonlinear problems, including those involving large deformations, making it possible to stably calculate buckling and fracture phenomena. Therefore, it is possible to accurately evaluate the collapse of a structure and determine its ultimate proof stress. Furthermore, given that the software can accurately analyze the contact state between parts using its own contact algorithm, it can be used to accurately model and evaluate an assembled structure with bolt joining. Therefore, this software should be suitable for the numerical analysis in this research. One of the recent good examples of this software's application to the architectural engineering field refers to Mizushima *et al*., 2018.

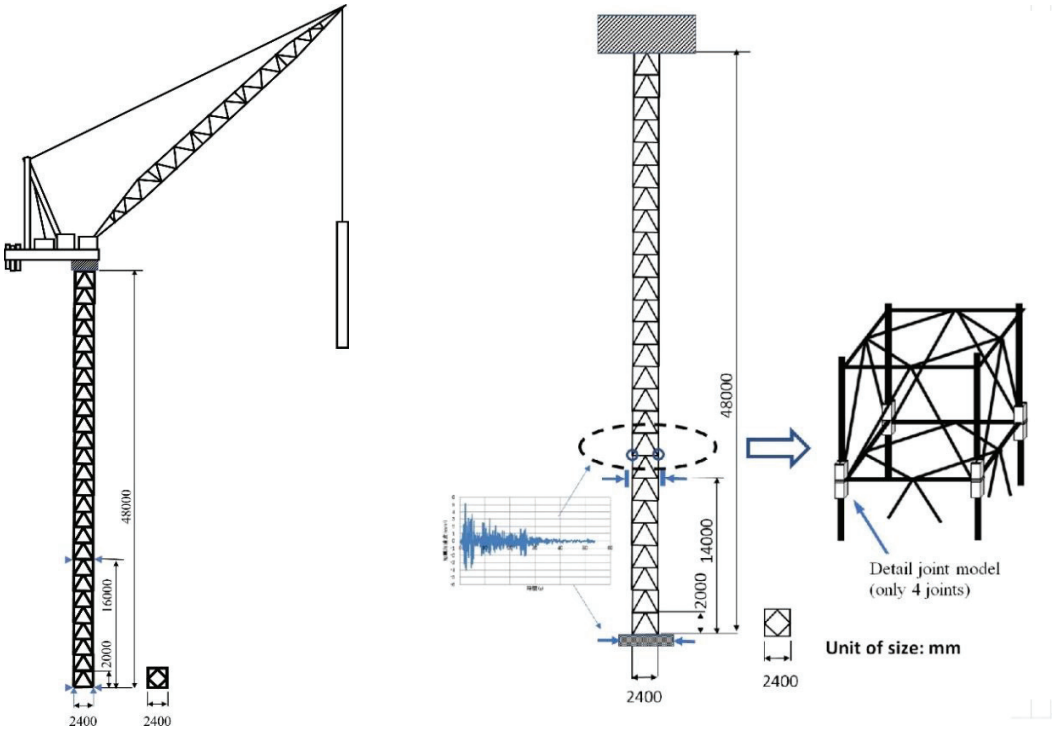

Fig. 4-1 Image of the analysis model for the FEM dynamic elastoplastic analysis of the tower crane

4.2.2 Modeling of the tower-crane mast

4.2.2.1 Outline of hybrid-element modeling

To model the tower crane for earthquake-response analysis, it was assumed that the mast was a three-dimensional truss structure and the crane-machine portion (lifting machine, counterweight, boom, sling wire, etc.) at the top of the tower crane was installed as one combined mass at the top of the mast structure. As shown in Fig. 4-1, in the HEM, detailed modeling was performed on the most critical four site joints near the position of horizontal support. Each of other site joints was assumed as a beam element composed of two end plates. When designing this modeling, the author considered the computing ability of the supercomputer of the University of Hyogo.

In the 3D truss structure of the tower crane mast, it was assumed that the entire joint system of the post members, vertical bracings, horizontal bracings, and horizontal members (beams) was joined rigidly, and the brace the horizontal members were connected eccentrically to the post members. Details of the joints of the actual tower crane are shown in Fig. 4-2.

4.2.2.2 Modeling the joint part in the HEM

Outline of modeling of the tower-crane site joint

The joint part, as shown in Fig.4-3, was the same shape as in the model, analyzed using the static elastoplastic FEM of the chapter 3, and the site-joint part of the tower-crane mast post was cut out at 450 mm above and below the joining face; the length was 900 mm. This length was determined as three times the width of the post members in consideration of the possibility of analysis when the reinforcing members of the joint part were applied. As for the shape of the joint, the post was H-shaped steel (H-305 × 305 × 10 × 15), the bolt was a large-diameter hexagon bolt M45 × 4, and the thickness of the end plate was 50 mm.

Initially, the earthquake-response analysis assumed that a joint-analysis model with the same solid-element subdividing system used in the chapter 3 was applied at the four joints and that the other members of the 3-D truss of the tower crane mast were composed of beam elements. However, after estimating the computer calculation time, it was found that it would take more than two thousand hours, which was not a reasonable amount of time. Therefore, we modeled the joint portion by introducing the new concept of the hybrid system with computer calculation time about 50 hours using the supercomputer of the University of Hyogo.

As shown in Fig. 4-4, the modeling assumed that the post part (450 mm above and below) made of H-shaped steel (H305 × 305 × 10 × 15) was the shell element model and the end plates and bolts were the solid-element models for the joint parts. The subdividing of the solid-element model was rougher than in the case of the static elastoplastic FEM analysis of the chapter 3. The element size was based on a cube with 10 mm sides. The end plates, consisting of solid elements, and the post, composed of shell elements, were rigidly joined. The numbers of elements and nodes of HEM and BEM are shown in Table 4-1.

Table 4-1 Structural system and number of elements of each part of the joint

Type of Model	Nodes	Beam elements	Shell elements	Solid elements
HEM	93,897	4,816	30,080	45,952
BEM	4,497	4,856	-	-

Contact condition

The bolted-joint connecting members were modeled in as real a situation as possible by defining the contact conditions at the surface between the end plates welded to the upper and lower posts and between the washers and end plates. The contact conditions were controlled by the "constrained method" using the contact determination function (* CONTACT_AUTOMATIC_ SURFACE_TO_SURFACE) (LS-DYNA KUM I, II) included in the software. The friction coefficient for these contact surfaces was assumed to be 0.1

Modeling of the site joint to the horizontal members and bracings

The horizontal members and vertical bracings, which were assumed to be composed of beam elements, were connected to the site joints, as shown in Fig. 4-5. The modeling of these connections was done in this analysis so that the horizontal members and the vertical bracings were eccentrically connected to the end plates and the flange/web of the H-shaped steel posts like the actual joints. Also, the edges of the beam-element model and shell-element model or solid-element model were connected using * CONSTRAINED_NODAL_RIGID_BODY" (LS-DYNA KUM I, II) with a length corresponding to the width of the horizontal member and bracing, as shown in Fig. 4-6

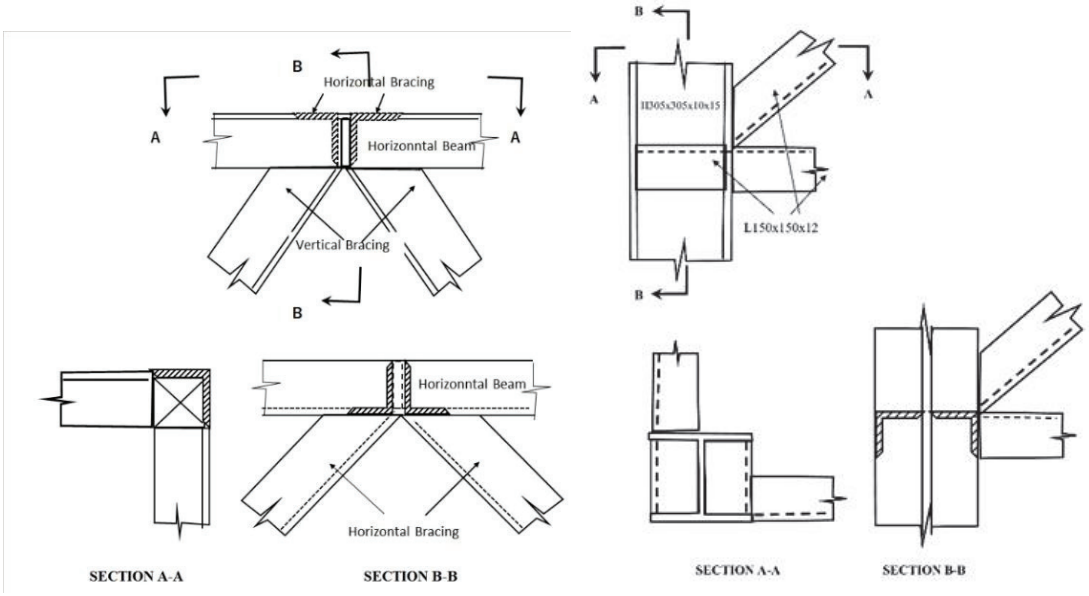

(a) Horizontal beams and bracings (b) Horizontal beams and bracings to the post

Fig. 4-2 Joint details; posts, horizontal beams, and bracings of tower crane mast members

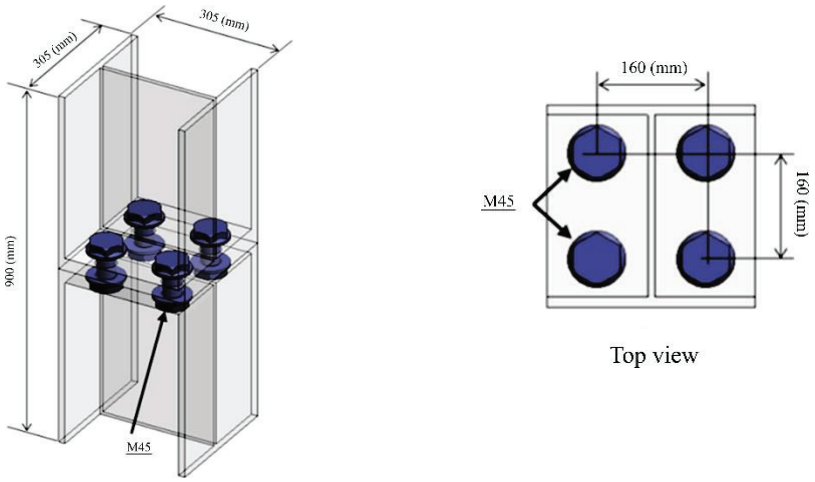

Fig. 4-3 Outline of the joint model

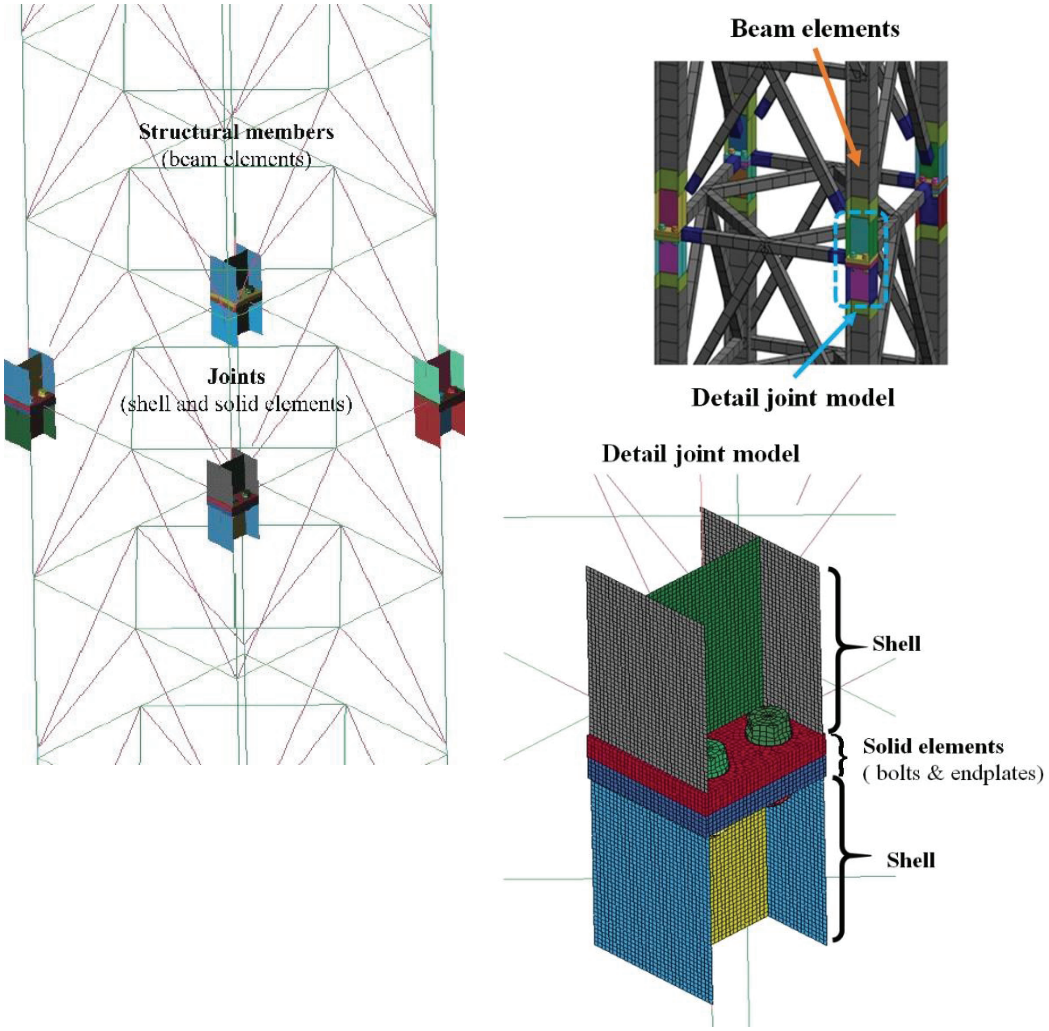

Fig. 4-4 Modeling of the tower crane mast (three-dimensional truss and site end-plate-type tensile bolted joint)

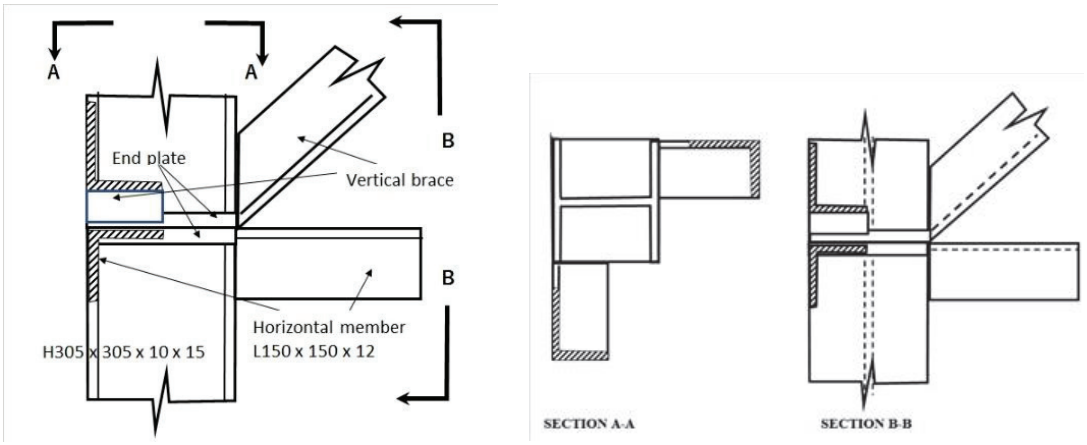

Fig. 4-5 Detail of a joint of the actual tower-crane mast

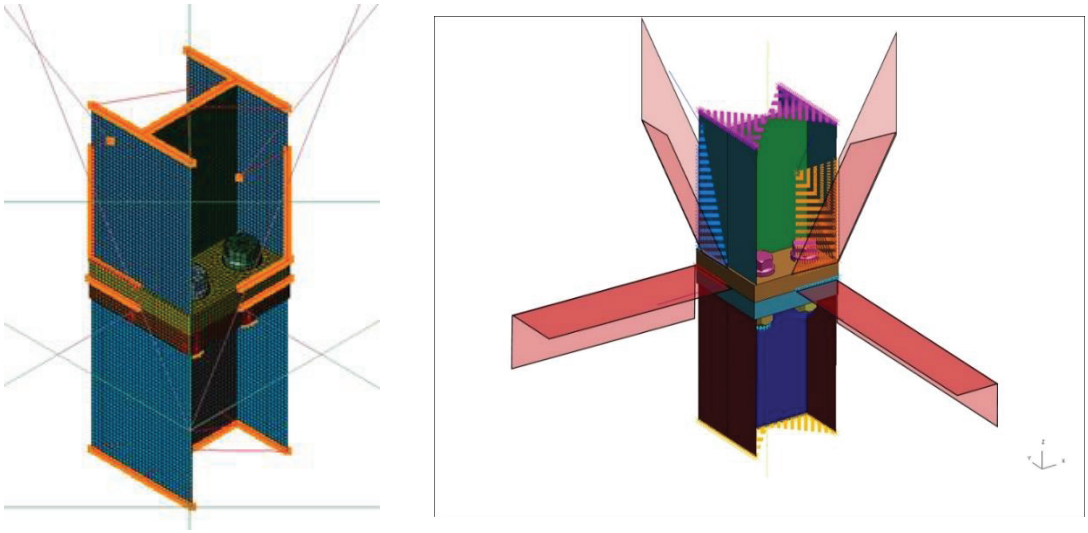

Fig. 4-6 Modeled connections between the end plate–type tensile bolted joint, horizontal members, and vertical bracings

4.2.2.3. Material model

An elastoplastic material model (* MAT_PLASTIC_KINEMATIC) (LS-DYNA KUM I, II), which is included in the software and considers kinematic hardening, was used for the modeling of material properties. In this model, it is possible to obtain both kinematic ($\beta = 0$) and isotropic hardening ($\beta = 1$) by setting the hardening parameter β ($0 < \beta < 1$). In this analysis, kinematic hardening ($\beta = 0$) was used (Fig. 4-7).

It is also possible to consider the fracture behavior after yielding, which was used for modeling the general metal materials, composite materials, plastics, and similar materials. Although it was also possible to consider the influence of the strain rate, no shock load was applied in this analysis; therefore, it was excluded. Furthermore, the breakage of elements was not considered. Table 4-2 lists the properties of the materials used.

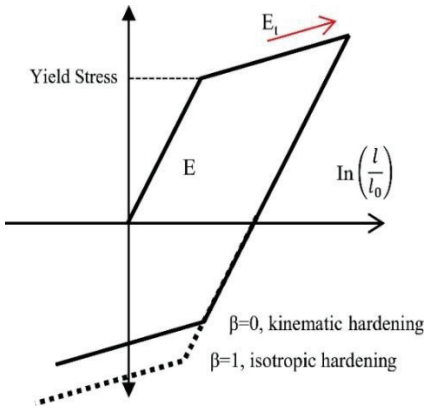

Fig. 4-7 Hardening

Table 4-2 Properties of steel materials

	Young's Modulus (MPa)	Density (ton/mm^3)	Poisson's Ratio	Yield Strength (MPa)
Post, end plates	2.06 x 10^5	7.89 x 10^9	0.3	340
Bracings beams	2.06 x 10^5	7.89 x 10^9	0.3	250
Bolts	2.10 x 10^5	7.89 x 10^9	0.3	900

4.2.3 Earthquake loading

The seismic force ELCENTORO - NS (v_{max} = 100 cm/s) was applied as the seismic loading on the bottom of the mast supporting the tower crane and at the horizontal support located 14 m above the base, as shown in Fig. 4-1. As mentioned above, considering the resonance of the building under construction and the tower crane, we used an earthquake strength twice as large as Japanese design seismic-intensity level 2 (v_{max} = 50 cm/s). The El Centro N–S seismic waves and their displacement response spectra are shown in Figures 4-8 and 4-9. The damping ratio of the mast structure is assumed as 3%. This number seems to be a little high but it was determined by referring to the section 5.2.4.3 of JCAS 1101-2018, which describes " The damping ratio of crane structures is 0.025 for welded structure, 0.04 for bolted structures and 0.03 for welded and bolted structures."

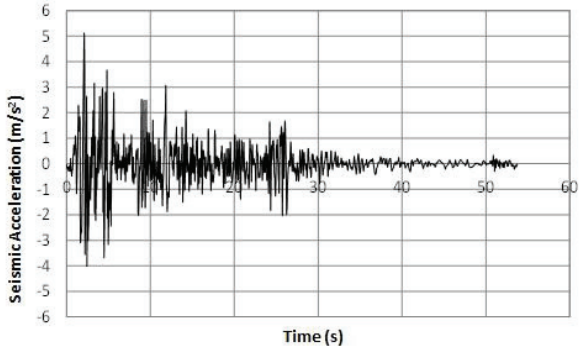

Fig. 4-8 Acceleration history of El Centro N–S waves

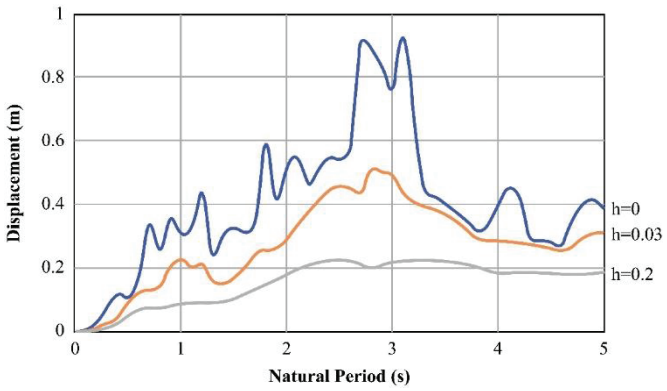

Fig. 4-9 Displacement spectra of El Centro N–S waves

4.3 Analysis results

4.3.1 Comparison of analytical results of the BEM and the HEM

4.3.1.1 Natural frequency and vibration mode of the tower crane

The natural frequencies of the BEM and HEM are shown in Table 4-3 up to the 10th-order mode, and the vibration modes are shown in Fig. 4-10. It was confirmed that there should be no problem with the various structural assumptions in the HEM creation because there was almost no difference between the natural frequencies and eigenmodes of both models.

Table 4-3 Natural frequency of each mode (Hz)

Mode	BEM	HEM	Mode	BEM	HEM
1	0.311	0.330	6	6.93	6.93
2	0.403	0.410	7	10.8	10.8
3	3.99	4.06	8	16.6	16.7
4	6.03	6.11	9	18.9	19.0
5	6.57	6.51	10	19.7	19.5

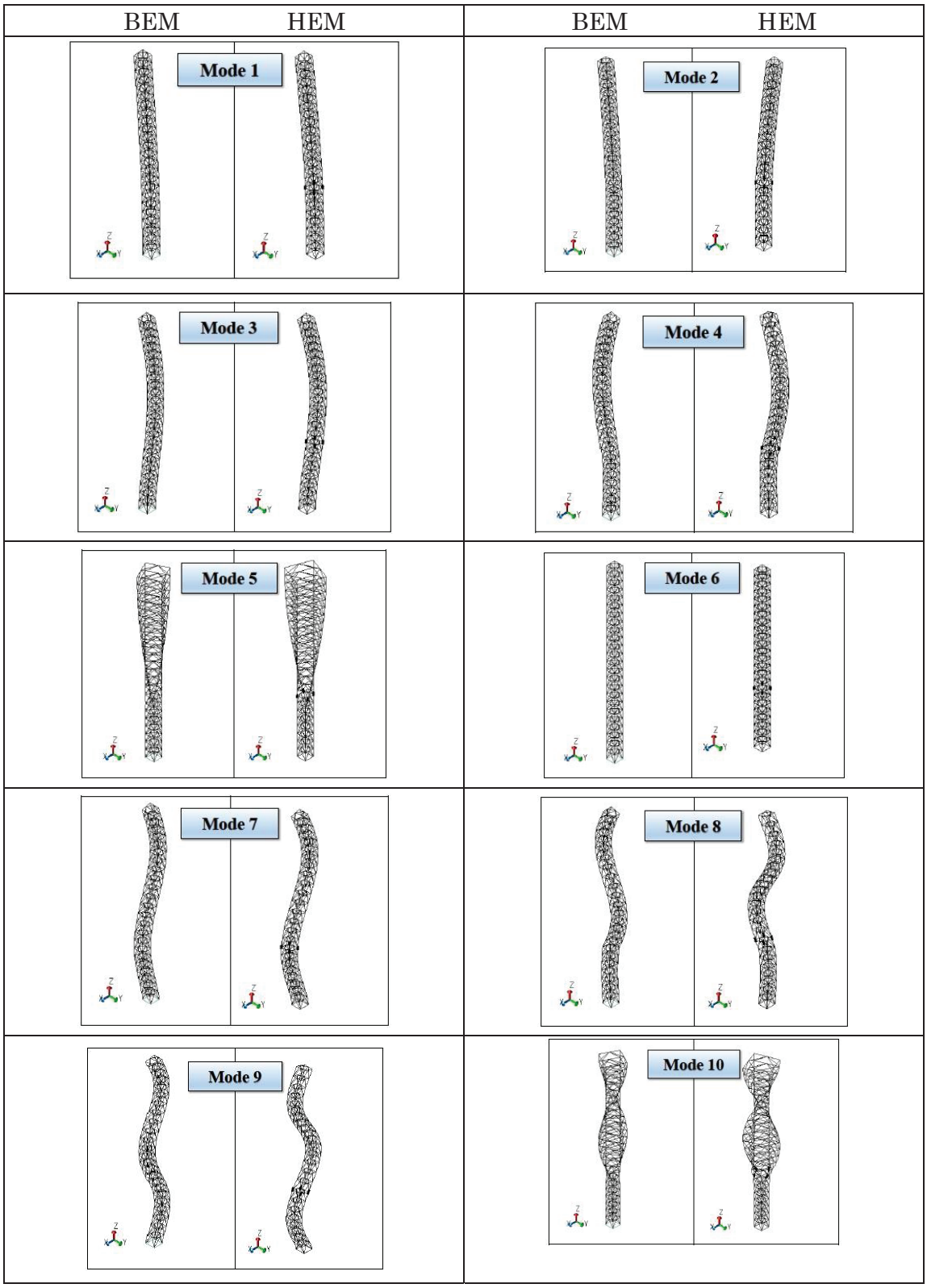

Fig. 4-10 Mode shapes of BEM and HEM

4.3.1.2 Comparison of displacement and acceleration history of the top of the tower-crane mast

Figures 4-11 and 4-12 compare the displacement history and acceleration history of the top of the tower-crane mast between the BEM and HEM. Although the influence of plasticization of the joint is somewhat observed in the HEM, the seismic response of the tower-crane mast is almost the same, and it seems that there is no problem with the structural assumption in the creation of the HEM.

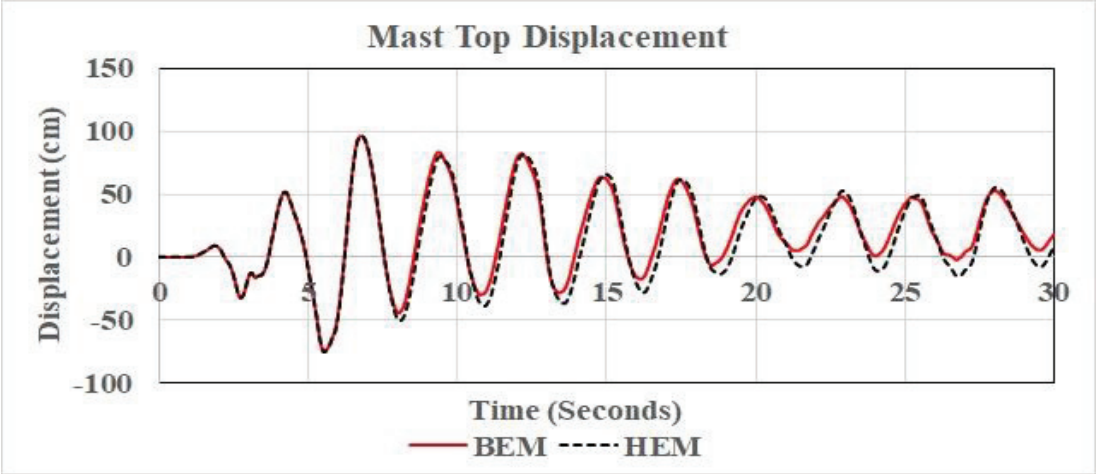

Fig. 4-11 Displacement history of the tower-crane top (BEM and HEM)

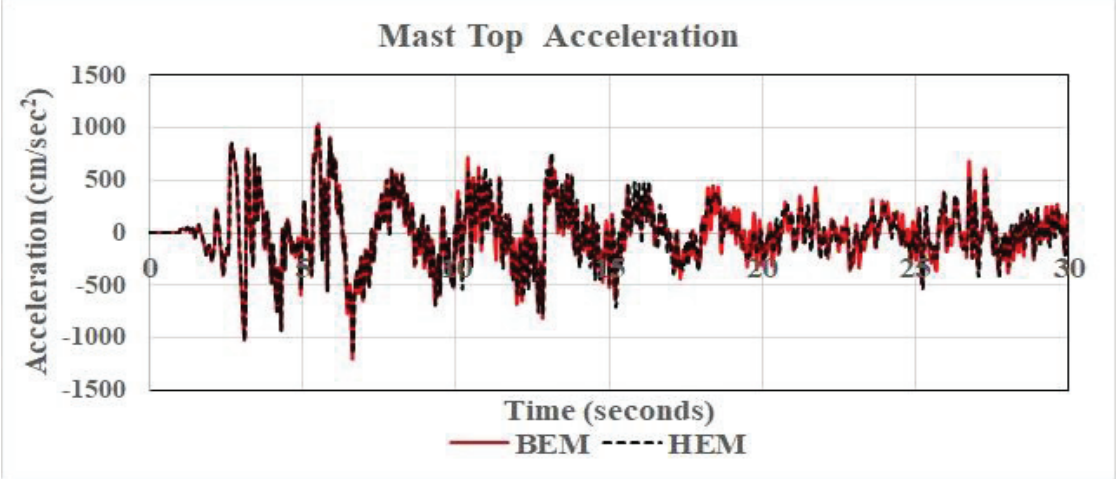

Fig. 4-12 Acceleration history of the tower-crane top (the BEM and the HEM)

4.3.1.3 Comparison of axial forces applied to a joint

The beam-elements (blue bold lines) at the location of a site joint with detailed modeling are shown in Fig. 4-13, and those of the detailed modeled joints in the HEM are shown in Fig. 4-14. The beam elements (one-dimensional of the joints) in the BEM connect rigidly to the members such as posts, beams and bracings. Figures 4-15 and 4-16 compare the axial forces applied to the joints at beam-element numbers 9129 and 9128 of the BEM and at Joints 1 and 3 of the HEM. The two joints have similar time-related

response of axial forces obtained from BEM and HEM.Given that the seismic force is loaded in the y-direction and the shape of the mast is symmetrical, Joints 1 and 2 and Joints 3 and 4 have almost the same response. Therefore, only the responses of Joints 1 and 3 are shown in the two figures.

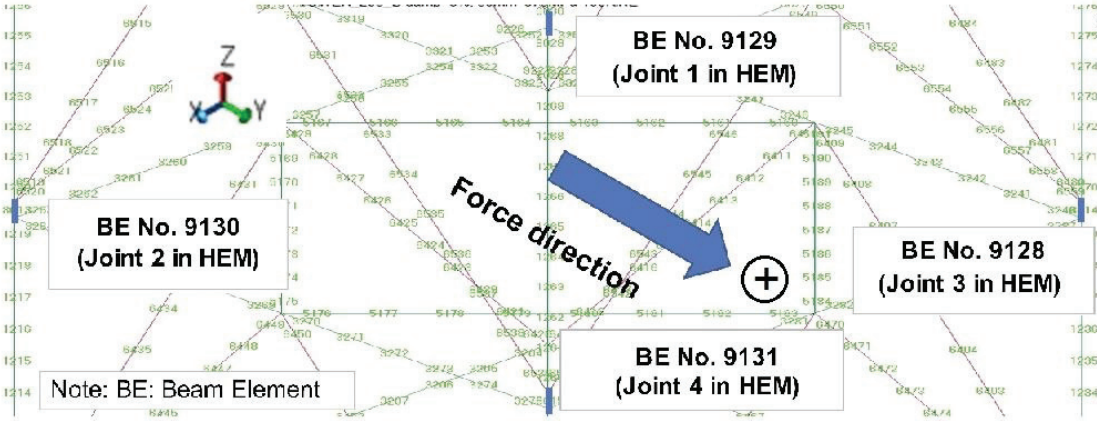

Fig. 4-13 Beam-element numbers of joints in the BEM

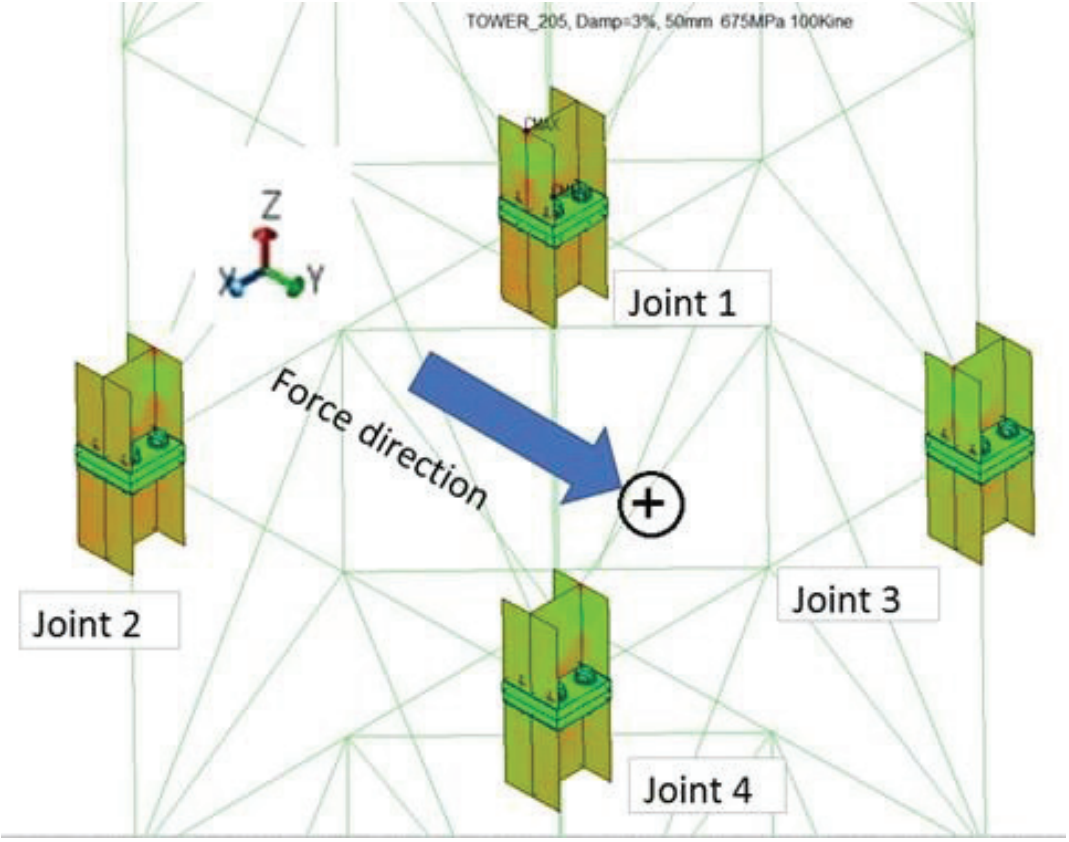

Fig. 4-14 Detailed model joint numbers in the HEM

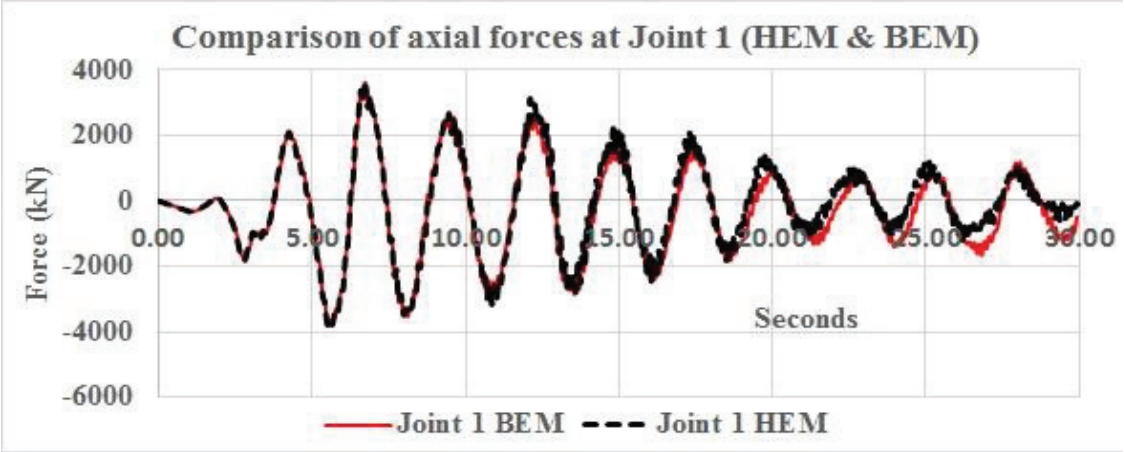

Fig. 4-15 Comparison of axial forces between HEM and BEM at Joint 1

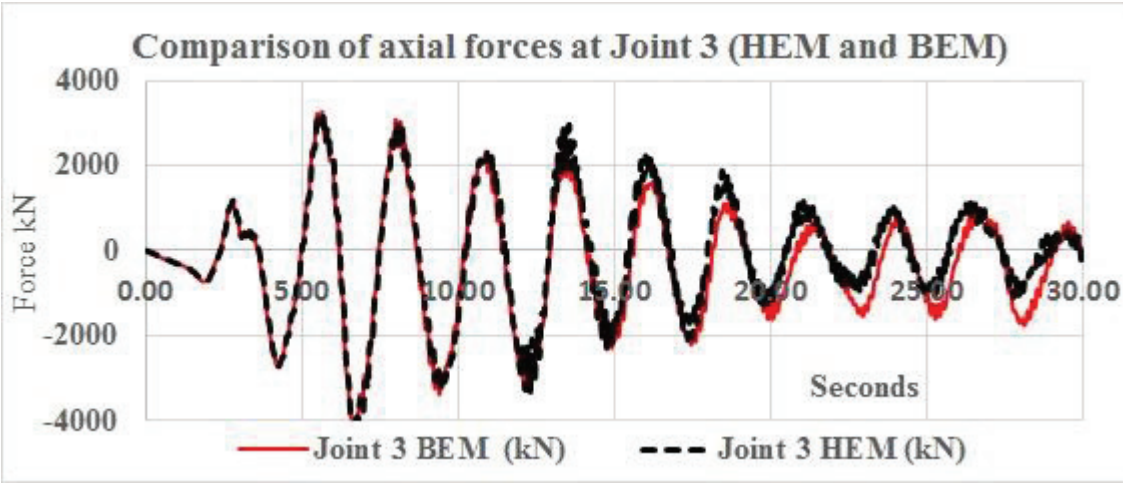

Fig. 4-16 Comparison of axial forces between the HEM and thhe BEM at Joint 3

4.3.2 Earthquake-response results at joints of the hybrid-element model

4.3.2.1 Changes in bolt and joint axial forces

Figures 4-17 and 4-18 show the time-response histories of the axial forces per one bolt in the z-direction of Joints 1 and 3 and the axial force in these bolts. The initial pretension axial force of each bolt is 75% of the yield strength of the bolts. The bolt tensile axial force slightly exceeds the initial tension axial force at 4.23 and 3.33 s of the first tension peak and shows the highest value at 6.72 and 5.5s of the second tension peak at Joints 1 and 3, respectively.

Notably, the initial pretension axial force of each bolt decreases after the second tension peak of the joints wherein the axial forces of these bolts considerably exceed their yield strength and remains constant as far as the bolt forces are within elastic range. Bolt No. 1 and No. 2 of Joint 1 as well as Bolt No. 3 and No. 4 of Joint 3 located outside the crane mast in the y-direction, which is the direction of earthquake loading, show higher force with more decrease in the initial pretension force compared with the other bolts after

yielding. The initial pretension force of Bolt No. 1 (a blue solid line) and No. 2 (a blue dotted line) of Joint 1 as well as Bolt No. 3 (a red solid line) and No. 4 (a red dotted line) of Joint 3 decrease by ~50% and ~15%, respectively. This implies that the extent of bolt yielding may have significant impact on the decrease in initial pretension forces and may cause bolt failure. These figures represent the joint force per one bolt as black solid lines for reference.

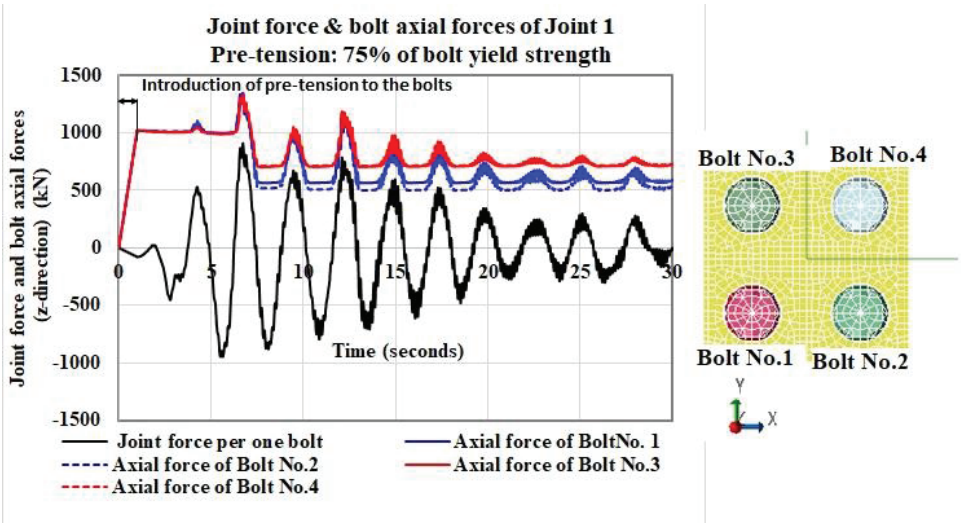

Fig. 4-17 Sesmic responses of bolt axial force and joint force on Joint 1

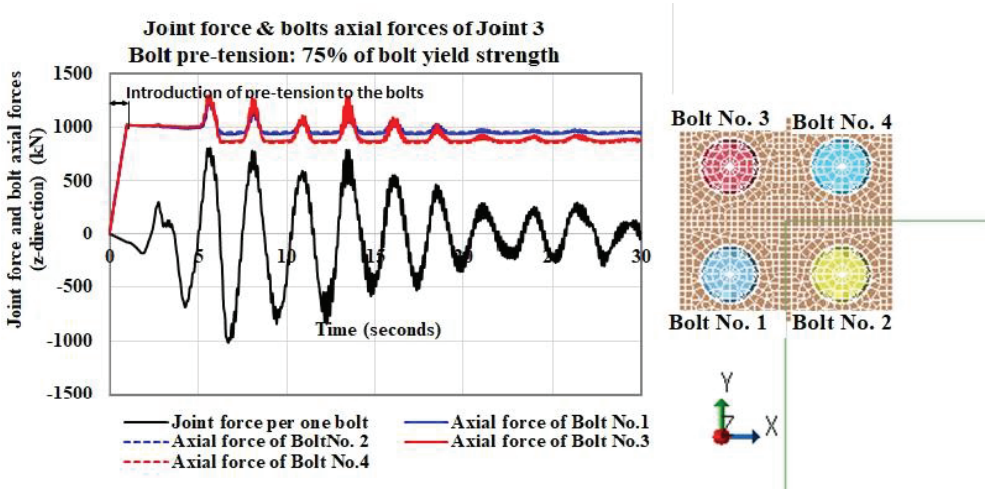

Fig. 4-18 Sesmic response of bolt axial force and joint force on Joint 3

4.3.2.2 Von Mises stress distribution of each part of the tower-crane mast joints

At Joint 1 and Joint 3, the maximum applied tensile forces are 3635 and 3171 kN at 6.72 and 5.5 s, respectively. Fig. 4-19 shows the contour plot of the von Mises equivalent stresses of the end plates in Joints 1 and 3 at 6.7 s. Because Joint 3 is compressed onto the end plate that is not bent, the stresses of the elements around the joints to the flanges of H shape post are large due to compression. Further, at Joint 1, tension is applied to the

joint portion, bending stress is generated in the end plate, and the von Mises equivalent stresses are large in the elements on the bolt lines parallel to the flange of the mast post.

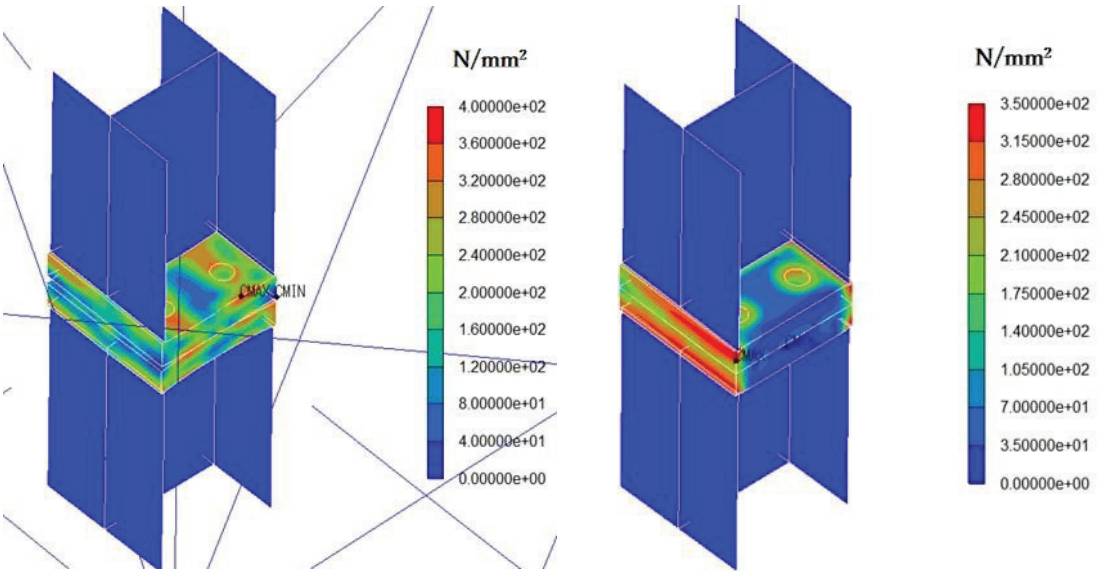

(a) Joint 1: von Mises stress (b) Joint 3: von Mises stress

Fig. 4-19 Contour plot of the von Mises stress for Joints 1 and 3 at 6.7 seconds

Figures 4-20 and 4-21 show the contour plots and time-related responses of the von Mises equivalent stresses in the end plates and bolts. From these figures, the detailed earthquake response of the components of the end-plate tension-bolt joint can be understood.

Figures 4-20 (a) and (b) show the von Mises stress contour plots of end-plate solid elements and the time-related responses of von Mises stresses of six end-plate solid elements with high stress in Joint 1, respectively. This end plate is the lower part of the two end plates, and Fig. 4-20 (a) details the end-plate deformation response for better comprehension. Fig. 4-20 (b) shows the stresses of the six elements of the end-plate exceed their yield strength (340 N/mm^2) when the joint force becomes the largest at about 6.7 s. and that after this peak, the stresses become peak value when the joint is compressed possibly due to the plastic deformation of the end-plate when the joint is subjected to maximum tension force at about 6.7 s. Figure 4-20 (b) shows the joint force per one bolt as black dotted lines for reference.

Figures 4-21 (a) and (b) show the von Mises stress contour plots of bolt solid elements during peak loading (6.7 s) and the time-related responses of von Mises stresses of three bolt solid elements in Joint 1, respectively. Figure 4-21 (a) also details the deformation of bolt with exaggeration for easy understanding and that the solid elements of bolts facing the flange of H-shaped post have higher von Mises stress which means bending moment is generated in the bolts. Fig. 4-21 (b), the stresses of No. 2 (a blue line) and No. 3 (a green line) elements of the bolts exceed their yield strength (900 N/mm^2) when the joint tensile force becomes the largest at about 6.7 s, and that after this peak, the pretension stresses decrease to a certain value and remain constant as long as the stresses do not exceed their yield strength. Conversely, the stress of No.1 element (a red line) is

maintained almost within the elastic range, without any decrease in the initial pretension stress. These results are consistent with those of Fig. 4-17 and indicate that the bending of bolt shaft must be considered for the design of end-plate-type tensile bolted joints with the bolts with large diameter. Figure 4-21 (b) also represents the joint force per one bolt as black dotted lines for reference.

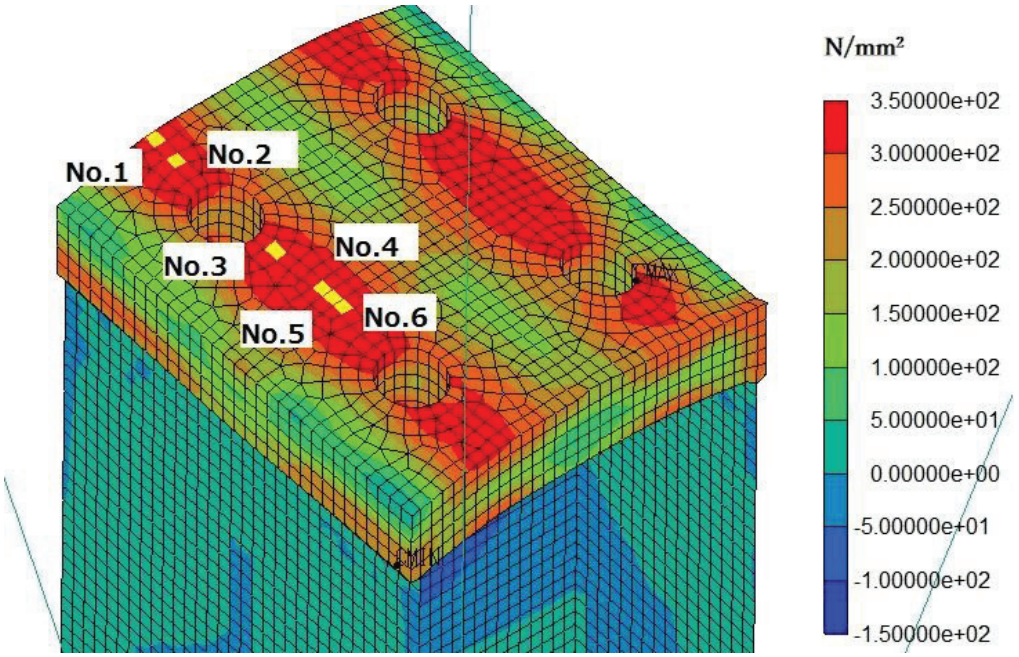

(a) End-plate von Mises stress counor plots and the solid-element number

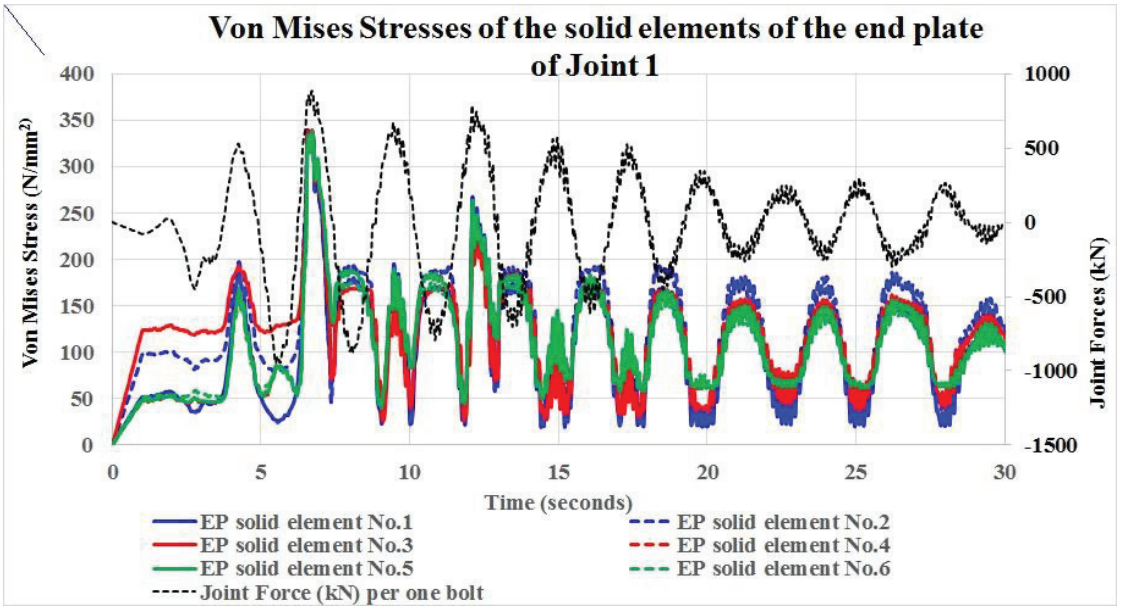

(b) Time-related responses of von Mises stress in the solid elements of the end plate

Fig. 4-20 Contour diagram and von Mises stress of the solid elements of the end plate

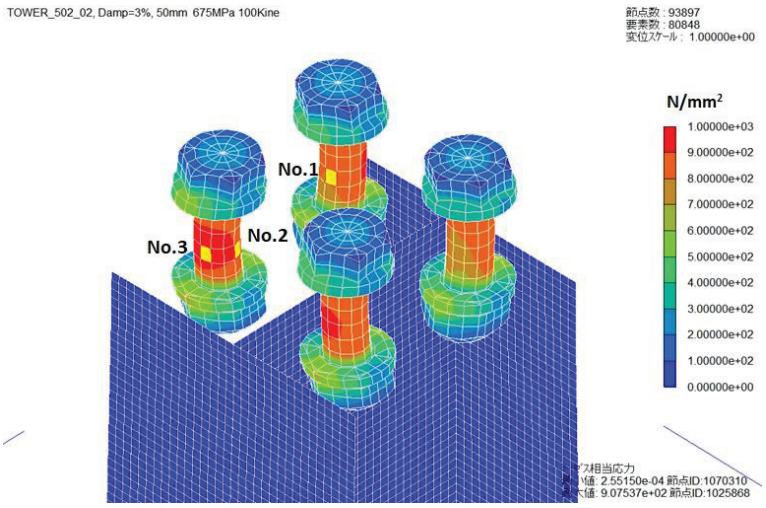

(a) Countor plots and solid-element numbers of the bolts

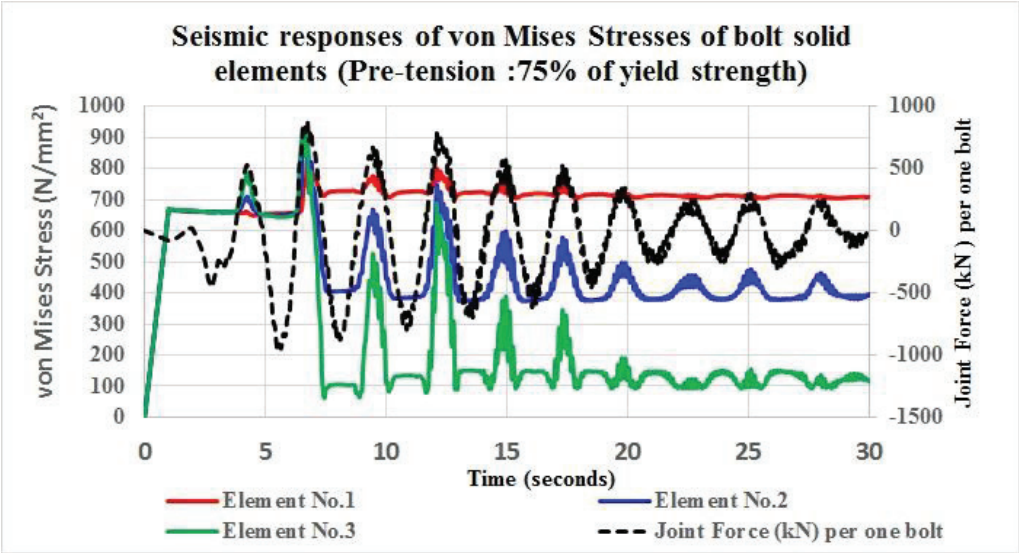

(b) Time related responses of von Mises stress of the solid elements of the bolt

Fig. 4-21 Contour diagram and von Mises stress in the solid elements of the bolts

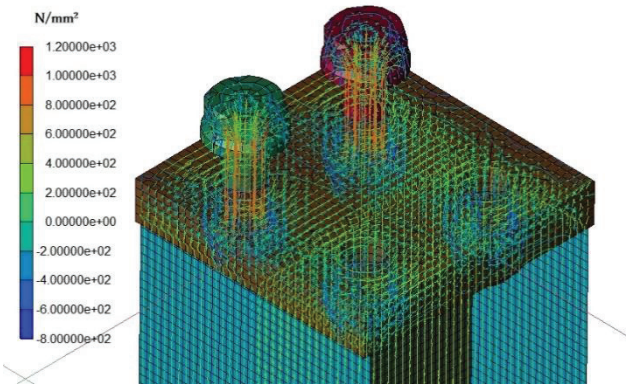

Fig. 4-22 Principal stress vectors

4.3.2.3 The gap between the two end plates and the principal stress vectors of the bolts and end plates

Fig. 4-22 shows, as results of the analysis, the principal stress vectors generated in the end plates and bolts when the largest gap between the two end plates is caused by the tensile load. Figures 4-23 (a) and (b) show the gap and time-related response of the gap sizes compared with the joint force indicated in black dotted line. These simulation results show the stress distribution of end plates and bolts and the relation of size of a gap between the two end plates and joint forces.

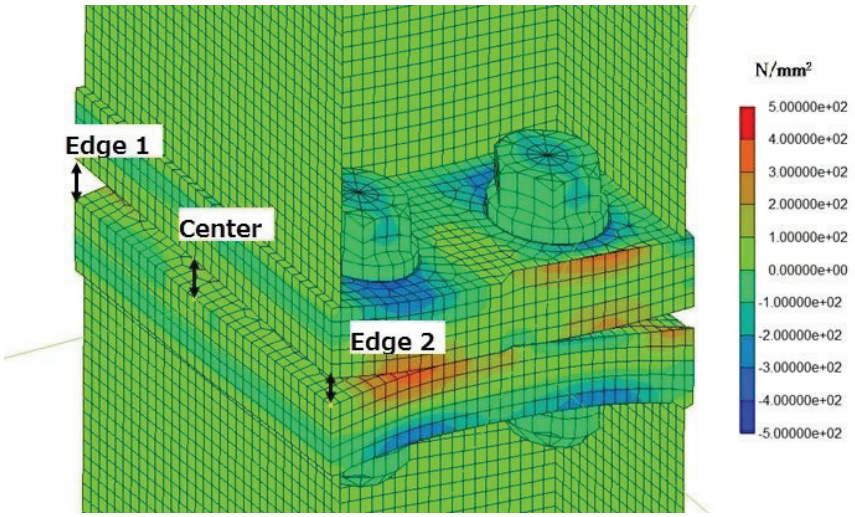

(a) Gaps between the two end plates

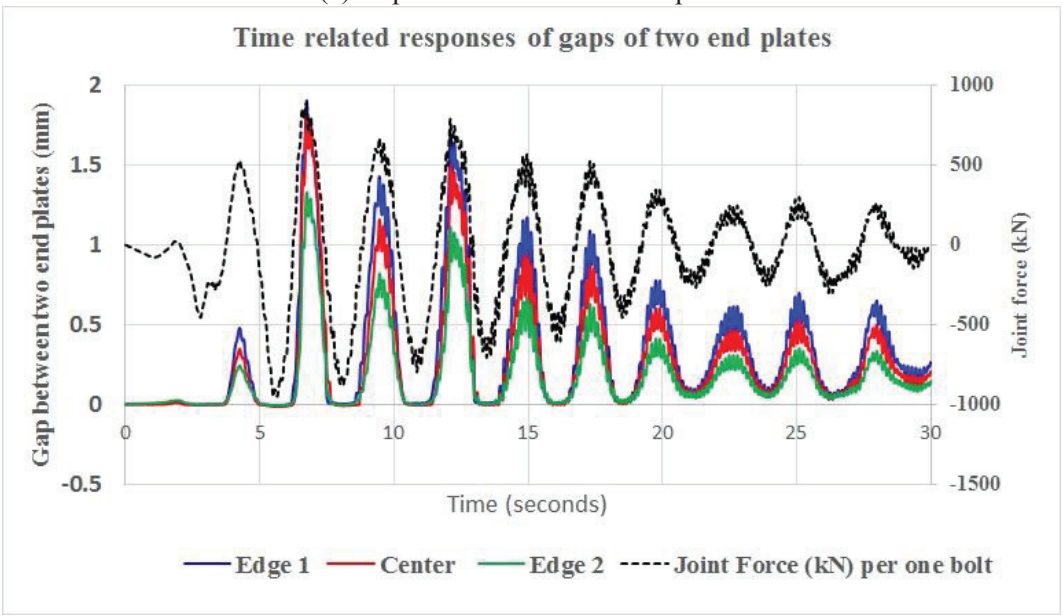

(b) Time-related gaps between the two end plates

Fig. 4-23 Gap between the two end plates

4.3.2.4 Case study on the seismic responses of the joint models with diferent initial pretention forces of bolts

By using this modeling and simulation method, it was studied how magnitude of initial pretention introduced to bolts will influence on seismic responses of the end-plate-type bolted tensile joints. Following two models were analyzed to compare.

Case 1 : the bolts of the joint with initial pretention axial force of 75% of yield strength of the bolts (882kN)

Case 2 : the bolts of the joint with initial pretention axial force of 25% of yield strength of the bolts (294 kN)

Fig. 4-24 shows time related response of bolt axial forces of the Bolt No.1 and the joint forces shared by one bolt at Joint 1 in Case 1 and Case 2. This figure expresses the response of Case 1 in red line and that of Case 2 in black line. In order to know visually the bolt deformation at the peak loadings at the joint, this figure also shows the contour plots of the bolts with exaggeration of bolt shaft deformation. This figure indicates that the time-related responses of the joint forces in the both cases are similar, but that the bolt's tensile axial forces of Case 2 are much smaller than that of Case 1. At the two peaks of joint's tension force, at 6.7 seconds and 12.1 seconds, the difference of them is as much as 11% and 14% respectively. Those bolt's tensile axial forces are described in the figure. This result suggests that initial pretention axial force of bolts should be critical factor for end-plate-type bolted tensile joints and recommends that the pretention force of bolts, 75% of bolt yield strength specified in AIJ Recommendation (2012) for firiction type joints, should be reduced to the proper value in consideration of the loading codition of the joints.

Fig. 4-25 shows time-related response of the gap sizes between the end-plates of Case 1 and Case 2 with that of the joint force indicated in black line. This figure also expresses the response of Case 1 in red line and that of Case 2 in black line. The gap location is at "center" shown in Fig. 4-23 (a). The maximum gap of Case 1 is 1.82mm and that of Case 2 is 2.21mm and difference is 0.0.39mm and 18%.

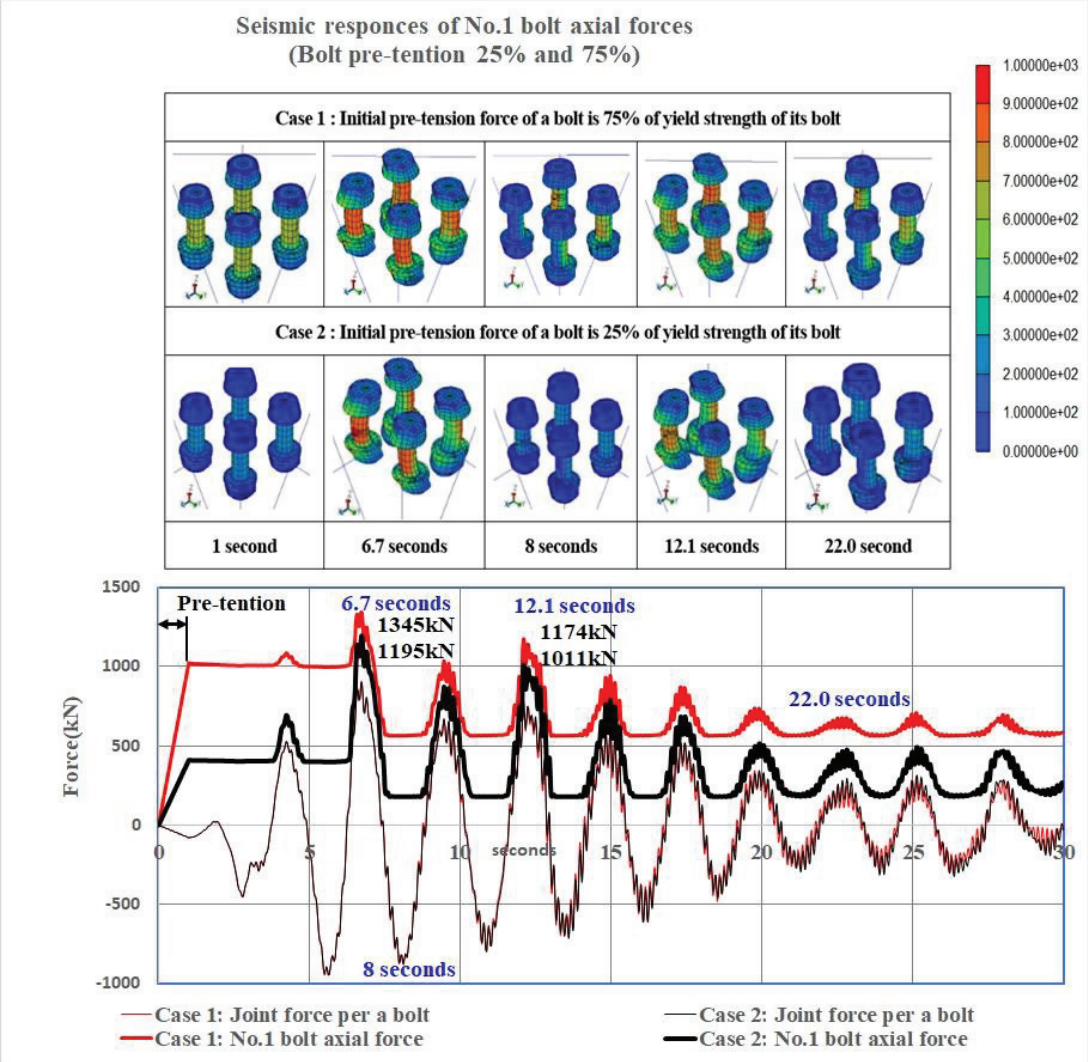

Fig. 4-24 Seismic responces on different initial pretention forces of bolts

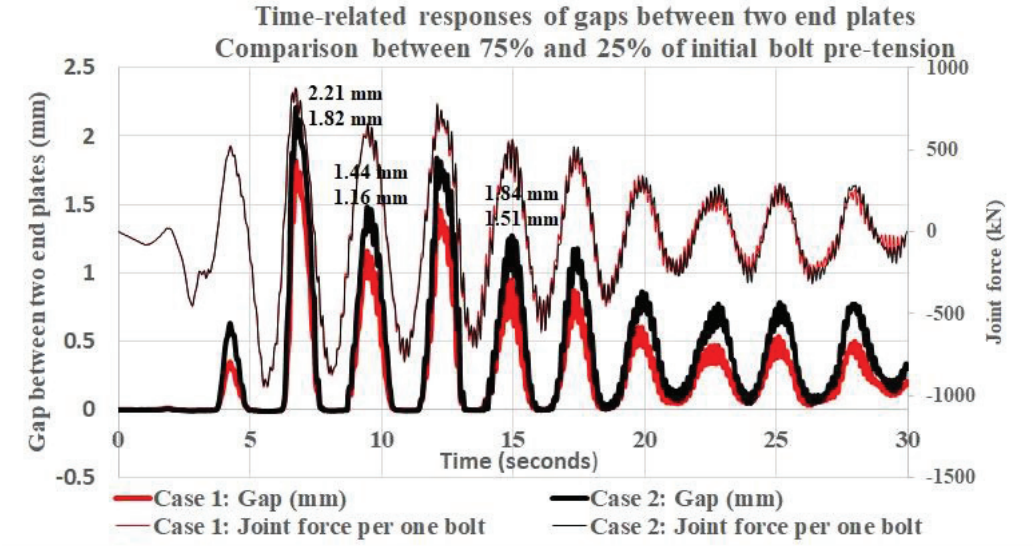

Fig. 4-25 Time-related responses of gaps between two end-plates

4.4 Conclusion

By creating a HEM of a tower-crane mast, we could obtain detailed mechanical behavior of the site joints (end-plate-type bolted tensile joints similar to the one of the tower crane mast joints used for Taipei 101) at the time of an earthquake with a reasonable calculation time using LS-DYNA and a supercomputer. We can replace the detailed joint model portion with a different, alternative joint model that could be used at any joints of the tower-crane mast.

Notably, this analysis showed that the joint behavior of the initial pretension axial force of a bolt is considerably reduced after the axial force of the bolt exceeds the yield strength. A maximum decrease of 50% in the initial pretension axial force under the El Centro N–S Wave (vmax = 100 cm/s) was observed. Results also showed the plastic bending deformation behavior of the large-diameter shafts of the bolts of the end-plate-type bolted tensile joints used herein. In addition, the case study on the seismic responses of the joint models with different initial pretention forces of bolts was done using this simulation analysis. This result suggested for end-plate-type bolted tensile joints that initial pretention axial force of bolts should be critical factor for designing of safer joint and recommended that the pretention force, 75% of bolt yield strength, specified in AIJ Recommendation (2012), should be reduced to .the proper value in consideration of loading condition of the joint using of the suitable analysis like the method proposed in this Chapter.

By using the structural model and simulation method proposed in this chapter, it is possible to provide effective information for designing safe joints of tower cranes during earthquakes, taking into consideration workability (control of bolt introduction axial force, etc.) and economy.

Future studies will use the proposed analysis method by considering parameters such as end-plate thickness, initial pretension axial force of a bolt, bolt strength and diameter, and configuration of bolts to determine the ultimate behaviors of site joints of tower-crane masts during earthquakes and to design safe joints with excellent earthquake resistance.

This method can also be applied to analyze the seismic responses of general temporary structures in which joints with lower strength than that of the jointed members are often applied in consideration of the ease of assembly and dismantling. Therefore, the method can contribute to the planning and implementation of earthquake-safety measures on construction sites.

Chapter 5

Conclusions

Fatal tower crane accidents because of natural and man-made causes are recorded globally each year. It is important to determine measures to prevent fatal tower crane accidents at construction sites during earthquakes because these accidents negatively impact construction projects, may result in losses of life and tremendous repair costs, and distort the construction schedule. However, in many cases, construction contractors follow only the structural design criteria for only cranes because tower cranes are facilities and structures that are needed only for a short term (e.g., less than two years). Owing to costs and other considerations, further countermeasures to prevent serious accidents during powerful earthquakes, similar to those taken for permanent buildings, are not considered.

According the author's experiences of tower cranes accident due to the earthquake at the construction site of the Taipei 101 building on 31st May 2002, the autor concluded that "resonance effects to a tower crane with the building where the tower crane is fixed" and "site joints of a tower crane mast" are key issues to prevent the fatal disaster of tower cranes at earthquake. Therefore, this research was conducted for the following purposes:

(4) To confirm the resonance effects of a tower crane seismic responses with the building, where the tower crane is installed, at construction sites of high-rise building, and propose countermeasures to prevent those effects and to minimize tower crane failures,

(5) To propose a new design method for end-plate type bolted tensile joints that are commonly applied to the site joints of tower crane masts owing to their site workability. The method uses the calculation results obtained using a supercomputer by an application of static elastoplastic finite element analysis (LS-DYNA R 9.2.0 _ Rev.119543, which was developed by Livermore Software Technology Company(LSTC)), to a tower-crane-mast structural models with extremely finely shaped solid elements, and

(6) To develop a modeling method for tower crane mast structures by creating a hybrid element model comprising solid, shell and beam elements for seismic response non-linear FEM analysis (LS-DYNA) to enable structural engineers to grasp the precise dynamic ultimate behavior of mast site joints during earthquakes, and to promote better structural design.

In chapter 2, based on the fact that the cause of the accident in the Taipei 101 building was mainly the resonance effects between the building and the tower crane according to the Investigation Report 2002, the author confirmed that similar phenomena should occur in general buildings. Simulation methods were used to describe the tower crane's response to an earthquake considering the construction progress. It also discussed the response amplification caused by resonance between the building and crane and between the building and earthquake ground motion during an earthquake. The analysis was done on a 14-story building designed according to the latest seismic design criteria. Lumped mass models of the six construction stages were prepared for seismic analysis; the building structural models were linear and nonlinear. El Centro NS (v_{max} = 50 cm/s and v_{max}=32.25 cm/s) seismic load was applied with a 3% damping ratio of the building and the tower crane structures. The seismic load (v_{max} = 50 cm/s) was large enough that some of the designed buildings' structural members should have experienced plastic

deformation, and the seismic load (v_{max}=32.25 cm/s) was the level that the designed buildings' structural members were all within elastic range. The results showed seriousness of the resonance effects caused by their close natural frequencies.

In addition, as a countermeasure, it was confirmed that this resonance effects could be suppressed by changing the rigidity of building and tower crane structures, or by giving temporary devices between the tower crane and the building for a damping function. Therefore, the author could show the importance of the study at the construction planning stage on the tower crane installation plan in consideration of the possibility of resonance effects of a tower crane by the building with tower crane installed at the time of the earthquake.

One of the causes of brittle tower crane collapses was the destruction of the site joints of the tower crane masts. Chapter 3 proposes a new design method for end-plate-type tensile bolted joints that are commonly applied to the site joints of tower crane masts. A tensile bolted joint possesses good workability for the joining of vertical members, such as the posts of a tower crane mast, at the time of assembly and disassembly, and moreover, it is structurally capable of transmitting large loads efficiently. However, the problem is that the design of the joints is difficult and complicated because the outer surface of the mast needs to be flat to enable climbing of the tower crane. Therefore, depending on the shapes of the post members of the mast, special joints such as large-diameter bolted (greater than 30 mm) and eccentric-bolted tension joints are applied to the site joints. This new design method uses the calculation results obtained using a supercomputer through static elastoplastic finite element analysis (LS-DYNA) applied to structural models with extremely fine cubic-shaped solid elements with side lengths of 2.5 mm. To prove the effectiveness of this method, the conventional design method was also described.

Using the design method proposed in this chapter, it is possible to realize not only more precise and reliable joint designs but also the design of various complicated joints in consideration of the construction conditions such as the pre-tension axial force on the bolts. By applying this method to, for example, a complex eccentric-tension bolt joint, the engineers can realize a detailed design in consideration of many parameters such as the enlargement of diameter of the bolts in response to a larger load in the eccentric joints, proper pre-tension of bolts, optimization of the bolt layout, etc.

We are confident that this new design method will help improve the earthquake resistance of tower cranes. Furthermore, this method is applicable not only to tower crane masts but also to bolted tension joints in all structures.

Chapter 4 proposed the modeling of structural analysis using a supercomputer and FEM elastoplastic analysis software (LS-DYNA) in order to accurately ascertain the ultimate behaviors of the tower crane's site joints at the time of the earthquake. The model is a hybrid element model (HEM) consisting of solid elements, shell elements and beam elements and keeping the computer calculation time to a realistic extent. The analysis results of detailed response of the tower crane joints to the EL Centoro-NS (Vmax = 100 cm / sec), which is a very large earthquake, were shown.

Notably, this analysis showed that the joint behavior of the initial pretension axial force of a bolt is considerably reduced after the axial force of the bolt exceeds the yield strength. A maximum decrease of 50% in the initial pretension axial force under the El Centro N–S Wave (v_{max} = 100 cm/s) was observed. Results also showed the plastic bending deformation behavior of the large-diameter shafts of the bolts of the end-plate-type bolted tensile joints used herein. In addition, the case study on the seismic responses of the joint models with diferent initial pretention forces of bolts was done using this

simulation analysis. This result suggested for end-plate-type tensile bolted joints that initial pretention axial force of bolts should be critical factor for designing of safer joint and recommended that the pretention force, 75% of bolt yield strength, specified in AIJ Recommendation (2012), shuld be reduced to the proper value in consideration of loading condition of the joint using of the suitable analysis like the method proposed in this Chapter.

By using the structural model and simulation method proposed in this chapter, it is possible to provide effective information for designing safe joints of tower cranes during earthquakes, taking into consideration workability (control of bolt introduction axial force, etc.) and economy.

Future studies will use the proposed analysis method by considering parameters such as end-plate thickness, initial pretension axial force of a bolt, bolt strength and diameter, and configuration of bolts to determine the ultimate behaviors of site joints of tower-crane masts during earthquakes and to design safe joints with excellent earthquake resistance. This method can also be applied to analyze the seismic responses of general temporary structures in which joints with lower strength than that of the jointed members are often applied in consideration of the ease of assembly and dismantling. Therefore, the method can contribute to the planning and implementation of earthquake-safety measures on construction sites.

This thesis recommends a computer-simulation method, which can generally be less expensive and can take more parameters into account in the study than laboratory experiments with specimens that are common in studies on the mechanical behavior of joints in steel structures. Therefore, when an analytical model that allows more reproducibility and less computation time as this thesis proposed is devised, the computer simulation tool become very useful and effective for detail and precise design of steel structure joints.

Finally, If the study had been conducted using this proposed analysis method for constructing the Taipei 101 Building, the behavior of site bolt joints of the tower-crane mast during the catastrophic earthquake could have been determined. However, in accordance with the author’s experiences of this disaster, and this research, it can be confirmed that such a study could not be conducted then in consideration of the seismic design standards of the time and the level of technologies in almost 20 years ago.

Acknoledgements

This study started for author's doctoral thesis in April of 2016 at the Department of Simulation Studies in the University of Hyogo to contribute to construction-site safety in the event of an earthquake based on the author's experiences on the tower crane fall disaster caused by the earthquake at the Taipei 101 Building, which occurred in 2002.

The author would like to pray for the souls of the people who were killed by the tower crane disaster in the Taipei 101 Building construction-site, and believe that the results of this study should help to prevent such fatal accidents.

First, the author would like to express his deep acknowledgement to Professor Yasuyuki Nagano, at the University of Hyogo, for his encouragement, helpful advice, and simulation ideas in various aspects. Under his guidance and support, the author began his research on this theme and had the opportunity to submit this thesis to the University of Hyogo.

The author would like to express his sincere appreciation to Professor Emeritus Eizaburo Tachibana, who was the author's adviser in the undergraduate thesis. He recommended the author to study at the University of Hyogo to obtain a doctoral degree, always offering encouragement and advice by telephone and e-mail.

The author would like to express his deep appreciation to Professor Emeritus Kozo Wakiyama, at Osaka University, for his valuable advice on bolted joints so the author could decide the research direction. He was an assistant professor when the author was a student at Osaka University and later recommended and greatly assisted the author to study in the University of Illinois in the USA.

The author is sincerely grateful to Associate Professor Susumu Kuwahara at Osaka University for very useful and practical advice on bolted joints through the joint research. He kindly agreed and implemented the experiments related to the contents of this thesis.

The author would like to express his deep acknowledgement to Mr. Tomoharu Saruwatari for assistance using the LS-DYNA. He prepared the data and operated LS-DYNA to analyze the structural models for this research, providing useful advice for modeling the structural system.

The author wishes to express sincere appreciation to Dr. Seiji Takanashi, senior researcher in the National Institute of Occupational Safety and Health, for providing valuable hints to focus the theme of this thesis and the author could get various information on the seismic design of tower cranes from his published papers.

The author is sincerely grateful to Mr. Masayuki Okano, an undergraduate student of the University of Hyogo in FY2016 and working for Obayashi Corporation now, for assisting with the study of the resonance effects between a tower crane and a building in computer calculation.

The author wishes to express sincere appreciation to the master and doctoral course students of the University of Hyogo, Mr. Lyu Zhilun, Miss. Maina Shirai and others to support the author in completing this thesis.

The author is sincerely grateful to Mr. Kento Shimada, an undergraduate student at Osaka University in FY2018 and working for Obayashi Corporation now, for assisting for preparation of this thesis through his research for graduation.

The author is owed a great deal of thanks to the Building Div. of Nippon Steel Cooperation (Now: Nippon Steel Engineering Co. Ltd.) for providing valuable experiences and information for him to complete this thesis.

The author also wishes to express deep appreciation to all the people in the International Cooperation Division of the Energy Conservation Center Japan (ECCJ), particularly Mr. Takakazu Oikawa and his group, for supporting the author's study by coordinating and rearranging the author's assignment in the ECCJ.

Finally, but not least, the author would like to thank his wife, Mrs. Mariko Ushio, and his daughter, Miss Mako Ushio, for their perpetual support and endless love.

References

References

Chapter 1

AIJ Recommendation (2012), Recommendation for Design of Connections in Steel Structure, (revised in March 2012), Architectural Institute of Japan.

ISO11031 (2016), Cranes-Principles for seismically resistant design, International Standard Organization.

JCAS1101(2008), Seismic Design Guideline for Cranes, the Japan Crane Association (JCA)

JIS B8821 (2013), Calculation standards for steel structures of cranes, Japanese Standards Association.

JIS B8831 (2004), Cranes-Design Principles for loads and load combination, Japanese Standards Association

JSS IV 05-2004, Recommendation for design of High Strength Tensile Bolted Connections for Steel Bridges, (revised in August 2004), Japanese Society of Steel Construction (JSSC).

Investigation Reports 2003, The causes of the 331 seismic disaster in Taipei 101 Building Construction dated June 5. 2002, the Taipei, *The Taipei Structural Engineers Association,* No.91-1395

Kobayashi, N. (2017), "ISO1131:craines-Principles for seismically resistant design and Seismic Design", *Journal of the Japan Crane Association*, **55**(635), 4-10

Loh, C.H., Tsai, K.C., Chung, L.L. and Yeh, C.H. (2003), "Reconnaissance report on the 31 March 2002 earthquake on the east coast of Taiwan", *Earthq. Spectra*, **19**(3), 531-556.

Takanashi, S. (2005), "Damage to the cranes and seismic design", *Journal of Reality Engineering Association of Japan (REAJ)*, **27**(8), (series No. 148).

Takanashi, S., Adachi, H. and Nakanishi, M. (2007), "Study on the seismic performance of the tower crane for construction", *Architectural Institute of Japan Technical Report*, **13**(26), 415-420.

Getines H. and Ushio Y. (2000), "Construction of the passenger terminal roof at Chek Lap Kok, Hong Kong" , *Journal of the Institution of Structural Engineer*s, Vol. 78 No.16, 15 Aug 2000:

Ushio, Y., Okano, M. and Nagano, Y. (2017), "The earthquake response of climbing-type tower cranes installed in high-rise buildings in consideration of various situation under construction", *Proceedings of 16th World conference on Earthquake Engineering, Santiago, Chile*. No. 3403

Chapter 2

Investigation Reports 2002, The causes of the 331 seismic disaster in Taipei 101 Building Construction dated June 5. 2002, the Taipei, *The Taipei Structural Engineers Association,* No.91-1395

Ai B., Yang J.L. and Pei, Z.Z. (2013), "Seismic response analysis of tower crane in consideration of the building-crane interaction", *Applied Mechanics and Materials, ISSN:1662-7482,* **353-356**, 1981-1985

Loh, C.H., Tsai, K.C., Chung, L.L and Yeh, C.H. (2003): "Reconnaissance Report on the 31 March 202 Earthquake on the East Coast of Taiwan", *Earthquake Spectra, Volume 19 No.3,* Page 531-556

Takanashi, S., Adachi, H. and Nakanishi, M. (2007), "Study on the seismic performance of the tower crane for construction", *Architectural Institute of Japan Technical Report Volume 13, No.26*, Page 415-420

Ushio, Y., Okano, M. and Nagano, Y. (2017), "The earthquake response of climbing-type tower cranes installed in high-rise buildings in consideration of various situation under construction", *Proceedings of 16th World conference on Earthquake Engineering, Santiago, Chile*. No.3403

Ushio, Y., Okano, M., Shirai, M. and Nagano, Y. (2017), The Seismic Response Analysis of Steel structure Building in Consideration of Construction Progress No.1 to No.3, Summary research reports presented at the annual conference in Hiroshima, organized by the Architectural Institute of Japan (AIJ) Aug. 2017, Structure Field Ⅱ、P57-62

JIS B 8821(2013) *Calculation standards for steel structures of cranes*, Japanese Standards Association

The book titled "*The Examples of Structural Design / Structural Member Sections*" (2007) , page 554-559, issued by The Japan Building Disaster Prevention Association

JIS B8831 (2004), Cranes-Design Principles for loads and load combination, Japanese Standards Association

Chapter 3

AIJ Recommendation (2012), Recommendation for Design of Connections in Steel Structure, (revised in March 2012), Architectural Institute of Japan.

ISO 11031 (2016), Cranes-Principles for seismically resistant design, International Standard Organization.

JCAS 1101 (2008), Seismic Design Guideline for Cranes, Japan Crane Association (JCA)

JICAS 1101 (2018), Guideline for seismic design of cranes, Japan Crane Association (JCA)

JIS B1082 (2009), Stress Area and bearing area for threaded fasteners, Japanese Standards Association

JIS B8821 (2013), Calculation standards for steel structures of cranes, Japanese Standards Association.

JIS B8831 (2004), Cranes-Design Principles for loads and load combination, Japanese Standards Association

JSS IV 05-2004, Recommendation for design of High Strength Tensile Bolted Connections for Steel Bridges, (revised in August 2004), Japanese Society of Steel Construction (JSSC).

LS-DYNA KUM **I** (2016), LS-DYNA Keyword User's Manual Volume I (LS--DYNA R8.0), JSOL Corporation, 2016.3

LS-DYNA KUM **II** (2016), LS-DYNA Keyword User's Manual Volume II (LS-DYNA R8.0), JSOL Corporation, 2016.3

Ai, B., Yang, J.L. and Pei, Z.Z. (2013), "Seismic response analysis of tower crane in consideration of the building-crane interaction", *Applied Mechanics and Materials, ISSN:1662-7482,* **353-356**, 1981-1985

Kobayashi, N. (2017), "ISO1131:craines-Principles for seismically resistant design and Seismic Design", *Journal of the Japan Crane Association*, **55**(635), 4-10

Loh, C.H., Tsai, K.C., Chung, L.L. and Yeh, C.H. (2003), "Reconnaissance report on the 31 March 2002 earthquake on the east coast of Taiwan", *Earthq. Spectra*, **19**(3), 531-556.

Mizushima,Y., Mukai, Y., Namba, H., Taga, K. and Saruwatari, T. (2018), "Super detailed FEM simulations for full-scale steel structure with fatal rupture at joints between members – Shaking table test of full-scale steel frame structure to estimate influence of cumulative damage by multiple strong motion: Part 1", *Japan Architectural Review published by John Wiley & Sons Australia, Ltd. On behalf of Architectural Institute of Japan,* **1**(1), 96-108

Takanashi, S., Adachi, H. and Nakanishi, M. (2007), "Study on the seismic performance of the tower crane for construction", *Architectural Institute of Japan Technical Report*, **13**(26), 415-420.

Ushio, Y., Okano, M. and Nagano, Y. (2017), "The earthquake response of climbing-type tower cranes installed in high-rise buildings in consideration of various situation under construction", *Proceedings of 16th World conference on Earthquake Engineering, Santiago, Chile*. No. 3403

Ushio, Y., Saruwatari, T., Nagano, Y. (2018), "Non-linear analysis on the end plate connections of tower crane mast structure", Research reports presented at the 2018 annual conference organized by the Kinki branch of the Architectural Institute of Japan, Structure field, 249-252

Ushio, Y., Saruwatari, T. and Nagano, Y. (2019b)," A New Design Method for Site-Joints of Tower Crane Mast by Non-linear FEM Analysis", *Advances Compuutational Des*ign**,** An International Journal, **4** (4) **(accepted for publication)**

Ushio, Y., Kuwahara, S. And Nagano, Y. (2019c), " Mechanical Property of Eccentric Bolted Joint Used in a Tower Crane Mast", Research reports presented at the 2019 annual conference organized by the Kinki branch of the Architectural Institute of Japan, Structure field,

Yang, J.G., Park, J.H., Kim, H.K., and Back, M. (2013), " A prying action force and contact force estimation model for a T-stub connection with high-strength bolts", *Journal of Asian Architecture and Building Engineering*, **12**(2), 309-316

Wang, X.Y., Luo, Y.F., Qiang, X.H. and Liu, X. (2015), "Review on high strength steel bolted end-plate connections", *Applied Mechanics and Materials, ISSN:1662-7482,* **744-746**, 265-273

Chapter 4

AIJ Recommendation (2012), Recommendation for Design of Connections in Steel Structure, (revised in March 2012), Architectural Institute of Japan.

JCAS1101 (2018), Seismic Design Guideline for Cranes, the Japan Crane Association (JCA)

LS-DYNA KUM I (2016), LS-DYNA Keyword User's Manual Volume I (LS--DYNA R8.0), JSOL Corporation, 2016.3

LS-DYNA KUM II (2016), LS-DYNA Keyword User's Manual Volume II (LS-DYNA R8.0), JSOL Corporation, 2016.3

Ai, B., Yang, J.L. and Pei, Z.Z. (2013), "Seismic response analysis of tower crane in consideration of the building-crane interaction", *Applied Mechanics and Materials,* **353-356**, 1981-1985

Loh, C.H., Loh, Tsai, K.C., Chung, L.L. and Yeh, C.H. (2003), "Reconnaissance report on the 31 March 2002 earthquake on the east coast of Taiwan", *Earthq. Spectra*, **19**(3), 531-556.

Mizushima, Y., Mukai, Y., Namba, H., Taga, K. and Saruwatari, T. (2018), "Super detailed FEM simulations for full-scale steel structure with fatal rupture at joints between members – Shaking table test of full-scale steel frame structure to estimate influence of cumulative damage by multiple strong motion: Part 1", *Japan Architectural Review,* **1**(1), 96-108

Ushio, Y., Okano, M. and Nagano, Y. (2017), "The earthquake response of climbing-type tower cranes installed in high-rise buildings in consideration of various situation under construction", *Proceedings of 16th World conference on Earthquake Engineering, Santiago, Chile*. No.3403

Ushio, Y., Saruwatari, T. and Nagano, Y. (2018), "Non-linear analysis on the end plate connections of tower crane mast structure", Research reports presented at the 2018 annual conference organized by the Kinki branch of the Architectural Institute of Japan, Structure field, 249-252

Ushio, Y., Saruwatari, T. and Nagano, Y. (2019a)" Elastplastic FEM analysis of earthquake responsee for the field-bolt joints of a tower crane mast", *Advances in Compuational Design***,** *An International Journal,* **4** (1), 53-72

Ushio, Y., Saruwatari, T. and Nagano, Y. (2019b)" A new design method for site-joints of tower crane mast by non-linear FEM analysis" , *Advances in Computational Design***,** *An International journal,* **4**(4)**,(accepted for publication)**

Zrnic, N. D., Bosnjak S. M., Gasic V. M., Arsic M. A. and Petkovic Z. D. (2011), "Failure Analysis of the Tower Crane Counterjib", *Procedia Engineering* **10** (2011) 2238-2243

Appendix

Structural member sizes of the 14-story building analyzed in Chapter 2

Reference:
The book titled "The Examples of Structural Design/Structural Member Sections" , Design Example S-10, page 558-559, published by the Japan Building Disaster Prevention Association in June 2007

Structural member sizes of the 14-story building analyzed in Chapter 2

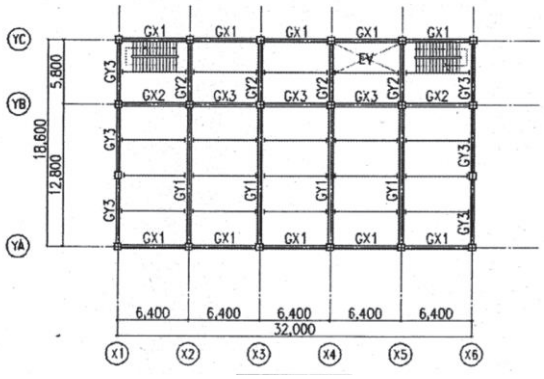

Typical floor plan

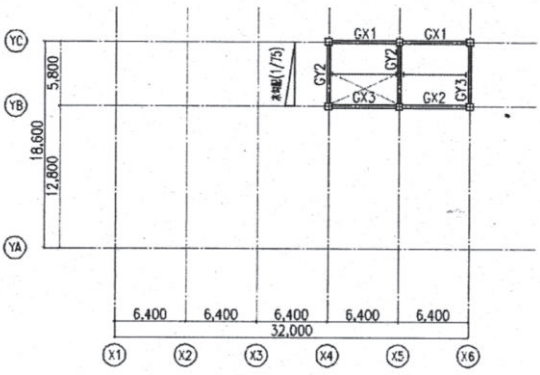

Floor plan at the roof level

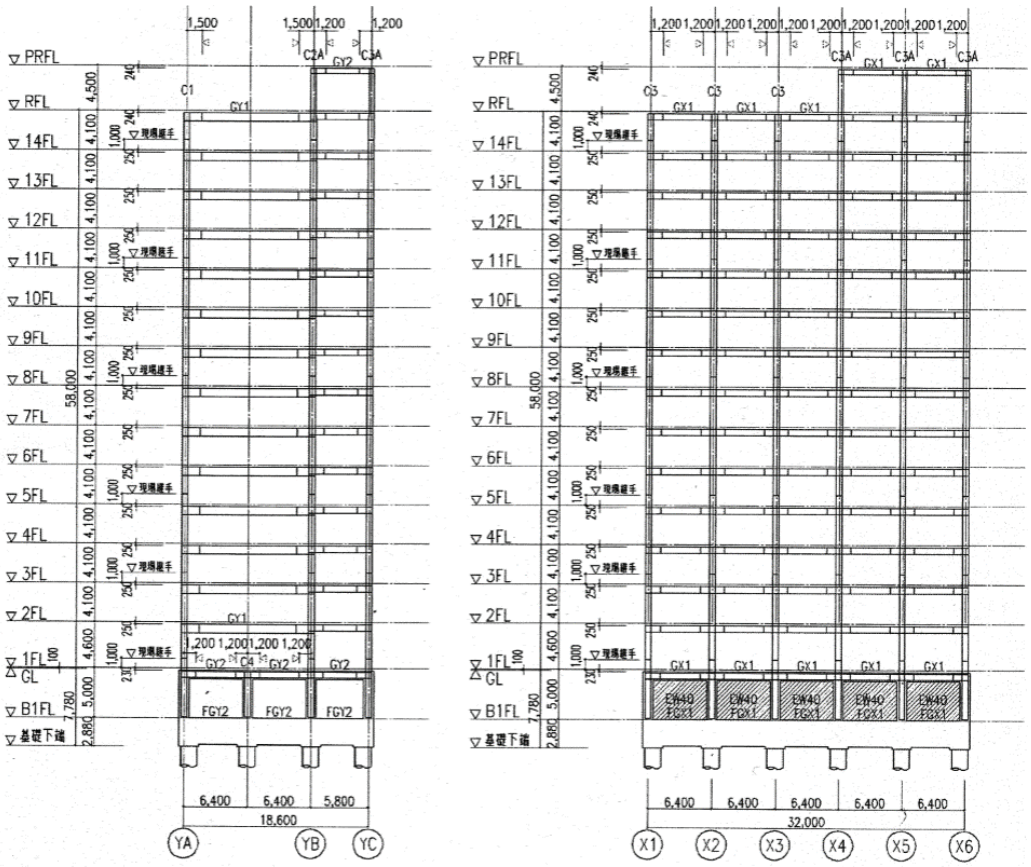

Elevation

List of sizes of beams and girders

Mark / Floor	GX1		GX2		GX3	
Location	Both sides	Center	Both sides	Center	Both sides	Center
PR	BH-500×250×12×19	H-500×250×9×16	BH-500×250×12×19	H-500×250×9×16	BH-500×250×12×19	H-500×250×9×16
12F-RF	H-650×250×12×19		H-650×250×12×19		H-650×250×12×19	
9F-11F	BH-700×250×14×22	BH-700×250×14×19	H-700×250×14×25	BH-700×250×14×22	H-700×250×14×25	BH-700×250×14×22
6F-8F	H-700×250×14×28	H-700×250×14×25	H-700×300×14×25	BH-700×300×14×22	H-700×250×14×28	H-700×250×14×25
2F5F	H-700×250×14×28	H-700×250×14×25	H-700×300×14×28	H-700×300×14×25	H-700×250×14×28	H-700×250×14×25
Mark / Floor	GY1		GY2		GY3	
Location	Both sides	Center	Both sides	Center	Both sides	Center
PR	-		BH-500×250×12×19	H-600×250×9×16	-	
12F-RF	H-850×350×16×25	BH-850×350×16×22	H-650×250×12×19		H-650×250×12×19	
9F-11F	H-900×350×19×25	BH-900×350×19×22	BH-700×250×14×19		BH-700×250×14×22	BH-700×250×14×19
6F-8F	H-900×350×19×25	BH-900×350×19×22	BH-700×300×14×22	BH-700×300×14×19	BH-700×300×14×22	BH-700×300×14×19
2F-5F	H-900×350×19×25	BH-900×350×19×22	BH-700×300×14×22	BH-700×300×14×19	H-700×300×14×25	BH-700×300×14×22

List of column sizes

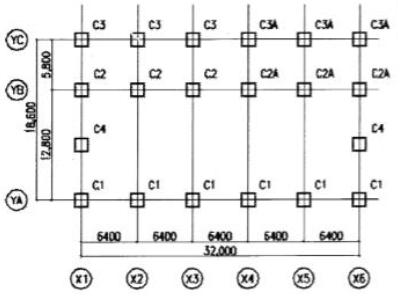

Key plan